MODELING SHOULDER LIGAMENT CONTRIBUTIONS AND THEIR EFFECTS ON MUSCLE FORCE PREDICTIONS

by

Sachin Raina

A thesis
presented to the University of Waterloo
in fulfillment of the
thesis requirement for the degree of
Master of Science
in
Kinesiology

Waterloo, Ontario, Canada, 2008

AUTHOR'S DECLARATION

I hereby declare that I am the sole author of this thesis. This is a true copy of the thesis, including any required final revisions, as accepted by my examiners.

I understand that my thesis may be made electronically available to the public.

Sachin Raina

ABSTRACT

Shoulder injuries are a common occurrence in both the workplace and everyday life. Mathematical musculoskeletal modeling and simulation provide a means for proactive injury prevention. To be effective, these models must physiologically replicate shoulder function. Although several muscle force prediction (MFP) shoulder models exist, few have attempted to integrate the force contributions of ligaments. In particular, no existing shoulder models have reported inclusion of the contributions of the glenohumeral ligaments. The purpose of the current study was to integrate seven shoulder ligaments into an existing computational shoulder model, and analyze both individual ligament characteristics and the influence that their inclusion has on the model outputs.

Using data from the literature, seven shoulder ligaments were integrated into a computational shoulder model: the costoclavicular, conoid, trapezoid, coracohumeral, superior glenohumeral, middle glenohumeral, and inferior glenohumeral, Ten subjects performed isometric exertions in 56 posture-force combinations. Upper body posture and hand force from these trials were used as inputs for three different model versions of increasing complexity; No-Ligaments (NL) included, Glenohumeral-Ligaments (GH) included, and All-Ligaments (AL) included. Electromyographic (EMG) signals from 11 muscle sites were recorded and used for comparison with model MFPs. The primary analysis focused on the differences between the GH and NL versions. Normalized EMG amplitudes were plotted against normalized MFPs from both

models. Ligament effects on model outputs were measured by comparing changes in correlation between EMG and MFP, changes in slopes regression lines relating EMG to MFP, and the frequency of zero-force prediction by the model. Paired Student's t-tests were used to measure significant differences.

Results showed significant correlations (Pearson product) between EMG amplitude and MFP in the lower trapezius and infraspinatus muscles ($p<0.01$). No significant differences were found in r-values for these muscles between the NL and GH model. Slopes of regression lines decreased when GH ligaments were added, while the change in zero-force predictions varied by muscle.

This study highlights the sensitivity of musculoskeletal models to the inclusion of ligament forces. Though correlations did not change, decreases in slope indicate increased force prediction by the GH model. Though zero-force predictions for some muscles increased, the results from those that decreased suggest muscles are active in postures where they were originally believed to be inactive. This finding suggests that inclusion of GH ligaments into our model may help predict antagonist muscle activity. However, further research is required to verify this claim.

ACKNOWLEDGEMENTS

Though only my name appears on this body of work, its creation would not have been possible if not for the efforts of a number of people.

I would first like to thank my advisor Dr. Clark Dickerson for taking me on as his first student. His patience, encouragement, sarcastic discouragement, funding, and overall ability to make me understand the world of shoulder biomechanics were greatly appreciated.

I would also like to thank my committee members, Dr. Richard Wells and Dr. Jack Callaghan, for their inputs and constructive criticisms throughout the stages of this thesis. I find it remarkable that two men who are always so busy, somehow always have the time to answer questions.

Sticking within the walls of the Burt Matthews Hall, I would like to thank Ruth Gooding, not only for her administrative assistance, but for her surrogate mothering. Most children turn to their moms in times of need, and in the Kin Department at Waterloo most students turn to Ruth.

My colleagues and laboratory mates also deserve thanks for keeping me sane, entertained, focused, and also distracted when it was necessary. In particular I would like to thank (in no particular order) Rebecca Brookham, Karen Van Ooteghem, Sam Howarth, Kevin Hurley, Kristen McFall, Alexis Cartwright, Lindsay Slater, and Diane Gregory. There are more whom I would like to thank, but I also hate writing.

I must thank Steve Brown, whom I lived with for two years. Not only did he pay all the bills on time and do the dishes far more often than I did, but he also played the role of a second advisor, and a fourth committee member.

Just as important as the people at school are the people outside. The support and encouragement from my friends and family never wavered; except from my grandfather who thinks I should be a surgeon. My parents have provided me with anything I have ever needed, and after all the proof reading I think my brother may know more about the shoulder than I do.

Though not statistically measurable, I'm pretty sure I have the best friends in the world. Though there is no gold standard to which to compare, I think this statement is qualitatively accurate. There is not enough room to name all of you, so I will name none of you – but you all know who you are.

Finally, to anyone who made this process easier, I thank you.

Sachin

TABLE OF CONTENTS

LIST OF TABLES

LIST OF FIGURES

I INTRODUCTION

Shoulder pain and injury are common events in occupational settings and everyday life. In some populations, 46% of those surveyed have reported shoulder complaints within a one year period (Brox, 2003). Along with discomfort and associated disruptions to daily life, musculoskeletal shoulder injuries represent both personal and financial burdens. A recent report estimated that shoulder injuries sustained in the workplace cost American businesses $1-2 billion annually (Reynolds, 1999).

Shoulder mechanical loading has been implicated as a probable cause of musculoskeletal disorders (Herberts, 1984). This loading is a function of not only the force on the hand, but also the posture of the upper extremity (Svendson, 2004). Attempts to estimate shoulder load and thereby develop methods to reduce the prevalence of shoulder injuries have been made through mathematical modeling (Hogfors, 1987, 1991; Dul, 1988; Wood, 1988a&b Van der Helm, 1994a; 1994b; Laursen, 1998; Holzbaur, 2005; Dickerson, 2006, 2007). These models employ either an optimization approach (Hogfors, 1987, 1991; Dul, 1988; Van der Helm, 1994a&b; Holzbaur, 2005; Dickerson, 2005, 2006) or an EMG-based approach (Wood, 1988a&b; Laursen, 1998) to predict the forces generated by individual shoulder muscles. Knowledge of individual muscle forces may allow researchers to identify dangerous load-posture scenarios. This identification is the first step in their prevention. The overall approach hinges on accurate quantification of muscle loads.

While the models mentioned above use similar parameters to model the muscles of the shoulder, none of them includes full ligament descriptions. The ligaments of the shoulder play a significant role in maintaining shoulder stability (Turkel, 1983; O'Connell, 1990; Seeley, 1999) and are known to be taut at extreme ranges of motions (Pronk, 1993; Culham and Peat, 1993; Itoi, 2004).

Notable attempts have been made to implement some ligaments into these models (Pronk, 1993; Makhsous, 1999). However, Pronk's attempts were unsuccessful, and the effectiveness of Makhsous's alterations remains unclear. Models of the glenohumeral ligaments exist, but none currently considers the impact of ligaments on muscle force predictions (Debski, 1999; Novotny, 2000).

Current muscle force prediction models may not sufficiently account for ligament contributions to intersegmental equilibrium or joint stability. In order to obtain more accurate muscle force predictions, the formulation of these predictions must include the forces generated by length changes in the ligaments.

1.1 Investigative Questions and Purpose

The purpose of this project is to incorporate mathematical descriptions of seven shoulder ligaments into a pre-existing muscle force prediction model of the human shoulder. Using data derived from the literature and empirical studies, two questions are addressed:

i) At what postures are ligaments most involved with shoulder function?

ii) How does the inclusion of these ligaments affect the output of a mathematical muscle force prediction model?

1.2 Hypotheses

Ligaments become taut in "extreme postures" (Culham and Peat, 1993; Itoi, 2004). However, the term "extreme" is not quantifiable. Therefore, it was hypothesized that:

i) The contribution of ligaments to shoulder function increases as arm posture deviates further from resting/anatomical position. Correspondingly, ligament length changes, and therefore force contributions, are greatest at the end ranges of motion in the humeral flexion/extension, abduction, axial rotation, and horizontal abduction planes.

ii) In situations where ligaments are taut, muscle force predictions for certain muscles decrease. External forces are resisted through muscle activity only in the original model. Ligament inclusion will lower these contributions.

iii) Due to increased physiological representation of the system, model-predicted muscle force predictions will improve with inclusion of these ligaments.

To address these hypotheses, three activities were undertaken:

1) Integration: The tensile properties of seven shoulder ligaments were integrated into a muscle force prediction model of the human shoulder. The integration was achieved by establishing attachment sites and reference lengths for the seven ligaments, and characterizing the mathematical force-length relationship for each ligament based on reported literature values.
2) Experimentation: Ten subjects performed tasks involving moderate and extreme shoulder postures in flexion/extension, abduction, and external rotation. EMG data for 11 muscles were collected for comparison with model predictions.
3) Comparison (Evaluation): Two versions of the model (with and without ligaments) were compared with the EMG data to determine the influence of ligament inclusion on the muscle force predictions. The data were compared using statistical measures including correlation coefficients and correlation slope values in conjunction with dependent t-tests.

II LITERATURE REVIEW

2.1 Musculoskeletal Structure of the Shoulder

The shoulder complex has both high mobility and low stability (Seeley, 1999). It is composed of three bones: the scapula, humerus, and clavicle; and contains three primary joints: the glenohumeral, acromioclavicular, and sternoclavicular (Culham and Peat, 1993). The ball-and-socket nature of the glenohumeral joint allows for large motion ranges in several principal movements, including flexion/extension, abduction, rotation, and circumduction (Seeley, 1999; Rockwood, 2004). Elevation, rotation, and axial rotation of the clavicle are achieved through articulation at the sternoclavicular and acromioclavicular joints. The joints also allow for elevation and rotation of the scapula. The primary function of ligaments in the shoulder is to provide joint stability (Turkel, 1983; O'Connell, 1990; Seeley, 1999). If a moment is generated at the shoulder, it is not necessarily the case that a ligament is contributing to the generation of this moment (Figure 1). Instead, it has been well documented that ligaments become taut only at extreme ranges of motion (Pronk, 1993; Culham and Peat, 1993; Itoi, 2004). The specific function and anatomical details of seven shoulder ligaments with respect to joint stability maintenance are discussed further. The ligaments considered are the costoclavicular, trapezoid, conoid, coracohumeral, superior glenohumeral, middle glenohumeral, and inferior glenohumeral. They are discussed from proximal to distal locations in the shoulder mechanism.

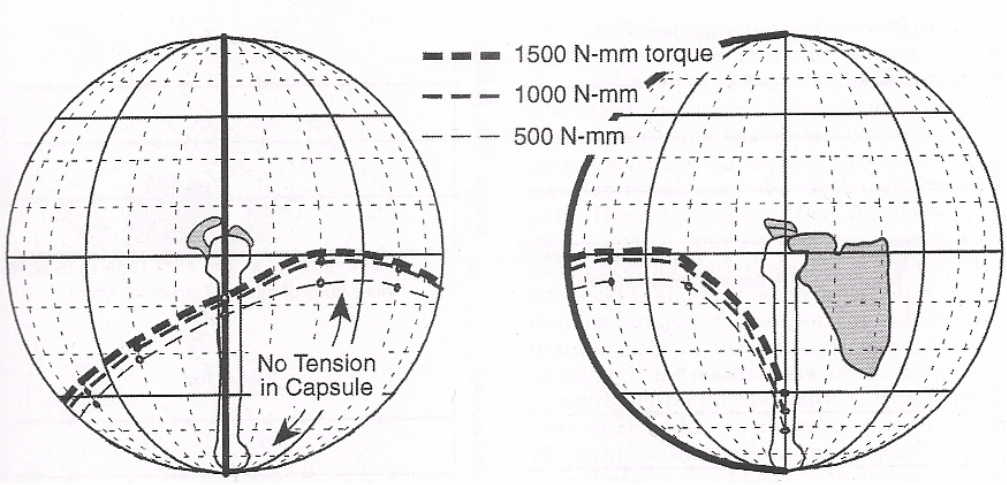

Figure 1: 3-dimensional illustration of shoulder torques that can be generated despite ligaments being lax. Left: lateral view. Right: Anterior view. (Frievalds, 2004)

2.2 Specific Ligament Function

2.2.1 Costoclavicular Ligament

The costoclavicular ligament (CCL) attaches the clavicle to the first rib, and functions to limit elevation of the clavicle and, in turn, the pectoral girdle (Cave, 1961; Pronk et al, 1993). Once a certain amount of elevation is achieved, the costoclavicular ligament serves as a fulcrum for clavicular rotation (Cave, 1961; Pronk 1993). While the costoclavicular ligament also helps resist anterior and posterior translation of the clavicle, its effect is insignificant when compared with the effects of other structures (Spencer et al, 2002).

2.2.2 Trapezoid and Conoid Ligaments

The trapezoid ligament (TRAP) and the conoid ligament (CON) combine to form the coracoclavicular ligament (Fukuda, 1986; Culham and Peat, 1993; Seeley, 1999). The trapezoid originates at the anterior portion of the

coracoid process and travels upwards to insert on the inferior surface of the clavicle (Fukuda, 1986; Culham and Peat, 1993). The conoid ligament originates posterior and medial to the trapezoid and inserts further medially on the clavicle (Fukuda, 1986; Culham and Peat, 1993). While both ligaments work to constrain the rotation and displacement of the clavicle, the conoid was shown to be more effective than the trapezoid in doing so (Fukuda, 1986). These ligaments have also been shown to become taut during scapular rotation (Itoi, 2004).

2.2.3 Coracohumeral Ligament

The coracohumeral ligament (CHL) originates at the base and lateral border of the coracoid process and travels laterally and inferiorly over the head of the humerus to insert at both humeral tuberosities (Neer, 1992; Culham and Peat, 1993; Itoi, 2004). The coracohumeral ligament is known to limit external rotation (Jerosch et al., 1990) and it also plays a prominent role in humeral suspension (Edelson, 1991).

2.2.4 Superior Glenohumeral Ligament

The superior glenohumeral ligament (SGHL) originates from the anterior rim of the glenoid and inserts on the head of the humerus, near the proximal tip of the lesser tuberosity (Culham and Peat, 1993; Itoi, 2004). When describing the origin of the glenohumeral ligaments, the glenoid is often referred to as a clock face (Figure 2), and the superior glenohumeral ligament

attaches at the one o'clock position (Steinbeck, 1998). The SGHL resists inferior translation of the humerus (O'Connell, 1990; Boardman, 1996) and maximum strain to this ligament occurs with the arm adducted and externally rotated (Itoi et al, 2004).

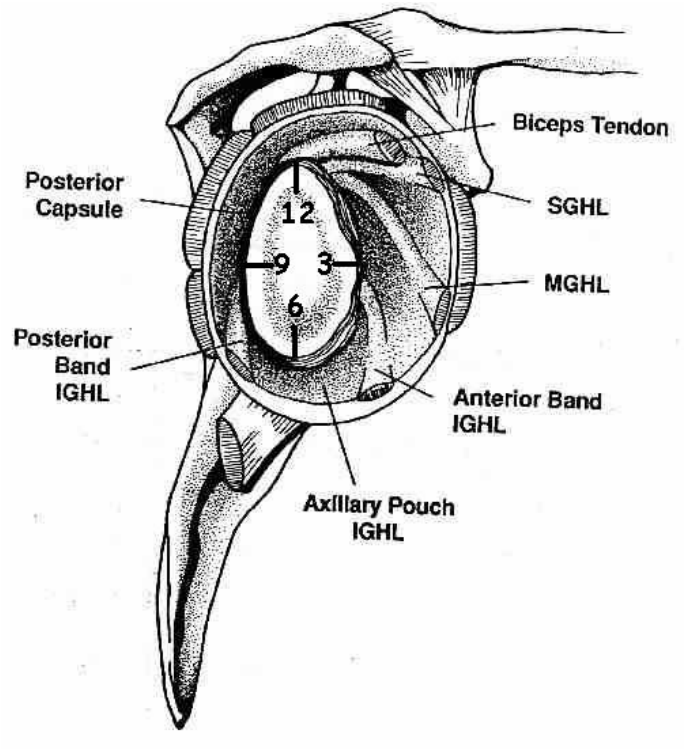

Figure 2: Lateral view of right glenoid fossa and insertions of glenohumeral ligaments (Culham and Peat, 1993). Hours of a clock face have been added to aid in locating insertion points of ligaments.

2.2.5 Middle Glenohumeral Ligament

The middle glenohumeral ligament (MGHL) originates between the one and three o'clock positions and attaches to the anterior aspect of the humerus, approximately 2cm medial to the insertion of the subscapularis (Culham and Peat, 1993; Steinbeck, 1998, Itoi, 2004). Turkel reported that at 45° of abduction the middle glenohumeral ligament are the main stabilizers of the

glenohumeral joint (Turkel, 1981). The MGHL becomes taut in movements where the shoulder is externally rotated and in an abducting position (Turkel, 1981).

2.2.6 Inferior Glenohumeral Ligament

The inferior glenohumeral ligament (IGHL) originates between three and eight o'clock and inserts on the anatomic neck of the humerus between the subscapularis and triceps (O'Brien, 1990; Steinbeck, 1998; Itoi, 2004). It is made up of three distinct bands; an anterior (IGHLA), an inferior (IGHLI), and a posterior (IGHLP) band (Turkel, 1981; Culham and Peat, 1993; Steinbeck, 1998). The inferior glenohumeral ligament is the primary stabilizer of the joint when the humerus is at 90° of abduction (Turkel, 1981). Furthermore, the inferior glenohumeral ligament is taut in abduction and external rotation (Itoi, 2004).

2.3 Recent History of Shoulder Muscle Force Prediction Models

Several attempts have been made by a number of research groups to create functional models of the shoulder. The two main types of muscle force prediction models are optimization-driven and EMG-driven. Optimization is a process in which predictions are calculated while a desired variable (i.e. energy) is minimized (Hogfors, 1987a, 1987b, 1991, 1995; Van der Helm 1992, 1994a, 1994b; Johnson, 1996; Dickerson, 2005). EMG-based models use measured EMG signals from a muscle to estimate the force produced by the muscle

(Wood, 1989; Laursen, 1998). Details regarding two of the more widely used shoulder models, the Gothenburg and Dutch models are discussed next.

2.3.1 Gothenburg Model

One of the earliest shoulder models developed is the Gothenburg model (Hogfors, 1987). This optimization-based model represents muscles as strings. Data obtained from three cadavers were used to estimate normalized origin and insertion points for each muscle (Hogfors, 1987). However, in this model it was assumed that ligament forces (excluding the CHL) could not produce moments about joints. Coordinates of the attachment sites of this ligament were provided; however, since the length at which the ligament becomes taut was unknown, the ligament was not included in the computation of any output variables, including muscle force. The coordinates for the conoid, trapezoid, and costoclavicular ligaments were also provided, but these ligaments were not incorporated into the model. Details for the insertion sites of the GH ligaments were not described for this model formulation.

The muscle force predictions of this model were evaluated by Karlsson and Peterson, and they found the predictions to be reflective of EMG in some postures (Karlsson and Peterson, 1992). However, they noted that their model could be improved with the inclusion of CH and GH ligaments (Karlsson and Peterson, 1992). Subsequent modeling work involving the costoclavicular, conoid, and trapezoid ligaments was performed by Pronk (1993) and Makhsous (1999). Details of these works are discussed below.

2.3.2 Dutch Shoulder Group

The parameters of the Dutch shoulder model are based on a data set presented by Veeger et al. (Veeger, 1991). These data were based on measurements made from the shoulders of seven cadaveric subjects. Included in this data set were anatomical and inertial properties of bones, attachment points of muscles and ligaments, and physiological cross sectional areas (PCSA) of muscles (Veeger, 1991).

These data were used to develop a finite-element model (FEM) of the shoulder. This model included three ligaments; the conoid, trapezoid, and costoclavicular ligaments (Van der Helm, 1994a). However, when a simulation was performed it was assumed that the conoid ligament was a rigid body instead of tensile (Van der Helm, 1994a). Furthermore, the researchers stated that the lack of stress/strain relationships and resting lengths of the ligaments prevented them from being able to accurately model these ligaments. It was proposed that their inclusion in the model would lead to high muscle force predictions and abnormal movements (Van der Helm, 1994a).

2.3.3 Other Models

Subsequent coordinate data and force prediction models have also failed to incorporate all the ligaments of the shoulder. Johnson et al. (1996) tried to produce a more accurate set of muscle anatomy using radiography and digitization, and dissection techniques. However, Johnson (1996) did not study any details of the shoulder ligaments, citing that the necessary data could be

found in Hogfors (1987). Laursen et al. (1998) developed an EMG-based model of the shoulder complex, but the impact of ligamentous structures was ignored. For the sake of simplicity it was assumed that external force would be linearly related to EMG amplitude.

2.4 Previous Attempts to Model Shoulder Ligaments

Very few attempts have been made at modeling the ligaments of the shoulder. Pronk et al. (1993) attempted to model the clavicular ligaments (costoclavicular, conoid, and trapezoid); however, a number of assumptions were made due to limitations that existed at the time. At the time, information on the stress/strain properties of the ligaments was unavailable. Attempts to model these ligaments were made using two approaches: 1) by treating the ligaments as rigid elements, and 2) by estimating the elastic material properties of ligament (Pronk et al., 1993). Simulations with the conoid as a rigid element reduced the load on the deltoid muscle when the humerus was abducted, but similar simulations with the trapezoid and costoclavicular ligaments were unsuccessful (Pronk et al., 1993). Estimation of the elastic material properties was done using an exponential equation relating stress of the ligament to the length of the ligament. The results of these simulations with elastic ligaments appeared to be qualitatively feasible, but their numerical accuracy could not be validated.

Makhsous (1999) attempted to incorporate the conoid and trapezoid ligaments into the Gothenburg model. Estimation of the material properties was

done in accordance with Pronk et al. (1993), but insertion points and lengths were based on a single cadaveric subject. A comparison with Laursen's EMG-based model showed improved similarity for many of the muscles measured. However, Makhsous used Laursen's experimental data, which were generated by subjects performing 43 isometric contractions in one standardized position (Laursen, 1998). The impact the ligaments had on the model in a full range of postures and scenarios was not provided.

Debski et al. (1999) estimated the forces in the GH ligaments by applying data collected in their lab to "Software for Interactive Musculoskeletal Modeling" (SIMM). Reference lengths for each of the GH ligaments were measured on ten cadaveric specimens, and tensile properties were obtained from Boardman (1996) and Bigliani (1992). Load-elongation relationships were defined using the stress-strain curve proposed by Bigliani (1992). However, the purpose of this model was to determine ligamentous contributions during anterior and posterior translation of the humerus. While his model suggested that the SGHL is the only taut ligament during forward flexion and extension, effects on muscle force levels were not discussed (Debski, 1999).

Detailed modeling techniques were used to model the glenohumeral ligaments by Novotny et al. (2000). The purpose of this model was to predict glenohumeral kinematics during the "cocking" phase of throwing as this posture has been shown to cause instability in the glenohumeral joint (Novotny et al., 2000). Useful ligament wrapping techniques specific to the glenohumeral ligaments are described in depth. However, as the investigation focused on GH

kinematics and not muscle force data, no information was available on muscle activation patterns.

Charlton (2006) proposed predicting ligament tensile properties by modeling the toe and linear regions of the stress-strain curve separately. He implemented the conoid ligament into the Newcastle shoulder model, but did not discuss the effects the changes had on muscle force predictions.

2.5 Dickerson Shoulder Model

The Dickerson shoulder model was initially conceived for primary use in ergonomic analyses and injury prevention (Dickerson, 2005 & 2006). The model includes four modules, including a muscle force prediction module. This optimization model uses several anatomical parameters and modeling concepts that are in concordance with the approaches of Hogfors (1987) and Van der Helm (1994). Muscles in the Dickerson model serve to achieve equilibrium with external moments while maintaining stability of the glenohumeral joint (Dickerson, 2007). As in all optimization models, an objective function is used to predict muscle forces. In the Dickerson model the objective function aims to minimize the sum of all cubed muscle forces (Equation 1).

$$\text{Objective Function} = \sum\left(F/_{CSA}\right)^3 \quad (1)$$

Where F is muscle force and CSA is muscle cross-sectional area. This cost function has been shown to better predict load sharing among agonist muscles compared to other functions (Herzog and Binding, 1993; Dickerson,

2007). However, it has been noted that optimization models typically under-predict antagonist activity.

While earlier models possessed much depth and detail, they lacked several distinguishing characteristics found only in the Dickerson model. These characteristics include: dynamic capability, anthropometric scalability, interfaces with modern job analysis software, and an improved shoulder rhythm formulation. Additionally, the Dickerson model has a unique glenohumeral stability constraint that is based on empirical shoulder dislocation data. Another advantageous feature of the model is the three-dimensional digital display of the musculoskeletal elements of the human shoulder. This display allows the user to visualize the postures and the movements of the body in space, including specific muscle paths.

However, as ligaments are usually only stressed at extreme postures, and since extreme postures are rarely seen in an ergonomic environment, ligaments were not included in the original version of this model (Dickerson, 2005). A primary goal of this work is to improve the model's ability to predict muscular activity in a wider range of potential postures. This improvement will expand the scope of application of the tool to include activities beyond midrange, common tasks.

2.6 Primary Contribution of the Work

The need and desire to include ligaments into shoulder models has been noted by the developers of several of these models (Karlsson and Peterson,

1992; Van der Helm, 1994a; Nieminen, 1995; Dickerson, 2005 & 2006). Seven shoulder ligaments, the costoclavicular, trapezoid, conoid, coracohumeral, superior glenohumeral, middle glenohumeral, and inferior glenohumeral, will be implemented as components to augment the Dickerson shoulder model. This study will add to the understanding of how and when ligaments contribute to maintain stability in the shoulder, and generate novel insights into primary shoulder function. Furthermore, a higher fidelity model should also provide more accurate muscle force predictions for different muscles in a wider range of scenarios. This information is integral for preventing musculoskeletal injuries to the shoulder region, as well as increasing the understanding of the mechanics of the shoulder complex.

III METHODOLOGY

3.1 Integrating Ligaments into the Biomechanical Shoulder Model

The following section explains the methods involved in integrating ligaments into the shoulder model. Two separate ligament models were created; one involving all 7 ligaments (AL model) and one involving only the ligaments crossing the glenohumeral joint (GH model). The GH model was of primary focus when comparing to the original no-ligament (NL) model.

3.1.1 Attachment Sites of Ligaments

To include the shoulder ligaments in a computational model, the precise location of the attachment sites of each ligament must be quantitatively specified. These data, combined with knowledge of shoulder structure and kinematics, allow for determination of ligament path and length throughout a movement and across postures. The origin and insertion points for the conoid, trapezoid, and costoclavicular ligaments were reported in previous studies (Van der Helm, 1994; Makhsous, 1999). These ligaments are geometrically defined in the current shoulder model, but do not appear in the cost function calculation, or any of the constraint equations in the optimization solution. The reason for their exclusion is that the model was originally implemented for analysis of midrange postures, and ligaments are most active in extreme ranges of movement (Dickerson, 2005). In our model, the coracohumeral ligament will originate at the lateral aspect of the coracoid process, and insert into the rotator

interval between the supraspinatus and subscapularis tendons (Neer, 1992). The exact coordinates of these attachment sites are provided by Hogfors (1987) and are listed in Table 1.

Table 1: Locations of attachments sites of the coracohumeral ligament in their respective coordinate systems (Hogfors, 1987).

Site	x-coordinate	y-coordinate	z-coordinate
Origin	$80 \times 10^{-3} s$	$80 \times 10^{-3} s$	$260 \times 10^{-3} s$
Insertion	$-35 \times 10^{-3} h$	$50 \times 10^{-3} h$	$53 \times 10^{-3} h$

As previously mentioned, the origins of the glenohumeral ligaments are often described by using a clock face as a reference system (Figure 2). Unfortunately, specific data for locally-defined insertion points are not reported in the literature, and thus these clock face-based descriptions must be used for ligament insertion point placement in our revised model. The SGHL originates from the one o'clock position on the glenoid and insert on the humerus near the proximal tip of the lesser tuberosity (Steinbeck, 1998; Itoi, 2004). The MGHL originates between one and three o'clock and inserts on the lesser tuberosity of the humerus (Steinbeck, 1998; Itoi, 2004). The origin of the IGHL capsule ranges from three o'clock to eight o'clock and inserts on the inferior margin of the neck of the humerus (Steinbeck, 1998; Itoi, 2004). As mentioned, exact coordinates are not provided in prior studies. Thus, the coordinates on the scapula and humerus will be estimated. To do so, it was assumed that each ligament originated on the lateral rim of the glenoid fossa, a scapular structure that was already geometrically defined in the model.

Distinguishing the lateral rim allowed definition of a glenoid coordinate system. Assuming a right shoulder, the positive z-axis traveled from the most

inferior point on the rim to the most superior point on the rim. The positive y-axis ran posterior to anterior through the midpoint of the z-distance. The x-axis was orthogonal to these two axes and ran positively in the medial direction. As indicated in Figure 3. The point [0, 0, 0] was assumed to be the middle of the glenoid. The clock-face locations were converted into angular locations; every hour was equivalent to 30°. In the z-y plane, vectors from the centre of the plane to the lateral rim were used to determine glenohumeral ligament insertion coordinates.

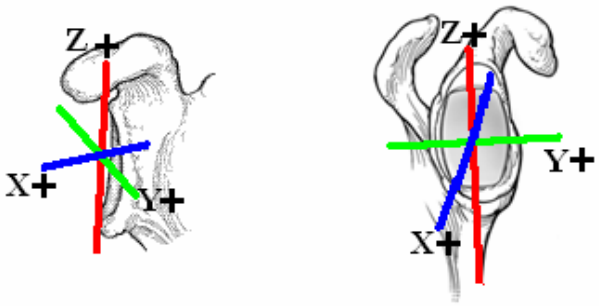

Figure 3: Anterior (left) and lateral views (right) of the glenoid coordinate system.

3.1.2 Reference Lengths of Ligaments

To measure the amount of force present in a given ligament, the length at which the ligament becomes taut, or "reference length", was used. This length should not be confused with "resting length" which is defined as the length of the ligament when the body is at rest in anatomical position. Many of these values have been determined experimentally (Table 2). Reference lengths of the costoclavicular and the coracohumeral ligaments were estimated using

the reference lengths of the coracoclavicular and glenohumeral ligaments, respectively.

Table 2: Reference lengths (mm) and cross sectional areas (mm2) for each ligament modeled using data from Bigliani (1992), Pronk (1993), Debski (1999), and Costic (2003).

Ligament	CCL	CON	TRAP	CHL	SGHL	MGHL	IGHLA	IGHLI	IGHLP
Ref. Length	10.4*	11.2± 4.1	9.6± 4.4	44.7*	44.1± 2.9	49.4± 8.1	41.3±4.5	39.8±5.6	41.0±4.2
LCSA	33.96	48.5	106.5	53.7	18	20	37.2	*18.5	18.5

* Not available from literature. Best estimate was made given available data.

After determining the reference lengths, a convention to calculate the amount of force generated by ligament length changes was required. This estimation necessitated the definition of ligament-specific tensile properties. For some ligaments, complete data were available in the literature allowing for modeling of the ligament as an inelastic element (Bigliani, 1992; Debski, 1999). For other ligaments only the stiffness of the ligament during the linear phase of the stress-strain curve was available (Boardman, 1996). Due to this limitation these ligaments were be modeled using a general equation for the stress-strain relation of elastic materials (Pronk, 1993; Makhsous, 1999). Knowledge of the relationship between the stress and strain in a ligament allowed us to determine the amount of tension in a ligament at any length. A viscoelastic muscle model was presented by Winters and Stark (1985), and this model was then modified by Pronk (1993) to apply to ligaments:

$$F_{max} = \sigma_{max} \times LCA \quad (2)$$

$$LE_1 = F_{max}/[\exp(LE_{sh})-1] \quad (3)$$

$$LE_2 = \exp(LE_{sh}/LE_{xm}) \quad (4)$$

$$F = LE_1 \times (LE_2^{\,l/lo-1} - 1) \quad (5)$$

Where F is the ligament force, F_{max} is the force at the maximum possible strain of the ligament, σ_{max} is the maximum ligament stress, LCA is the ligament cross sectional area (Table 2), *l* is the ligament length, *lo* is reference length, LE_{xm} is the maximum ligament length, LE_{sh} is the shape parameter for the curve, and LE_1 and LE_2 are material parameters (Winters and Stark, 1985; Pronk, 1993; Makhsous, 1999). Maximum ligament stress (σ_{max}) was assumed to be 5MPa (Bigliani, 1992; Makhsous, 1999). A shape parameter of 3 was used, in accordance with Pronk (1993) and Makhsous (1999). A typical stress-strain curve using the proposed equation is seen in Figure 4. No force is produced when ligament strain was below the reference length. Maximum strain was assumed to be 40% of reference length (Pronk, 1993, Makhsous, 1999). If a ligament exceeded this length its force was constrained to its maximum value (F_{max}).

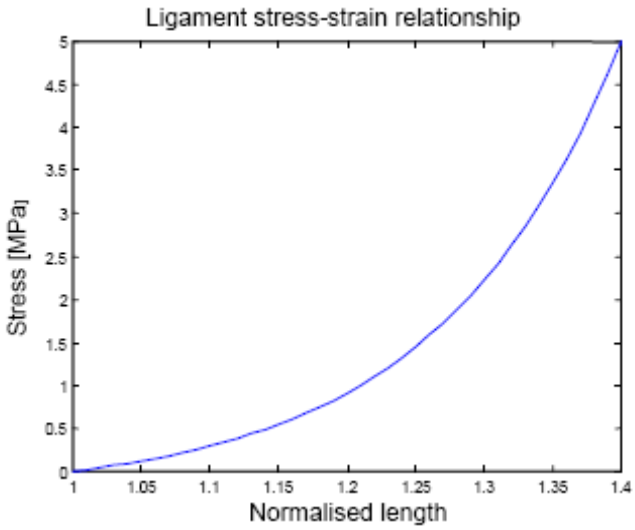

Figure 4: Typical stress-strain relationship for a ligament derived using equation 3 (adapted from Makhsous, 1999).

3.1.3 Single Lines of Action vs. Wrapping

The conoid, trapezoid, and costoclavicular ligaments do not travel around any objects from origin to insertion and thus were modeled as direct origin-to-insertion lines of actions (Culham and Peat, 1993; Pronk, 1993; Makhsous, 1999). The coracohumeral ligament and elements of the glenohumeral ligaments, however, travel around the head of the humerus, and thus are not adequately described linearly. These ligaments were modeled using previously developed geodesic line-of-action wrapping techniques (Hogfors, 1987; Van der Helm, 1994; Novotny, 2000; Charlton, 2001; Dickerson, 2005).

3.2 Experimentation

3.2.1 Subject Pool

Ten participants, five males and five females (mean age = 23.9, height = 175.9cm, weight = 72.9kg), were recruited from the University of Waterloo population. Each subject was free of shoulder discomfort and shoulder injury within the previous six months. Subjects who had experienced a shoulder injury that resulted in potential structural deformations (i.e. broken clavicle) were omitted from this study. Subjects' ranges of shoulder motion were in agreement with published standards (Table 3, Boone, 1979., Murray, 1985). The study was approved by the Office of Research Ethics at the University of Waterloo.

Table 3: Average (±SD) range of motion (in degrees) of the arm for ten subjects in seven directions. Data is also separated by gender and compared against published values (Murray, 1985).

	ALL	M	MURRAY M	F	MURRAY F
No. of Subjects	10.0	5.0	20.0	5.0	20.0
Abduction	171.1 ± 14/1	163.4 ± 16.5	178.0 ± 1.0	178.8 ± 5.0	180.0 ± 1.0
Extension	68.8 ± 12.9	65.2 ± 12.2	57.0 ± 3.0	72.4 ± 13.9	58.0 ± 3.0
Flexion	163.1 ± 11.2	158.8 ± 10.7	170.0 ± 2.0	167.4 ± 11.1	172.0 ± 1.0
Internal Rotation	62.1 ± 11.1	59.0 ± 11.0	49.0 ± 3.0	65.2 ± 11.4	53.0 ± 3.0
External Rotation	102.0 ± 12.0	98.8 ± 16.5	94.0 ± 2.0	105.2 ± 5.1	101.0 ± 2.0
Horiz. Adduction	48.5 ± 9.0	47.8 ± 9.9	NA	49.4 ± 9.2	NA
Horiz. Abduction	108.5 ± 10.2	102.2 ± 9.9	122.0 ± 2.0	114.8± 6.1	129.0 ± 2.0

3.2.2 Maximal Voluntary Contraction and Range of Motion Normalization

Prior to performing the movement tasks, subjects performed a set of maximal voluntary contractions (MVCs), which were used to normalize EMG signals. Arm positions and movements recommended in Cram and Kasman (1998) were used to elicit MVCs. Two MVCs were performed for each muscle site with at least two minutes between contractions.

To normalize postures, subjects were asked to demonstrate their maximum voluntary range of motion for each of the seven arm movements discussed below (Table 4). These ranges of motion were reached without aid of the experimenter. Measurement of the arm angle in each range of motion was done by the experimenter with the use of a goniometer. Though not a clinician, the experimenter had experience measuring arm angles with a goniometer.

3.2.3 Experimental Postures

Four sets of postural ranges were tested. These ranges were chosen to create ligament tension according to the literature. An illustration of the anatomical planes used to define arm postures is shown in Figure 5.

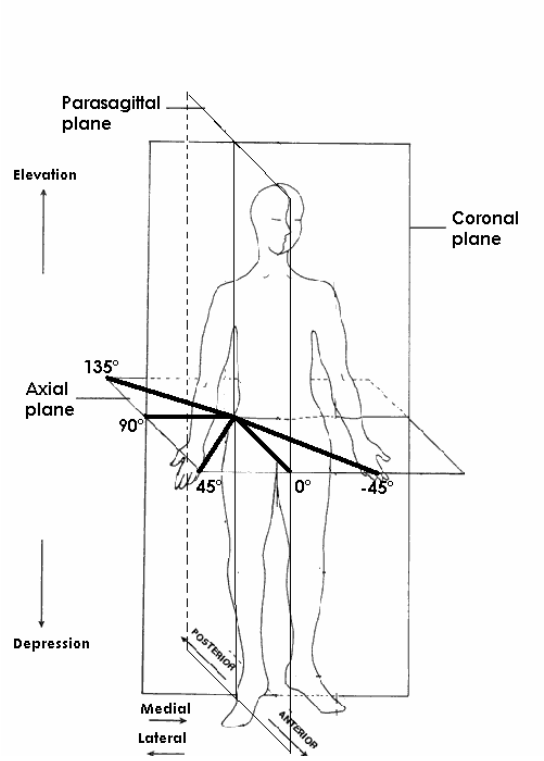

Figure 5: Anatomical planes of human body used to define arm postures.

In total, 56 experimental posture-force combinations were tested in this study (a list is given in Appendix A, page 86). These combinations were distributed unequally across four different ranges of motion. The first set of postures was abduction of the arm at seven different angles (Figure 6a) with the elbow fully extended.

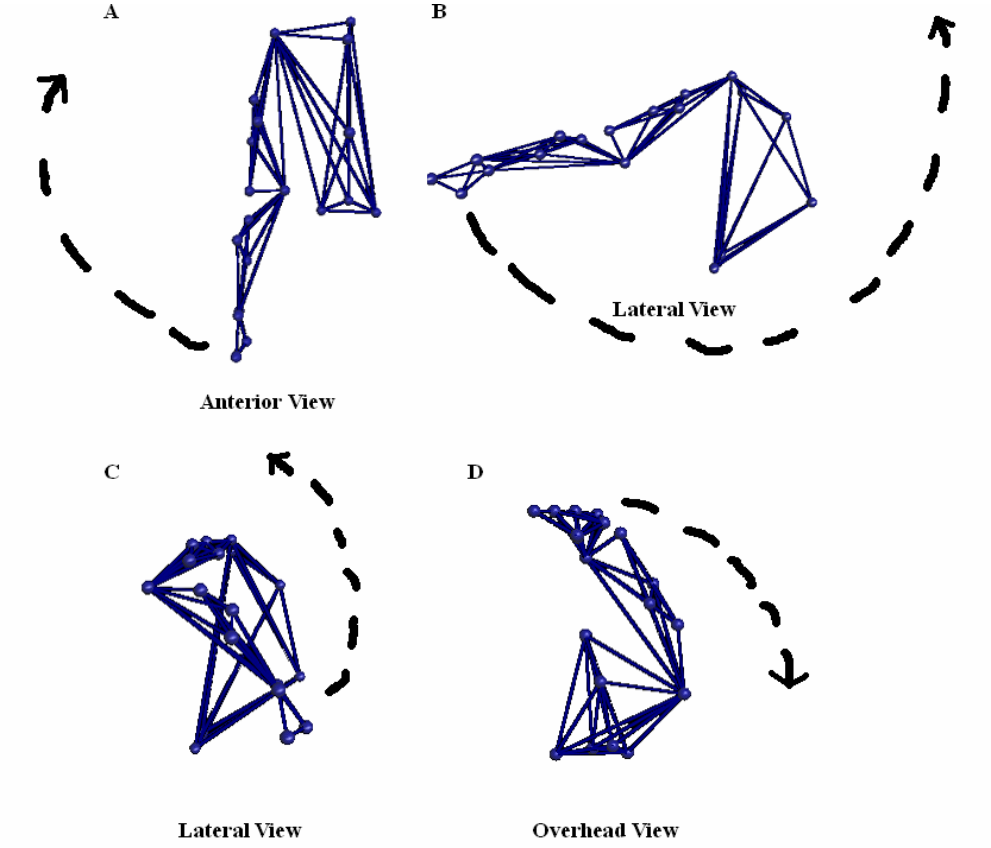

Figure 6: Illustration of arm movements about the shoulder. a) Abduction, from anterior view; b) flexion, from lateral view; c) external rotation d) horizontal abduction, from overhead view.

The next set consisted of nine different postures of flexion ranging from maximal extension to maximal flexion with a straight arm (Figure 6b). These two ranges of motion were expected to cause the costoclavicular, the inferior glenohumeral, and coracoclavicular ligaments to become taut and generate force. The third set involved seven different postures of internal and external rotation (Figure 6c). Internal-external rotation postures were performed with the arm abducted to 90° and the elbow flexed to 90°. The final five postures involved flexing the arm to 90°, flexing the elbow to 90°, and ranged in the horizontal abduction (parallel to the axial plane) (Figure 6d). The internal-

external rotation and horizontal ab/adduction postures were used to engage the CHL and GH ligaments. All postures are summarized in Table 4.

Table 4: Arm movements and final postures for experimental trials.

Plane of Elevation	Range of Elevation (% of MVROM)	Hor Ab/Ext Rotation	Elbow Angle	Direction of Force	Ligaments Involved	# of Trials
Abduction/ Coronal Plane	0%-100%, every 17%.	None	5°	Abduction/ Adduction	TRAP,CON, CCL, IGHL	7
Flexion/ Parasagittal Plane	Max extension (0%)- Max flexion (100%), every 12.5%	None	5°	Flexion/ Extension	TRAP,CON, CCL,SGHL	9
Abduction	90°	Max Int.Rot (0%) – Max Ext.Rot (100%), every 33%	90°	Internal/ External Rotation	CHL, AGHL, MGHL, IGHL	7
Flexion	90	Max Hor Ad (0%) – Max Hor Ab (100%)	90	Horizontal Abduction/ Adduction	MGHL,	5

3.2.4 Force Exertion Task

In randomized order, subjects assumed one of the 28 postures, while producing a "comfortable" level of force, in one of two directions. This procedure yielded 56 posture-force combinations. Forces were exerted against a uniaxial force transducer being held perpendicular to the hand by an experimenter. Subjects were seated upright with their arm at their side, and were instructed by the experimenter as to how to attain the given posture. For example, if the posture required the hand to be directly above the shoulder, the subject was asked to either flex or abduct to said position. Correct arm angles and positions were ensured by the use of a goniometer by the experimenter who measured the range of motion. The subject then pushed against the force transducer in this posture for six seconds while EMG and motion tracking data were synchronously collected. Force outputs were monitored on an external

digital display that provided the subject with instantaneous feedback to help maintain a constant level of force production (Figure 7). The subject was then allowed to relax before assuming the next posture. A minimum of one minute of rest was given between trials.

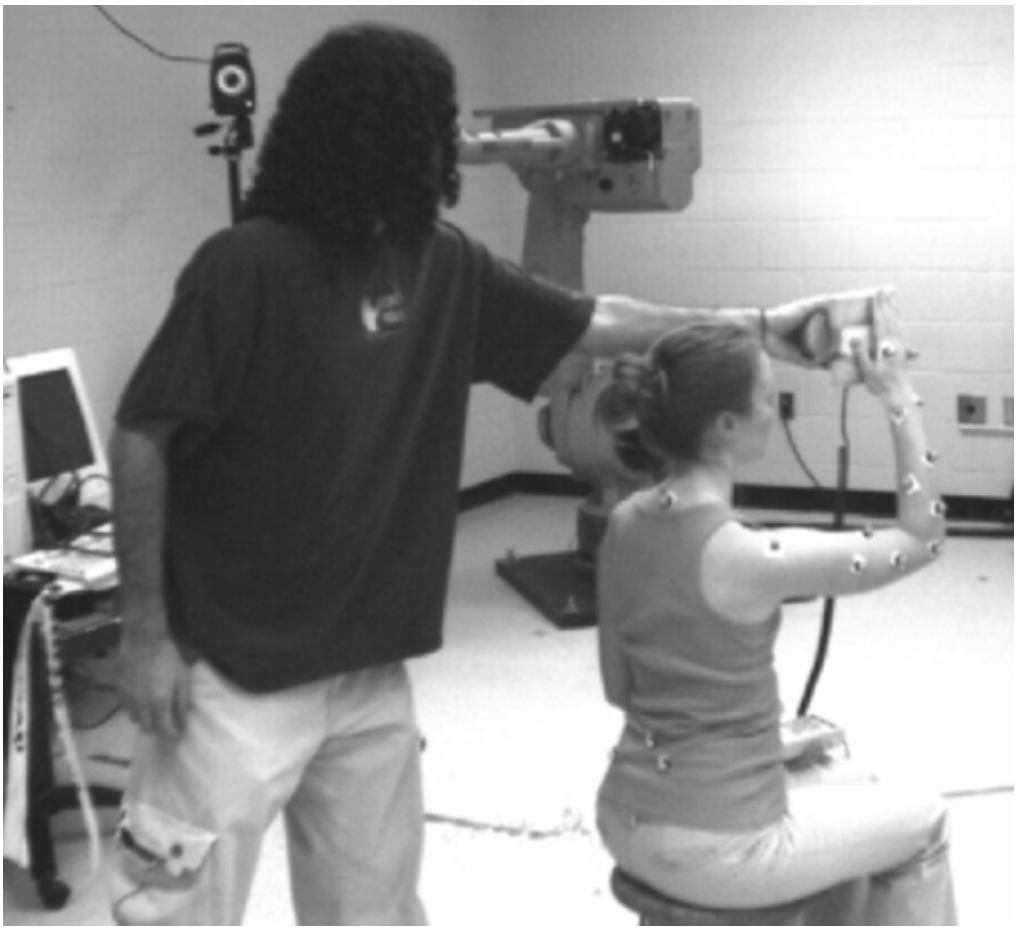

Figure 7: Photo of experimental trial. Subject is horizontally adducting against force transducer held by experimenter. Digital display in left hand was used to help maintain constant force. Direction of force was assumed to be perpendicular to the palm of the hand.

3.2.5 EMG Recording and Processing

Electromyographic signals were collected from 11 sites (Table 5) using a 16 channel Noraxon EMG system throughout the experimental protocol. Disposable Noraxon EMG electrodes were used and placed in accordance with standard descriptions (Cram and Kasman, 1998).,Raw EMG signals were filtered with a bandpass ranging from 10-500Hz and sampled at 1500 Hz due to the default settings of the hardware. and The data were converted from analog to digital form using a 16-bit card (Noraxon) and stored on a laboratory computer. All EMG data were linear enveloped using a single pass of a second order, lowpass Butterworth filter with a 2.5Hz cut off frequency. Processed data were subsequently normalized to 100% MVC using data from the maximal trials. Once the EMG data had been normalized, a two second window during the static phase was averaged and used for comparison to the muscle force prediction of the model (Seen in "Statistical Analysis")

Table 5: Muscle sites and electrode placements to be used for EMG collection (Cram and Kasman, 1998)

Muscle	Electrode Position
Latissimus Dorsi	Approximately 4 cm below inferior scapular tip, halfway between spine and lateral torso edge
Pectoralis Major, Sternal Insertion	Approximately 2 cm medial from axillary fold, horizontal
Pectoralis Major, Clavicular Insertion	2 cm below the clavicle, medial to axillary fold and at an oblique angle towards the clavicle
Upper Trapezius	Parallel to muscle fibers, along shoulder ridge, halfway between seventh cervical vertebra and acromion
Lower Trapezius	Approximately 5 cm below scapular spine, on medial edge, at 55-degree oblique angle, immediately lateral to spine
Middle Deltoid	On the lateral aspect of the arm, approximately 3 cm below the acromion, parallel to muscle fibers
Posterior Deltoid	Approximately 2 cm below the scapular spine, parallel to the muscle fibers at an oblique angle to the arm
Anterior Deltoid	Approximately 4 cm below the clavicle parallel to muscle fibers on the anterior aspect of the arm
Infraspinatus	Parallel to scapular spine, approximately 4 cm below and on the lateral aspect
Biceps Brachii	Parallel to muscle fibers and in the center of the muscle belly
Triceps Brachii, Long Head	Approximately 2 cm medial to arm midline, approximately halfway between acromion and olecranon

3.2.6 3-Dimensional Motion Tracking

Motion tracking of the upper limb and torso was done using eight Vicon MX20 cameras at a sampling rate at 50Hz. Digital re-creation of the segments was done using Vicon Nexus software. Reflective markers were placed unilaterally at specified bony landmarks on the hand, forearm, arm, and torso (Table 6, Figure 8).

Table 6: Marker names and locations used for digital reconstruction.

Marker Name	Location
C7/T1	Protuberance of 7th cervical vertebrae
L5/S1	Joint of 5th lumbar and 1st sacral vertebrae
LPSIS	Left posterior inferior iliac spine
RPSIS	Right posterior inferior iliac spine
SS	Suprasternal notch
XP	Xiphoid process
ACR	Flat side of right acromion process
A1	1st arm marker; non co-linear to A2 and A3
A2	2nd arm marker; non co-linear to A1 and A3
A3	3rd arm marker; non co-linear to A1 and A2
ME	Medial Epicondyle
LE	Lateral Epicondyle
FA1	1st forearm marker; non co-linear to FA2 and FA3
FA2	2nd forearm marker; non co-linear to FA1 and FA3
FA3	3rd forearm marker; non co-linear to FA1 and FA2
US	Ulnar Styloid
RS	Radial Styloid
MCP5	5th metacarpal
MCP2	2nd metacarpal

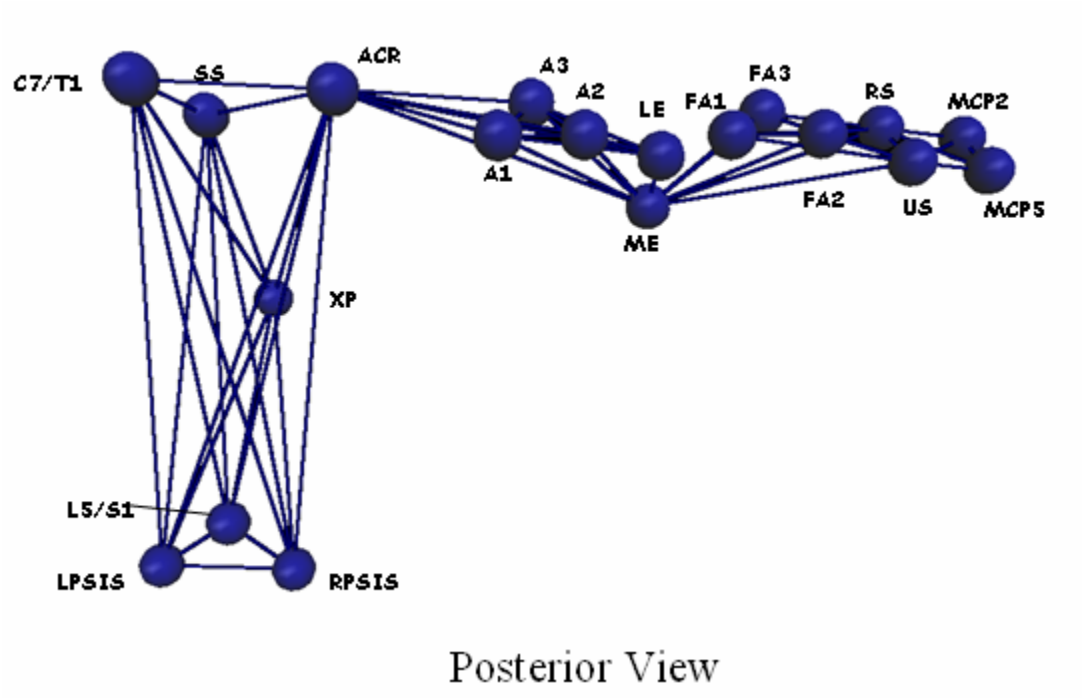

Figure 8: 3-D reconstruction of marker arrangement. Labels correspond with anatomical locations specified in Table 6. Lines connecting markers indicate that those markers are on the same segment.

Markers were placed at either end of the segment, and at least one other was placed non-co-linearly in between. These markers created a plane for each segment which allowed for the determination of segment lengths and joint centres. Motion data were filtered using a 2nd order dual pass Butterworth filter with a cut off frequency of 6Hz prior to inputting it in the model. Full marker setup and an image of the 3D reconstruction can be seen in Figure 9.

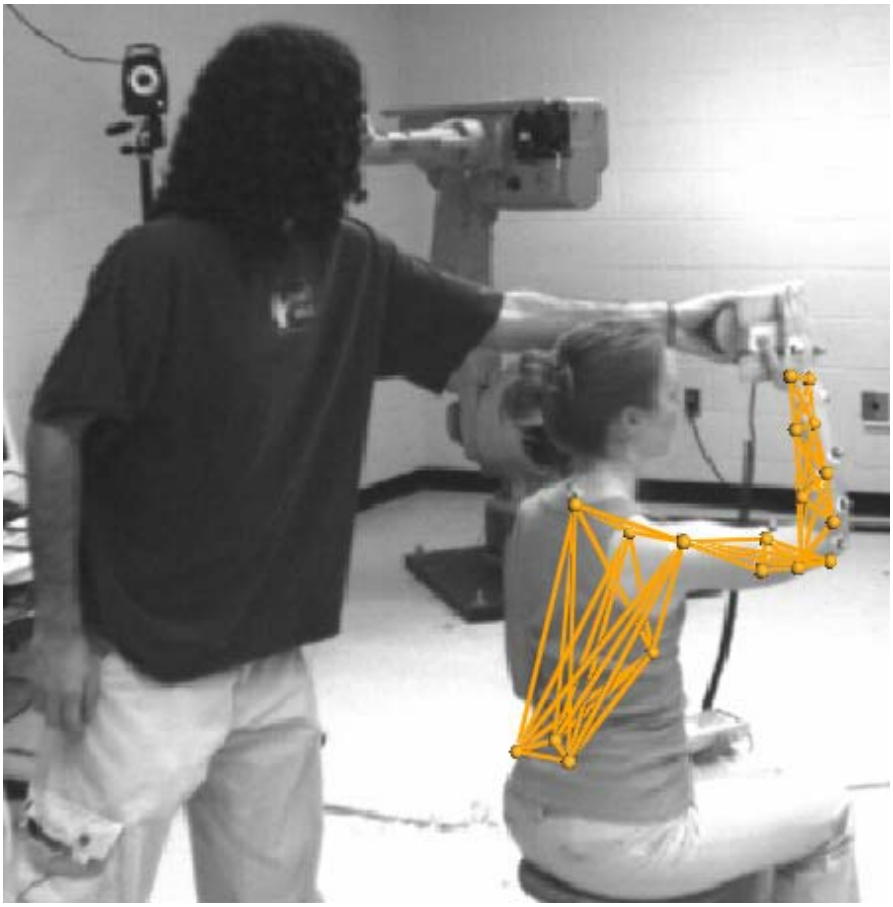

Figure 9: 3-D reconstruction of marker placement and segments overlaid on subject.

3.2.7 Mathematical Shoulder Model Inputs and Outputs

Joint centre coordinates were calculated from the marker data and were put into the model to recreate subject postures using a technique developed by Nussbaum and Zhang (2001). The other input of the model was force acting at the hand, which was assumed to be acting perpendicularly to the palm of the hand. The palm of the hand was defined as the plane created by the MCP2, MCP5, and US markers. The equilibrium constraints of the model attempts to achieve segmental translational and rotational equilibrium by counteracting external moments at the shoulder by generating forces in a combination of muscles. The external moment is derived by a combination of hand force and the force of gravity acting on the arm in a static situation. It is expected that the equilibrium constraints will be affected by the addition of ligaments, as ligaments produce forces that will create additional moments at the shoulder. The moments created by the ligaments can act to cause either higher or lower muscle activations to be needed to achieve equilibrium. The optimization routine is driven by the cost function (Equation 1), which minimizes the sum of all muscle stresses cubed while satisfying equilibrium and stability constraints. Ligaments do not appear in the cost function and therefore their addition will not affect the means by which an optimal solution is determined.

When an optimal solution was found by the model, force predictions were generated for each of the 38 muscles elements. If a solution could not be found for a particular trial, that trial was not used in the statistical analysis. The model

also calculated ligament lengths (total distance between origin and insertion of a ligament) and ligament forces (Equation 5).

3.2.8 Statistical Analysis

Predicted muscle force was compared against EMG amplitude for each of the 11 muscles at the 56 different postures. A correlation coefficient between the predicted force and EMG amplitude was determined for each muscle. A correlation of 1.0 indicates a perfect relationship, while 0 indicates no relationship at all. Coefficients were calculated for each muscle using muscle force predictions from the model before and after ligament implementation. A dependent t-test was used to compare the differences in correlation coefficients for each muscle between the 'old' and 'new' models. The slope of each regression line was also calculated and compared with a dependent t-test to assess any changes in the relationship between EMG amplitude and MFP between the two models. These t-tests were both two-tailed, with alpha = 0.05. To further evaluate the effects of the ligament additions, the number of zero muscle force predictions were counted and compared for each muscle between the two models. A zero-force was defined as any occurrence where normalized MFP was less than 1%. This comparison was also done with a two tailed t-test, but an alpha level of 0.01 was used to ensure differences were significant. The three variables used for comparison are shown diagrammatically in Figure 10.

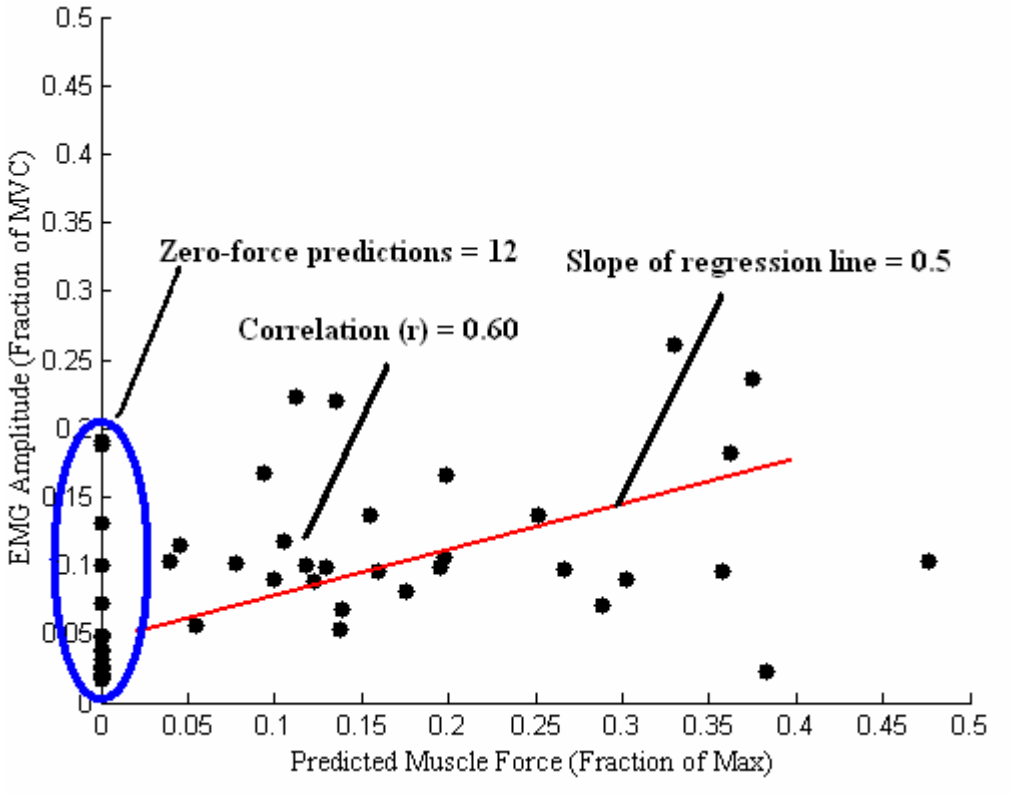

Figure 10: Scatterplot showing typical relationship between EMG amplitude and predicted muscle force. The three variables being used for comparison (correlations, slope, and zero-force count) are labeled accordingly.

Since ligaments become most engaged in extreme postures differences in correlation coefficient between extreme and non-extreme postures will be analyzed. McAtnamey (1993) has highlighted the risks of flexion angles greater than 90°, and Janwantanakul (2001) treated postures equal to 90% max ROM as extreme. Using these guidelines, all maximal ranges of motion were deemed extreme. Furthermore, the three most flexed and abducted postures were also treated as "extreme" as they were often greater than 90°. These postures are summarized in Table 7.

Table 7: List of postures deemed "extreme" and "non-extreme"

	Extreme	**Non-Extreme**
Postures	5, 6, 7, 8, 14, 15, 16, 17, 23, 24, 28, 33, 34, 35, 36, 42, 43, 44, 45, 51, 52, 56	1, 2, 3, 4, 9, 10, 11, 12, 13, 18, 19, 20, 21, 22, 25, 26, 27, 29, 30, 31, 32, 33, 37, 38, 39, 40, 41, 46, 47, 48, 49, 50, 53, 54, 55

IV RESULTS

Ligament length, force, and predicted muscle force were computed with all three versions of the model. Specific characteristics for individual ligaments are noted, but only the effects of GH ligaments on muscle force predictions were analyzed.

4.1 Non-convergence Rate of Models

The model was unable to find a feasible solution (converge) for some combinations of posture and hand force. For the three versions of the model, No Ligaments (NL) included, All Ligaments (AL) included, and only Glenohumeral Ligaments (GHL) included, the number of non-converging trials is summarized in Table 8. Detailed results of non-convergence are presented in Appendix C (page 88).

Table 8: Summary of incidences of non-convergence of the No Ligament (NL), Glenohumeral Ligament (GHL), and All Ligament (AL) models.

	No Ligament	GH Ligaments	All Ligaments
S1	0	4	6
S2	5	7	18
S3	1	3	11
S4	1	1	4
S5	4	4	9
S6	0	0	3
S7	2	3	7
S8	1	3	23
S9	0	2	8
S10	0	0	5
Total	14	27	94
Percentage	2.5	4.82	16.8

Due to the large number of non-convergent trials in the AL model only the GH model was compared to the original NL model.

4.2 Ligament Length and Force

Ligament lengths and ligament forces were calculated by the model in each posture using the described methods. Ligament length was modeled to be completely posture dependent as was ligament force. Average length of each ligament as a function of posture is shown in Figure 11, and shows how length increases throughout specific ranges of motion. A similar trend is seen in a plot of force vs. posture for all ligaments (Figure 12). However, it is important to note that force is only generated at lengths exceeding the reference length. Data for individual subjects can be found in Appendices D and E (page 89, page 99).

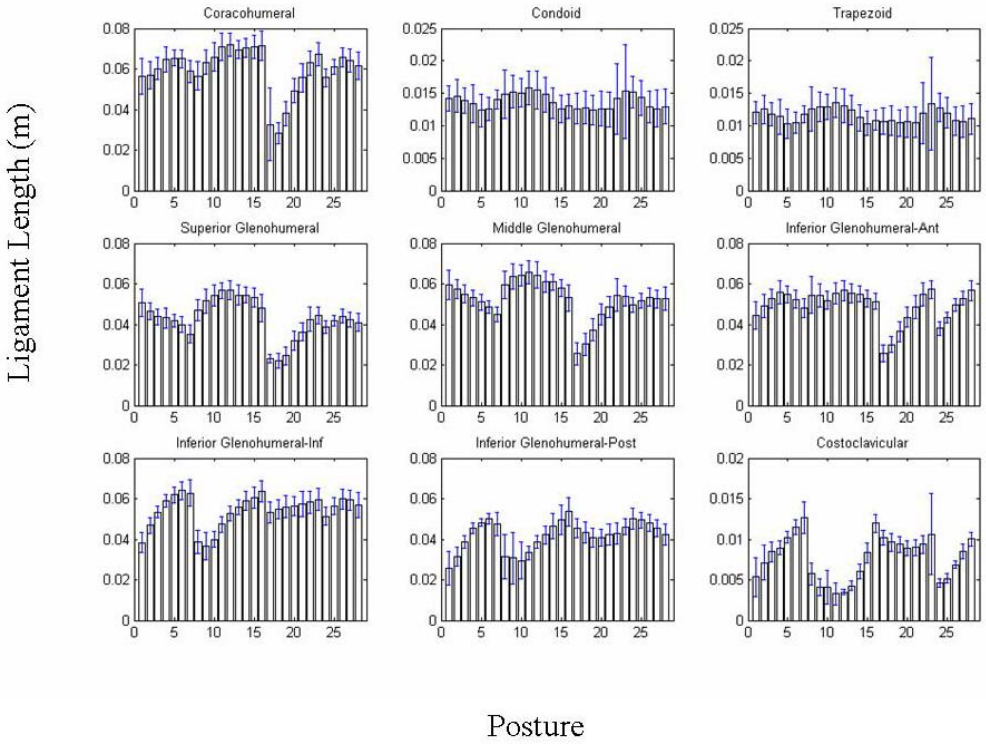

Figure 11: Average subject's ligament length across 28 experimental postures. Postures 1-7: Abduction; Postures 8-16: Extension-Flexion; Postures 17-23: Internal/External rotation; Postures 24-28: Horizontal Ad/Abduction. Note that postures 1-28 are the same as 29-56. To show all 56 postures would be redundant.

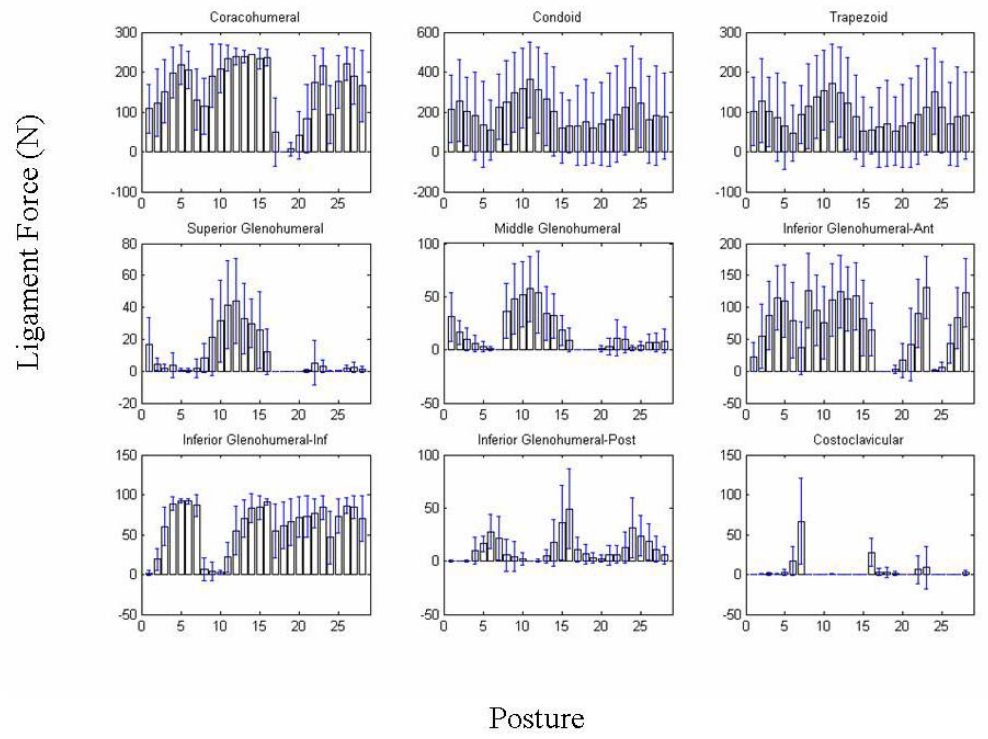

Figure 12: Average subject's ligament force across 28 experimental postures. Postures 1-7: Abduction; Postures 8-16: Extension-Flexion; Postures 17-23: Internal/External rotation; Postures 24-28: Horizontal Ad/Abduction. Note that postures 1-28 are the same as 29-56.

In several cases maximum producible ligament force was predicted by the model. Maximum force values as determined by maximum strain were found to range from 90N to 532.5N (Table 9).

Table 9: Maximum force values as determined by maximum strain (140% reference length).

Ligament	CCL	CON	TRAP	CHL	SGHL	MGHL	IGHLA	IGHLI	IGHLP
Max Force(N)	169.8	532.5	268.5	244.75	90	100	186	92.5	92.5

4.3 Effects of Ligaments on Muscle Force Prediction Model

4.3.1 Effect on Correlation Coefficients

Normalized MFP values were correlated with experimental normalized EMG values. The resulting coefficients were used to help evaluate model performance. Normalized MFP values across all trials correlated poorly with

EMG for most muscles. Strongest correlations were seen in the lower trapezius and infraspinatus muscles (both significant, $p<0.01$), while poorest correlations were seen in the upper trapezius and triceps muscles (Table 10 and Table 11).

Table 10: Pearson r correlation coefficients showing relationship between EMG amplitude and predicted muscle force for No-Ligament model. The lower trap and infraspinatus muscles showed significant correlations.

	Lat. Dorsi	Pec Stern	Pec Clav	Upper Trap	Lower Trap	Mid Delt	Post Delt	Ant Delt	Infra	Biceps	Triceps
S1	0.34	0.25	0.07	-0.33	**0.39**	0.29	0.16	0.28	**0.62**	0.26	-0.20
S2	0.05	0.38	-0.17	-0.21	**0.64**	0.33	0.18	0.11	**0.48**	0.01	-0.13
S3	0.26	0.23	0.27	-0.26	**0.71**	0.00	0.03	0.29	**0.63**	-0.22	-0.17
S4	0.22	0.42	-0.01	0.43	**0.57**	0.06	0.11	0.29	**0.68**	0.18	0.18
S5	0.04	0.03	0.15	-0.30	**0.27**	0.00	0.17	0.18	**0.47**	-0.12	-0.18
S6	-0.20	0.10	-0.10	0.06	**0.20**	0.18	0.40	0.26	**0.40**	0.00	-0.21
S7	0.03	0.37	0.33	-0.13	**0.43**	0.11	0.04	0.34	**0.62**	0.17	-0.18
S8	0.07	0.05	0.13	-0.04	**0.42**	0.10	0.27	0.06	**0.66**	0.07	0.01
S9	0.21	0.04	-0.11	-0.17	**0.29**	0.33	0.40	0.16	**0.47**	0.07	-0.14
S10	0.11	0.05	0.05	-0.19	**0.31**	-0.01	0.01	0.04	**0.46**	-0.13	-0.18
AVG	**0.11**	**0.19**	**0.06**	**-0.12**	**0.42***	**0.14**	**0.18**	**0.20**	**0.55***	**0.03**	**-0.12**
SD	**0.15**	**0.16**	**0.16**	**0.22**	**0.17**	**0.14**	**0.14**	**0.11**	**0.10**	**0.15**	**0.12**

Table 11: Pearson r correlation coefficients showing relationship between EMG amplitude and predicted muscle force for Glenohumeral-Ligament model. The lower trap and infraspinatus muscles showed significant correlations.

	Lat. Dorsi	Pec Stern	Pec Clav	Upper Trap	Lower Trap	Mid Delt	Post Delt	Ant Delt	Infra	Biceps	Triceps
S1	0.06	0.06	0.00	-0.33	**0.60**	0.47	0.02	0.37	**0.68**	0.47	-0.12
S2	0.08	0.16	0.08	0.00	**0.46**	0.24	0.07	0.27	**0.62**	0.36	-0.27
S3	0.13	0.06	0.33	-0.23	**0.76**	0.15	0.07	0.30	**0.71**	0.10	-0.08
S4	0.18	0.31	-0.03	0.33	**0.52**	0.08	0.09	0.21	**0.56**	0.26	0.11
S5	0.07	0.01	0.19	-0.31	**0.23**	0.08	0.07	0.03	**0.36**	0.05	-0.13
S6	-0.16	0.05	-0.05	0.04	**0.39**	0.20	0.35	-0.09	**0.21**	0.10	-0.01
S7	0.00	0.32	0.28	-0.04	**0.42**	0.15	-0.15	0.28	**0.46**	0.17	-0.04
S8	0.09	-0.14	0.21	0.02	**0.04**	0.16	0.25	0.28	**0.41**	0.15	-0.04
S9	0.07	0.08	-0.02	-0.11	**0.15**	0.24	0.20	-0.10	**0.05**	0.14	0.08
S10	-0.06	-0.07	0.04	-0.15	**0.34**	0.01	0.10	-0.01	**0.61**	-0.04	-0.15
AVG	**0.05**	**0.08**	**0.10**	**-0.08**	**0.39***	**0.18**	**0.11**	**0.15**	**0.47***	**0.18**	**-0.07**
SD	**0.10**	**0.15**	**0.14**	**0.19**	**0.21**	**0.13**	**0.14**	**0.18**	**0.21**	**0.15**	**0.11**

When correlation coefficients were compared between the two models, significant differences were seen between the sternal portion of the pectoralis muscle, upper trapezius, and biceps muscles as seen in Table 12 (9df, $p<0.05$).

Table 12: Results of statistical analysis measuring difference in correlation coefficients between NL and GH models. A H_o value of 1 indicates significant difference.

Muscle	NL Average	SD	GH Average	SD	H_o	P-value
Lat Dorsi	0.11	0.15	0.05	0.10	0	0.082
Pec Stern	**0.19**	**0.16**	**0.08**	**0.15**	**1**	**0.003**
Pec Clav	0.06	0.16	0.10	0.14	0	0.176
Upper Trap	-0.12	0.22	-0.08	0.19	0	0.180
Lower Trap	0.42	0.17	0.39	0.21	0	0.581
Mid Delt	0.14	0.14	0.18	0.13	0	0.187
Post Delt	**0.18**	**0.14**	**0.11**	**0.14**	**1**	**0.045**
Ant Delt	0.20	0.11	0.15	0.18	0	0.434
Infraspinatus	0.55	0.10	0.47	0.21	0	0.196
Biceps	**0.03**	**0.15**	**0.18**	**0.15**	**1**	**0.002**
Triceps	-0.12	0.12	-0.07	0.11	0	0.184

Results seen in a typical subject are shown using scatter plots in Figure 13. Full data for all subjects is presented in Appendices F and G (page 109 and page 119).

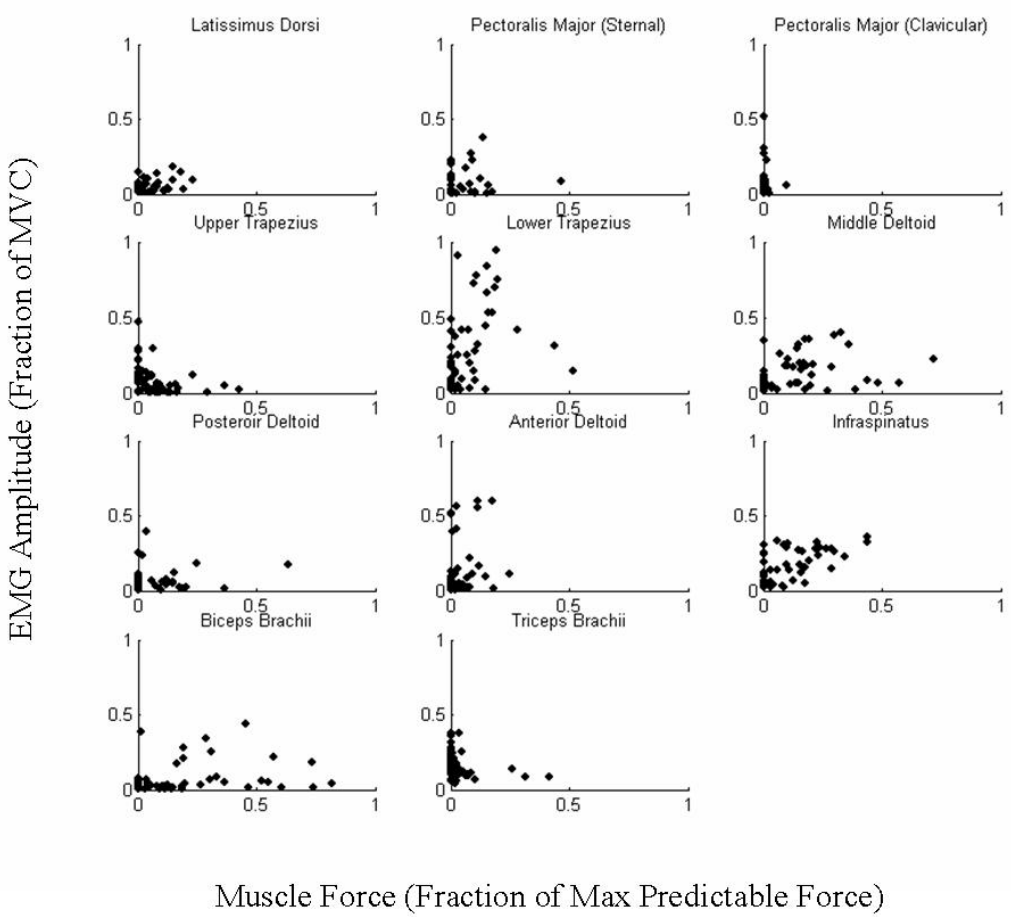

Figure 13: Typical scatter plots showing relationship between predicted muscle force and EMG amplitude.

4.3.2 Effect on MFP:EMG Ratio

The ratio between MFP and normalized EMG was measured by fitting the data with a linear regression line and calculating its slope. For the NL model, slope values ranged from -0.17 to 1.73 (Table 13Table 13), while for the GH model the values ranged from -0.12 to 0.86 (Table 14).

Table 13: Slope of regression line fit between normalized EMG and normalized MFP as calculated using the NL model

	Lat. Dorsi	Pec Stern	Pec Clav	Upper Trap	Lower Trap	Mid Delt	Post Delt	Ant Delt	Infra	Biceps	Triceps
S1	0.22	0.27	0.46	-0.35	0.97	0.20	0.10	0.86	0.56	0.12	-0.23
S2	0.04	0.69	-0.93	-0.32	4.18	0.56	0.32	0.30	0.36	0.01	-0.16
S3	0.38	0.11	1.00	-0.25	2.99	0.00	0.03	0.74	0.37	-0.30	-0.13
S4	0.17	0.54	-0.13	0.58	2.11	0.07	0.12	1.63	0.96	0.15	0.18
S5	0.02	0.02	0.37	-0.37	0.49	0.00	0.15	0.34	0.32	-0.06	-0.14
S6	-0.16	0.03	-0.53	0.02	0.53	0.15	0.31	0.72	0.11	0.00	-0.22
S7	0.04	0.12	2.32	-0.32	1.41	0.11	0.05	0.67	0.50	0.16	-0.41
S8	0.07	0.06	0.91	-0.05	3.54	0.15	0.31	0.31	0.54	0.08	0.01
S9	0.20	0.01	-1.00	-0.35	0.34	0.56	0.71	0.78	0.60	0.05	-0.43
S10	0.03	0.02	0.04	-0.19	0.71	-0.01	0.01	0.05	0.21	-0.04	-0.15
AVG	**0.10**	**0.19**	**0.25**	**-0.16**	**1.73**	**0.18**	**0.21**	**0.64**	**0.45**	**0.02**	**-0.17**
SD	**0.15**	**0.24**	**1.00**	**0.29**	**1.40**	**0.21**	**0.21**	**0.44**	**0.24**	**0.14**	**0.18**

Table 14: Slope of regression line fit between normalized EMG and normalized MFP as calculated by GH model.

	Lat. Dorsi	Pec Stern	Pec Clav	Upper Trap	Lower Trap	Mid Delt	Post Delt	Ant Delt	Infra	Biceps	Triceps
S1	0.03	0.06	-0.02	-0.45	1.28	0.33	0.02	0.92	0.35	0.25	-0.24
S2	0.07	0.21	0.67	-0.01	1.20	0.34	0.16	0.53	0.30	0.26	-0.67
S3	0.16	0.03	1.68	-0.26	1.77	0.17	0.07	0.49	0.29	0.15	-0.09
S4	0.10	0.36	-0.29	0.52	1.53	0.15	0.10	0.64	0.66	0.24	0.11
S5	0.04	0.01	0.50	-0.40	0.30	0.13	0.05	0.05	0.16	0.03	-0.14
S6	-0.09	0.01	-0.21	0.01	0.89	0.16	0.28	-0.14	0.03	0.01	-0.01
S7	0.00	0.08	2.33	-0.09	0.94	0.16	-0.12	0.35	0.26	0.15	-0.08
S8	0.04	-0.10	1.76	0.03	0.08	0.29	0.26	0.82	0.17	0.08	-0.02
S9	0.03	0.01	-0.11	-0.30	0.11	0.34	0.29	-0.21	0.03	0.08	0.11
S10	-0.01	-0.02	0.03	-0.14	0.46	0.01	0.07	-0.01	0.19	-0.01	-0.16
AVG	**0.04**	**0.07**	**0.63**	**-0.11**	**0.86**	**0.21**	**0.12**	**0.34**	**0.24**	**0.12**	**-0.12**
SD	**0.07**	**0.13**	**0.95**	**0.28**	**0.60**	**0.11**	**0.13**	**0.40**	**0.18**	**0.10**	**0.22**

Significant decreases in slope with the addition of GH ligaments were seen in the sternal portion of the pectoralis muscle and the infraspinatus, while a significant increase was seen in the biceps muscle (Table 15, 9df, $p<0.05$).

Table 15: Results of statistical analysis measuring difference in slopes between NL and GH models. A H_o value of 1 indicates significant difference.

Muscle	NL Average	SD	GH Average	SD	H_o	P-value
Lat Dorsi	0.10	0.15	0.04	0.07	0	0.065
Pec Stern	**0.19**	**0.24**	**0.07**	**0.13**	**1**	**0.028**
Pec Clav	0.25	1.00	0.63	0.95	0	0.083
Upper Trap	-0.16	0.29	-0.11	0.28	0	0.216
Lower Trap	1.73	1.40	0.86	0.60	0	0.066
Mid Delt	0.18	0.21	0.21	0.11	0	0.544
Post Delt	0.21	0.21	0.12	0.13	0	0.061
Ant Delt	0.64	0.44	0.34	0.40	0	0.103
Infraspinatus	**0.45**	**0.24**	**0.24**	**0.18**	**1**	**0.004**
Biceps	**0.02**	**0.14**	**0.12**	**0.10**	**1**	**0.043**
Triceps	-0.17	0.18	-0.12	0.22	0	0.585

4.3.3 Zero-force Predictions by Model

The number of zero-force predictions for the two models are summarized in Table 16 and Table 17. The number of zero-force predicting trials was subsequently normalized to the number of convergent trials per subject to account for the non-converging trials. Student's t-tests were run using an alpha of 0.01, and results are summarized in Table 18.

Table 16: Number of zero-force predictions calculated by NL model

	Lat Dorsi	Pec Stern	Pec Clav	Upper Trap	Lower Trap	Mid Delt	Post Delt	Ant Delt	Infra	Biceps	Triceps
S1	29	39	51	21	24	21	37	29	23	14	32
S2	24	27	39	12	28	21	40	21	26	18	29
S3	22	32	47	13	36	19	36	24	26	15	31
S4	26	35	46	16	32	25	34	25	25	18	29
S5	25	32	46	19	32	17	29	21	24	18	26
S6	28	38	50	31	20	19	31	25	28	14	33
S7	26	30	45	27	25	22	33	22	27	14	28
S8	32	32	48	27	30	22	40	25	25	18	30
S9	34	33	52	30	24	17	29	20	29	16	32
S10	33	35	44	24	32	17	36	27	25	19	31
AVG	**27.9**	**33.3**	**46.8**	**22.0**	**28.3**	**20.0**	**34.5**	**23.9**	**25.8**	**16.4**	**30.1**
SD	**4.0**	**3.6**	**3.8**	**6.9**	**4.9**	**2.7**	**4.0**	**2.9**	**1.8**	**2.0**	**2.1**

Table 17: Number of zero-force predictions calculated by GH model

	Lat Dorsi	Pec Stern	Pec Clav	Upper Trap	Lower Trap	Mid Delt	Post Delt	Ant Delt	Infra	Biceps	Triceps
S1	26	34	44	32	16	24	41	16	10	6	29
S2	20	25	40	26	23	28	40	15	11	12	36
S3	23	31	46	20	34	26	44	21	17	13	34
S4	27	30	50	29	26	27	38	19	12	14	31
S5	25	29	45	24	31	19	33	19	19	15	26
S6	28	32	52	39	20	26	39	19	16	4	35
S7	24	26	48	35	18	25	34	18	18	10	28
S8	24	29	47	31	27	24	42	16	20	15	33
S9	25	31	50	45	14	20	38	5	5	11	32
S10	32	37	46	36	23	22	46	18	12	12	38
AVG	**25.4**	**30.4**	**46.8**	**31.7**	**23.2**	**24.1**	**39.5**	**16.6**	**14**	**11.2**	**32.2**
SD	**3.2**	**3.5**	**3.5**	**7.4**	**6.4**	**3.0**	**4.1**	**4.5**	**4.8**	**3.7**	**3.8**

Table 18: Results of statistical analysis measuring difference in zero-force predictions between NL and GH models. Average values are expressed as percentage of the number of convergent trials in each model. A H_o value of 1 indicates significant difference.

Muscle	NL Average	SD	GH Average	SD	H_o	P-value
Lat Dorsi	51.0	0.06	47.5	0.04	0	0.0990
Pec Stern	60.9	0.05	57.0	0.05	0	0.0179
Pec Clav	85.6	0.05	87.7	0.04	0	0.1545
Upper Trap	**40.1**	**0.12**	**59.3**	**0.13**	**1**	**0.0000**
Lower Trap	**51.9**	**0.10**	**43.6**	**0.12**	**1**	**0.0023**
Mid Delt	**36.7**	**0.05**	**45.3**	**0.06**	**1**	**0.0001**
Post Delt	**63.3**	**0.08**	**74.2**	**0.08**	**1**	**0.0003**
Ant Delt	**43.7**	**0.05**	**31.2**	**0.08**	**1**	**0.0004**
Infraspinatus	**47.3**	**0.03**	**26.3**	**0.09**	**1**	**0.0001**
Biceps	**30.1**	**0.04**	**21.1**	**0.07**	**1**	**0.0002**
Triceps	55.1	0.03	60.4	0.07	0	0.0165

No trends are obvious; however, it appears that muscles that share similar lines of action to ligaments experienced an increase in zero-force predictions. Muscles without similar lines of actions to ligaments appear to have decreased in the number of zero-force predictions.

4.4 Correlation Differences in Extreme and Non-extreme Postures

The 56 postures were divided into two types of postures: “extreme” and “non-extreme” postures. Correlation coefficients were grouped by posture type and were compared. Coefficient data are summarized in Table 19 and Table 20. T-test results are shown in Table 21. Because groups were of different sizes and the definitions of “extreme” and “non-extreme” carry some subjectivity, an alpha level = 0.01 instead of 0.05 was used to test for significant differences.

Table 19: Pearson product correlation coefficients showing relationship between EMG amplitude and predicted muscle force non-extreme ranges of motion with the GH model.

	Lat. Dorsi	Pec Stern	Pec Clav	Upper Trap	Lower Trap	Mid Delt	Post Delt	Ant Delt	Infra	Biceps	Triceps
S1	0.07	-0.01	-0.02	-0.38	0.54	0.69	0.37	0.45	0.66	0.41	-0.08
S2	0.09	0.30	0.25	0.06	0.69	0.57	0.00	0.26	0.73	0.15	-0.23
S3	0.19	0.28	0.35	-0.12	0.84	0.31	0.11	0.21	0.75	0.02	-0.24
S4	0.34	0.35	-0.11	0.67	0.58	0.36	0.03	0.26	0.63	0.17	0.18
S5	0.03	0.11	0.33	-0.20	0.47	0.06	0.11	0.15	0.40	0.04	-0.31
S6	-0.23	0.33	-0.04	0.22	0.55	0.37	0.45	-0.12	0.25	0.13	-0.37
S7	-0.05	0.37	0.37	-0.26	0.44	0.22	-0.10	0.46	0.45	0.34	-0.07
S8	0.10	0.01	0.33	0.17	0.03	0.32	0.34	0.11	0.49	-0.02	-0.05
S9	0.05	0.36	0.00	0.10	0.24	0.37	0.32	0.05	0.17	0.07	0.03
S10	-0.07	0.07	0.18	-0.02	0.57	0.38	0.12	0.15	0.76	0.17	-0.16
AVG	**0.05**	**0.22**	**0.17**	**0.02**	**0.50**	**0.36**	**0.17**	**0.20**	**0.53**	**0.15**	**-0.13**
SD	**0.15**	**0.13**	**0.18**	**0.26**	**0.22**	**0.13**	**0.17**	**0.15**	**0.20**	**0.10**	**0.16**

Table 20: Pearson product correlation coefficients showing relationship between EMG amplitude and predicted muscle force extreme ranges of motion with the GH model.

	Lat. Dorsi	Pec Stern	Pec Clav	Upper Trap	Lower Trap	Mid Delt	Post Delt	Ant Delt	Infra	Biceps	Triceps
S1	0.20	0.10	0.04	-0.10	0.81	0.10	-0.16	0.25	0.78	0.55	-0.25
S2	0.13	0.35	-0.13	0.09	0.27	0.17	0.28	0.39	0.35	0.45	-0.31
S3	-0.06	-0.11	0.38	-0.32	0.65	-0.10	-0.12	0.44	0.63	0.11	-0.02
S4	0.05	0.29	0.30	-0.13	0.37	-0.10	0.21	0.29	0.33	0.37	0.16
S5	0.33	-0.13	-0.15	-0.44	-0.03	0.27	0.01	-0.17	0.07	-0.03	0.36
S6	-0.04	-0.18	-0.08	-0.19	0.29	0.14	0.31	0.02	0.18	0.03	0.04
S7	0.17	0.26	0.21	0.12	0.39	0.26	-0.21	0.03	0.44	-0.04	-0.16
S8	0.17	-0.29	0.13	-0.09	0.02	0.31	-0.05	0.35	0.31	0.20	-0.03
S9	0.24	0.05	0.76	-0.32	-0.02	0.16	0.07	-0.18	-0.06	0.01	-0.05
S10	-0.15	-0.19	-0.16	-0.28	0.14	-0.18	0.07	-0.14	0.43	-0.19	-0.18
AVG	**0.10**	**0.01**	**0.13**	**-0.17**	**0.29**	**0.10**	**0.04**	**0.13**	**0.35**	**0.15**	**-0.04**
SD	**0.15**	**0.23**	**0.29**	**0.18**	**0.21**	**0.17**	**0.17**	**0.24**	**0.20**	**0.20**	**0.18**

Table 21: Results of statistical comparison of correlation coefficients between extreme and non-extreme postures. A Ho value of 1 indicates significant difference.

	Non Extreme		Extreme			
	Avg	**SD**	**Avg**	**SD**	**H_o**	**P-value**
Lat. Dorsi	0.05	0.15	0.10	0.15	0.00	0.14
Pec Stern	0.22	0.13	0.01	0.23	0.00	0.45
Pec Clav	0.17	0.18	0.13	0.29	0.00	0.35
Upper Trap	0.02	0.26	-0.17	0.18	0.00	0.51
Lower Trap	0.50	0.22	0.29	0.21	0.00	0.53
Mid Delt	**0.36**	**0.13**	**0.10**	**0.17**	**1.00**	**0.48**
Post Delt	0.17	0.17	0.04	0.17	0.00	0.37
Ant Delt	0.20	0.15	0.13	0.24	0.00	0.34
Infra	0.53	0.20	0.35	0.20	0.00	0.48
Biceps	0.15	0.10	0.15	0.20	0.00	0.25
Triceps	-0.13	0.16	-0.04	0.18	0.00	0.15

V DISCUSSION

This study involved adding seven shoulder ligaments, consisting of nine elements into a musculoskeletal model of the human shoulder. Of particular interest was the response of the ligaments in various postures, and the effects the addition of these ligaments had on the muscle force predictions of this model. This section will discuss the findings of this study, identify some of its limitations and assumptions, and suggest future directions for this work.

5.1 Convergence

The model used predicts muscle forces through the use of optimization. Given an upper body posture and force at the hand, the optimization algorithms predict muscle forces by minimizing a cost function (in this case the sum of the cubed muscle stresses). Due to equilibrium constraints and boundaries placed on the force producible by muscles of the shoulder, instances occur where a feasible solution cannot be found to satisfy all of the constraints. Instances of non-convergence were minimal for the NL and GH models, but much greater when all ligaments (AL) were included.

The dramatic increase in non-convergence was attributed to inclusion of the conoid ligament, trapezoid ligament, and costoclavicular ligament. A bar graph of normalized trapezoid ligament force from subject 8 shows that approximately 50% of trials caused the ligament to exceed maximal force (Figure 14).

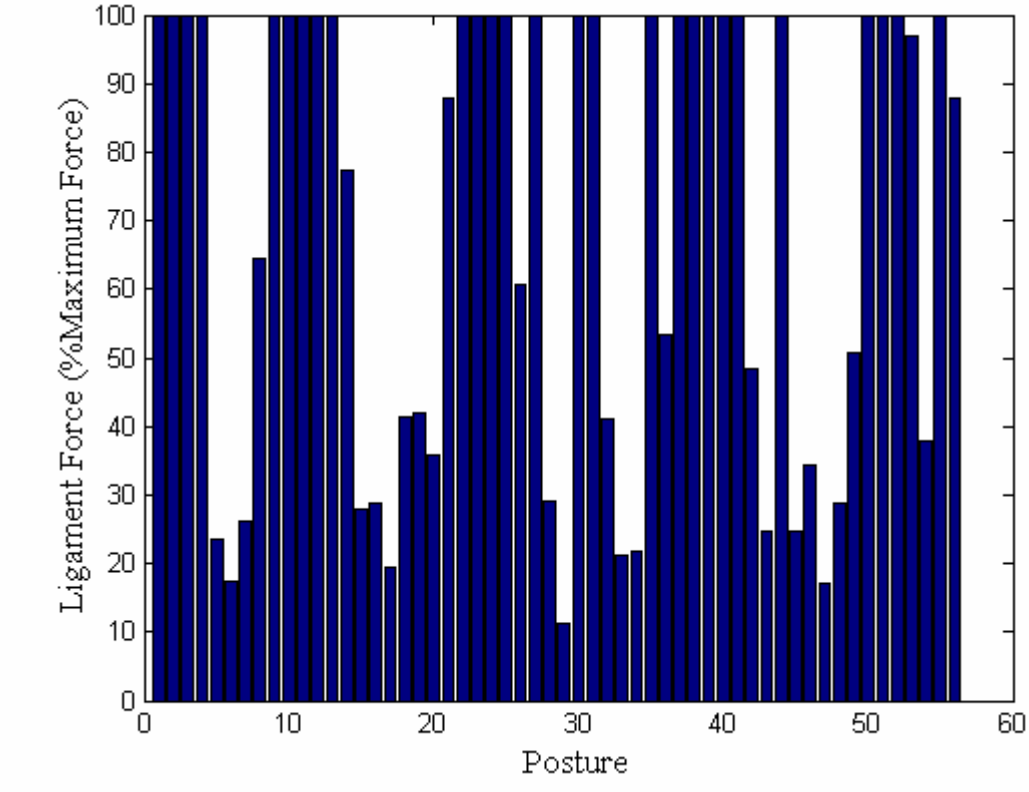

Figure 14: Bar graph of normalized trapezoid ligament force in all 56 postures for subject 8. Results indicate nearly 50% of trials produced maximal ligament force.

Similar findings were seen in the CCL and CON. The force values assigned to the CON, TRAP, and CCL at or beyond maximum strain were 532.5, 268.5, and 169.8 Newtons, respectively. To understand the magnitude of these forces, consider that 532.5N is greater than the maximum allowable force for all but one muscle included in the model (Wood, 1989; Karlsson, 1992; Dickerson, 2007). The high magnitudes of these ligament forces led us to believe that inclusion of the CON, TRAP, and CCL ligaments is placing a demand on some muscles that exceeds the physiological limits of those muscles (as specified in the model). The high rate of non-convergence for the AL model indicates that either some muscle boundaries are underestimated, ligament

forces are being overestimated, or a combination of the two. Nonetheless, it is clear that the properties of the CON, TRAP, and CCL ligaments are being poorly modeled. The difficulty of modeling these particular ligaments will be further discussed in a later section.

5.2 Ligament Length vs. Posture

With respect to the first investigative question, the hypothesis presented was correct. Just as has been noted in the literature (Culham & Peat, 1993; Pronk, 1993; Debski, 1999; Makhsous, 1999; Seeley, 1999; Itoi, 2004), the lengths of the modeled ligaments increased steadily as the arm deviated from rest. More specifically deviation within certain ranges of motion caused length increases for certain ligaments. These results are not surprising given that ligament length is influenced by joint angle and segment rotation (Jerosch, 1990; Culham and Peat, 1993; Uruyama, 2001). Since there is not a "gold standard" against which to compare, only qualitative assessments and comparisons were made between the outputs and clinical findings cited in the literature. In order to assess the magnitude of a ligament's contribution, it was assumed that ligaments contribute most to shoulder function when they reach their greatest length. Comparisons between current study and previous attempts to model ligaments were made where possible. However, to the best of our knowledge, this is the first time glenohumeral ligaments have been incorporated into a musculoskeletal model of the shoulder.

5.2.1 Costoclavicular Ligament

Elevation of the arm caused rotation of the clavicle, resulting in an increase in CCL length. This increase in length was expected and is in accordance with previous model findings, and with anatomical studies (Pronk, 1993; Cave, 1962). However, when compared to predictions of Pronk (1993), our model predicts both a shorter resting length, and a shorter length at maximum angle of abduction (Figure 15). Also, while Pronk's (1993) simulations show a peaking of CCL length at approximately 150°, our model, on average, peaks at maximum range of abduction. Though there is a difference in terms of absolute lengths, the maximum percent increase in CCL length is similar (approx. 250% vs. approx. 280%).

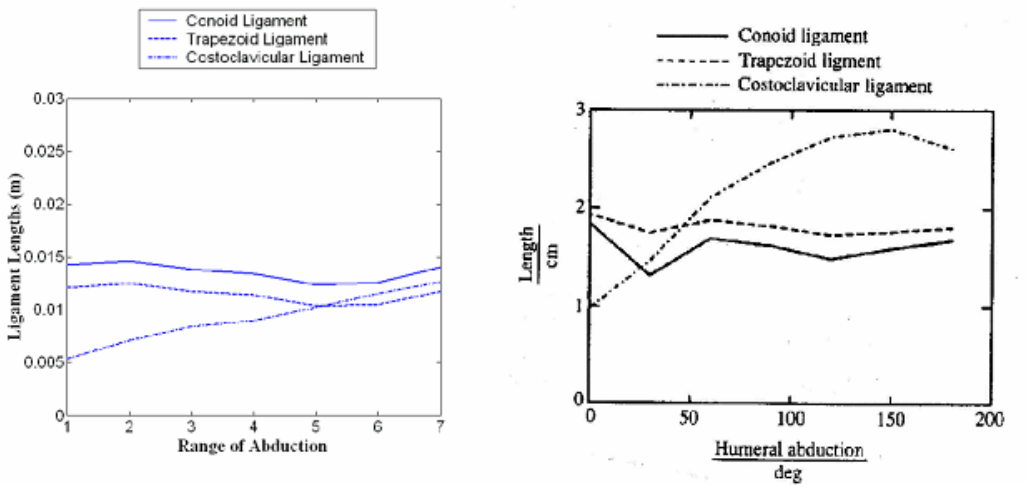

Figure 15: Comparison of CON, TRAP, and CCL lengths in Dickerson Model (left) and Dutch Model (Pronk, 1993) (right). Though magnitudes of lengths vary, trends are similar.

Before attempting to explain these differences it is important to note that Pronk (1993) plots his lengths against humeral abduction angle, while the present data are plotted against a percentage of maximum abduction (expressed

in seven intervals). Thus, some of the variance can be attributed to varying postures. With that said, the discrepancy in absolute length values is likely due to the differing locations of CCL attachment sites between the two models. The difference in shape indicates a difference in the structural composition of the two models. While the results from our model indicate the distance between the first rib and the clavicle continues to increase throughout abduction, Pronk's (1993) findings suggest a decrease beyond 150°.

5.2.2 Trapezoid and Conoid Ligaments

Our results showed that the CON and TRAP ligaments were longest when the arm was most extended and most internally rotated (Figure 16). These findings are confirmed by findings in the literature that state the TRAP and CON ligaments work towards preventing rotation of the clavicle about its long axis (Culham and Peat, 1993; Pronk, 1993). Little difference was found between the model's results and those of Pronk's (1993) when comparing CON and TRAP lengths produced over a range of abduction. Although our ligament lengths are once again shorter than Pronk's, the general trend seen is similar. The only other noticeable difference is that Pronk predicts the TRAP to be longer than the CON, while we predict the opposite. These discrepancies are likely once again simply due to the difference in attachment sites. However, the similarity in ligament trends seen between the two models shows that there is consistency between the results of the two models.

More differences are noticeable when the characteristics of our CON and TRAP ligaments are compared to those of Makhsous (1999). Not only are the lengths in our model shorter than those in Makhsous' (1999), but the shape of the curve of the trapezoid ligament is also different (Figure 16). Our model predicted a decrease in TRAP length during the mid-ranges of abduction, while Makhsous' (1999) predicted a steady increase. The discrepancies in TRAP length were not expected considering both the Dickerson (2007) model and Makhsous' (1999) model are based on the same anatomical data (Hogfors, 1987; Makhsous, 1999; Dickerson, 2007). These input similarities lead us to believe the differences are controlled by differences in the shoulder rhythm. The shoulder rhythm refers to the interplay between the bones of the shoulder, and is estimated using a set of polynomials. The rhythm in this model is different from that used by Makhsous, and could be the reason for the differences seen in TRAP length.

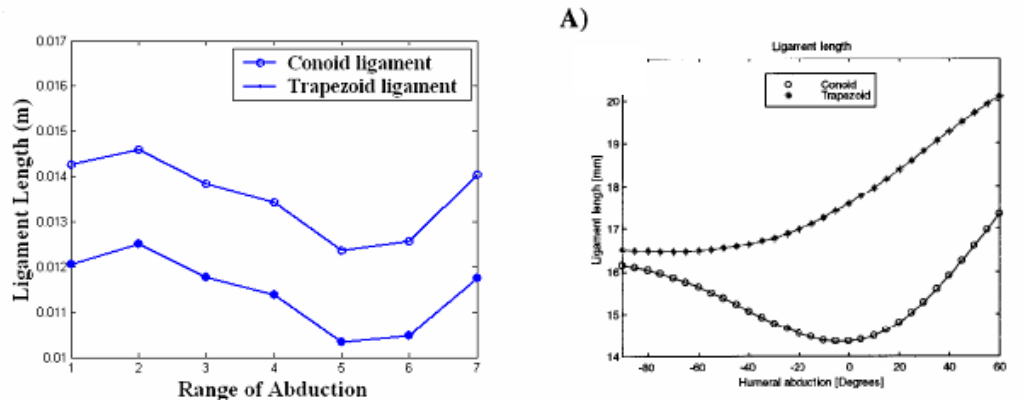

Figure 16: Comparison of CON and TRAP lengths throughout a range of minimal to maximal abduction in Dickerson Model (left) and Gothenburg Model as modified by Makhsous (1999) (right).

5.2.3 Coracohumeral, Superior Glenohumeral, and Middle Glenohumeral Ligaments

The CHL and SGHL contribute most to shoulder function during external rotation, a result that is in accordance with the literature (Jerosch et al., 1990, Itoi, 2004). The SGHL is actually most strained when the arm is near 0° of flexion and externally rotated, a result that agrees with reports by Itoi (2004). Debski et al. (1999) reported that all glenohumeral ligaments increase in length during both forward flexion and extension. This claim disagrees with our findings. Our results show peak length near neutral flexion, and a steady decrease in both flexion and extension. Debski el. al. (1999) also found that the SGHL is most stressed (and therefore strained) when the arm is at the end ranges of flexion and extension, a result that also contradicts our findings. A graph of GH ligament force as predicted by Debski (1999) can be seen below in Figure 19.While such substantial discrepancies are alarming, the differences could be attributed to the degree of rotation of the humerus. Debski (1999) predicted SGHL tension by moving cadaveric arms through a range of flexion/extension with the humeral epicondyles aligned in the scapular plane. The present study had the humeral epicondyles parallel to the transverse plane, resulting in approximately 60° more external rotation. The greater amount of external rotation is the likely cause of the differences seen in ligament strain in the SGHL when compared to Debski (1999).

While it is known that the MGHL is a primary stabilizer during abduction and external rotation, our results showed most ligament strain during flexion

(Figure 11). These findings are once again due to the high degree of external rotation during the flexion postures.

5.2.4 Inferior Glenohumeral Ligament

The primary functions of the three bands of the IGHL are to stabilize the joint when the arm is above 90° abduction and when the arm is abducted and externally rotated (Turkel, 1981; Culham and Peat, 1993; Itoi, 2004). Our model results are consistent with the literature, as the lengths of each of the three bands peak when the arm is in some degree of abduction (Figure 11).

When compared to Debski (1999), our results show some similarities. The anterior portion of the IGHL increases with extension, but decreases as it approaches maximum flexion. The posterior aspect of the IGHL only lengthens as the arm is flexed, not extended. However, this comparison is limited to a qualitative discussion as Debski (1999) only reports ligament forces and not lengths.

5.3 Ligament Force

5.3.1 Comparison with Literature

Pronk et al. (1993) calculated ligament forces for the CON, TRAP, and CCL at different degrees of abduction (Figure 17). Their results show inconsistent force patterns for the CON and TRAP, whereas ours show a steady decrease followed by an increase near maximum abduction. Calculated forces for the CCL resemble those of the current study, excluding the significant drop

at maximum abduction seen in Pronk's (1993) model. The magnitude of force for each ligament was strikingly greater in our model than calculated by Pronk (1993). Possible explanations for this observance are discussed at the end of this section.

a) Conoid Ligament

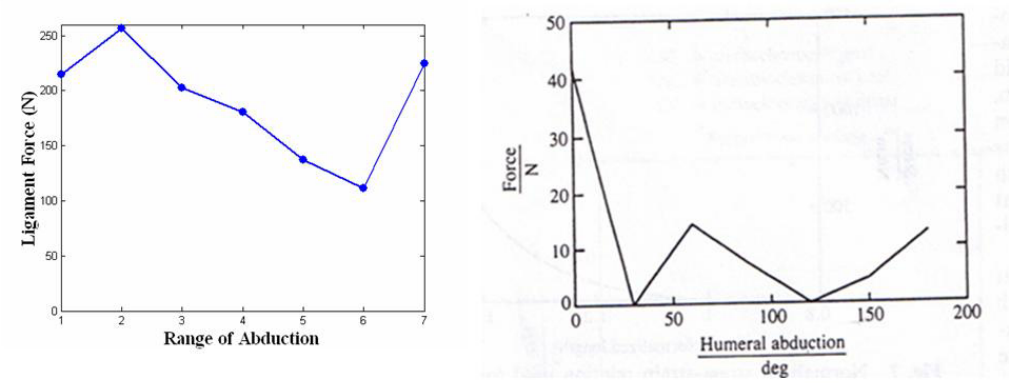

b) Trapezoid Ligament

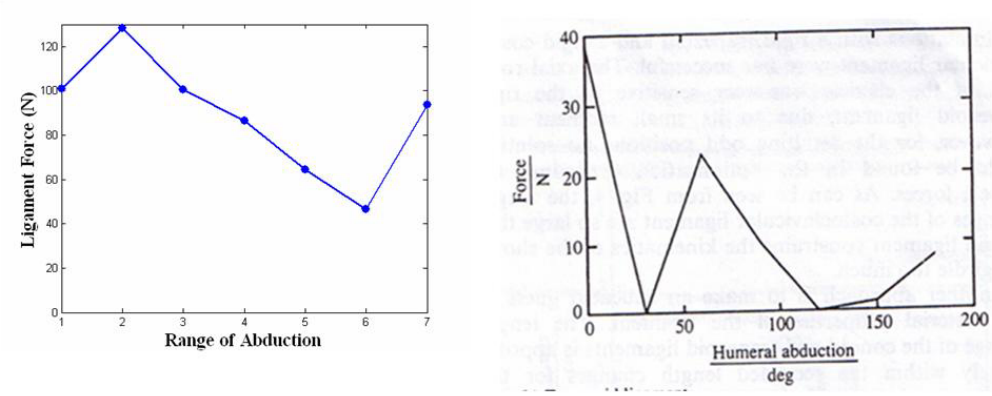

c) Costoclavicular Ligament

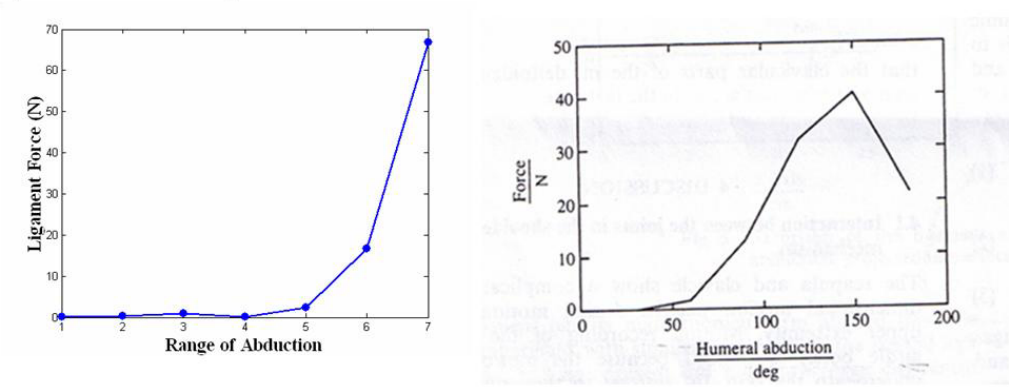

Figure 17: Forces in three ligaments in Dickerson Model (left) and Dutch Model (Pronk, 1993) (right); a) conoid ligament; b) trapezoid ligament; c) costoclavicular ligament.

Force profiles for the TRAP and CON throughout the range of abduction were compared to predictions made by Makhsous (1999) for these same ligaments. The shapes of the force curves predicted by Makhsous (1999) differ from those in our model in the same way as do the ligament lengths discussed above (Figure 18). This result was anticipated as similar force estimation techniques are employed by the two models. However, such large discrepancies in force magnitude were not expected.

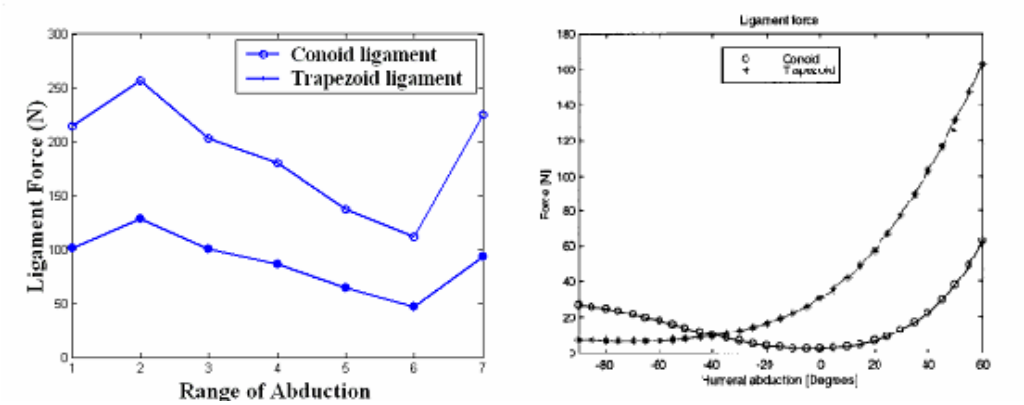

Figure 18: Comparison of CON and TRAP forces throughout a range of minimal to maximal abduction in Dickerson Model (left) and Gothenburg Model as modified by Makhsous (1999) (right).

Though the attachment sites were similar, different reference lengths and cross sectional areas were used. While the cross sectional areas used were of similar magnitude, the reference lengths used in this model were approximately two-thirds the length of those used by Makhsous (1999). As was mentioned, low reference length values can result in overestimations of ligament force. While Makhsous' (1999) estimations are not perfect, it is possible that our estimations may over-predict force in the CON and TRAP ligaments.

As previously mentioned, Debski et al. (1999) studied the change in force in the glenohumeral ligaments throughout the range of forward flexion-extension. A comparison between their forces and the forces predicted by our model is found in Figure 19.

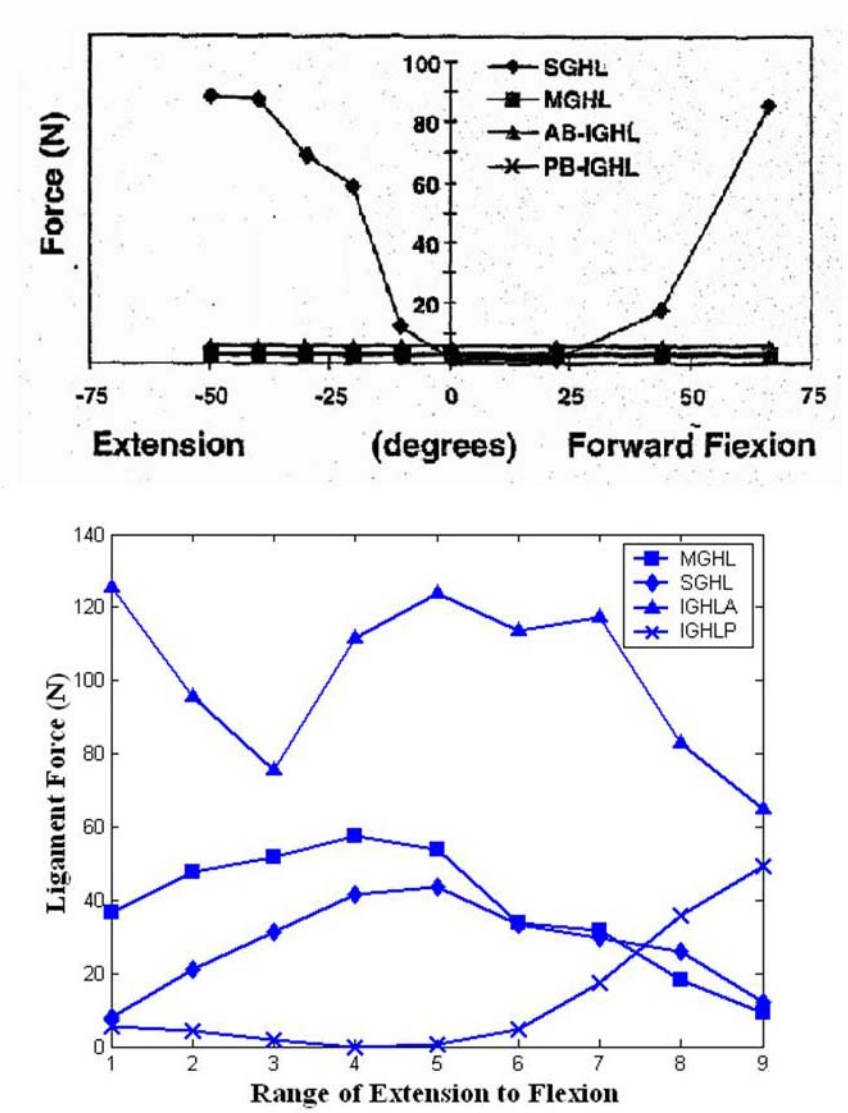

Figure 19: Comparison of force in GH ligaments predicted by Debski (1999)(top) and modified Dickerson Model (bottom). X-axis in Dickerson model ranges from maximum extension (1) to maximum flexion (9).

An explanation for the differences in SGHL length was given above, and applies to the differences seen in force. In the other three ligaments measured Debski (1999) found 0N of force produced. Our findings show some force in all of the glenohumeral ligaments at some point during forward flexion-extension. The reason for these differences is not clear; given that similar reference lengths were used, our model appears to be overestimating the ligament length.

Equation 1 shows how ligament force was modeled to be a function of ligament length. Thus, it is logical that ligament force increased with ligament length, and that peak force values coincided with peak length values. However, it is surprising that the modeled ligaments sometimes (depending on the posture and subject) exceeded maximum length criteria, resulting in prediction of maximal force. This prediction was not always representative of what occurred during experimentation. Exceeding maximal length would indicate likely tearing of the ligament and would cause the subject significant pain or discomfort, none of which was reported. Comparisons with previous studies in the literature also suggest that our model is overestimating ligament forces.

The overestimation of ligament forces is a function, and more than likely a combination, of two contributing factors;

i) Underestimation of ligament *reference* length.

ii) Overestimation of ligament length.

Underestimation of ligament reference length:

As we can see from Equation 1, ligament reference length is not only used to determine at what length tension is generated, but is also used to determine the maximum ligament force. Thus, underestimating the reference length of a ligament will not only result in greater forces at shorter lengths, but will also result in an underestimation of the maximum ligament force.

Overestimation of ligament length:

As tension is dependent on ligament length, systematic Overestimation of ligament length will create non-physiological tension in the ligament. Furthermore, because tension is proportional to ligament length, overestimating the length will also result in inflated ligament force values. While all ligaments are prone to inaccurate modeling, shorter ligaments such as the CCL, CON, and TRAP are most sensitive to these errors (Pronk, 1993). A constraint was placed on ligament force so that it did not exceed its maximum force value (derived from its maximum strain value). When ligament force is plotted against posture, "plateaus" indicate the ligament was predicted to exceed its maximal strain and therefore force. Figure 20 shows plots of the forces of the CON, and TRAP ligaments throughout the 28 different postures. As we can see from the Figure 20, these ligaments were often predicted to reach or exceed their maximal force.

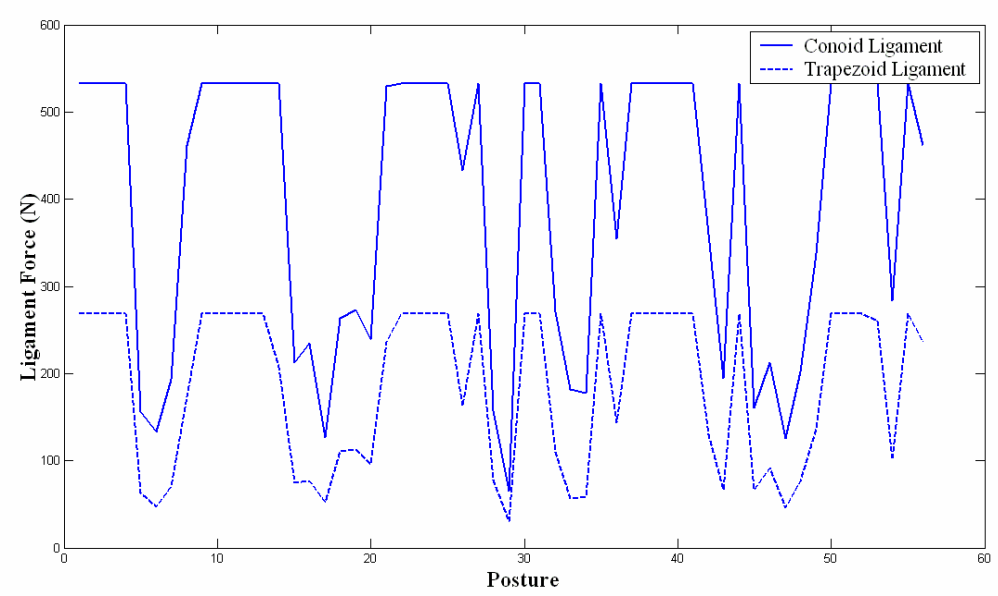

Figure 20: Force of Conoid and Trapezoid throughout the 56 experimental trials from subject 8. Flat horizontal lines, or "plateaus", indicate the ligament is producing maximum allowable force.

While we cannot quantify the magnitude of ligament force over-estimations, it is likely that the errors are large in some cases, as it is unlikely that any of our subjects' ligaments reached their maximum lengths. A recent study of collegiate level baseball pitchers showed that their maximum passive range of external rotation was 126° (Werner, 2007). Although these pitchers are an elite proportion of the population in terms of shoulder range flexibility, these values are still dramatically greater than our average of 102° of maximal active shoulder external rotation. While our subjects were actively ranging as far as possible, they likely could have achieved greater ranges of motion if taken there passively. Thus, the overestimation of shoulder ligament forces is likely greater than it appears.

5.3.2 Factors Influencing Ligament Length

Ligament lengths may be influenced several factors, such as height, flexibility, and age. Any combination of these factors, as well as others, could have contributed to the model's over predictions of length and, hence, ligament force. Of greatest concern was the potential impact subject height might have on ligament length. Ligament attachment sites in the model were scaled as a proportion of bone length for each subject, and that ligament length is determined by calculating the distance between attachment sites. Given a constant posture, two subjects who differ in stature will have different ligament lengths. While ligament lengths were scalable, ligament reference lengths were not. Thus, a subject with longer bones (likely a taller subject) will have longer ligament lengths than a subject with shorter bones, even if they were in identical arm postures. To assess the model's sensitivity to varying subject size, subject height was compared to ligament length in eight randomly selected trials. Strong correlations ($r > 0.6$) were seen between ligament length and subject height (Table 22). These findings indicate that height could be a primary cause of over estimation of ligament lengths.

Table 22: Correlation coefficients between subject height and ligament length for 8 randomly selected postures. Two postures were randomly selected within each of the four ranges of motion.

Posture	CHL	CON	TRAP	SGHL	MGHL	IGHLA	IGHLI	IGHLP	CCL
5	-0.08	0.35	0.34	-0.13	0.50	0.29	0.74	0.36	0.84
7	-0.36	0.82	0.80	-0.57	-0.03	0.26	0.53	0.27	0.50
9	0.25	0.25	0.25	0.55	0.61	0.24	0.11	-0.31	0.60
14	0.26	0.56	0.55	-0.47	0.33	-0.24	0.73	0.83	0.23
19	0.61	0.17	0.10	0.52	0.59	0.61	0.76	0.70	0.52
22	0.57	0.17	0.17	0.50	0.60	0.62	0.72	0.69	0.69
26	0.70	0.43	0.43	0.64	0.73	0.72	0.76	0.77	0.40
27	0.45	0.33	0.35	0.46	0.67	0.58	0.69	0.57	0.46

These findings indicate that height could be a primary cause of over estimation of ligament lengths. Scatter plots of ligament length plotted against height for a posture 26 are seen in Figure 21.

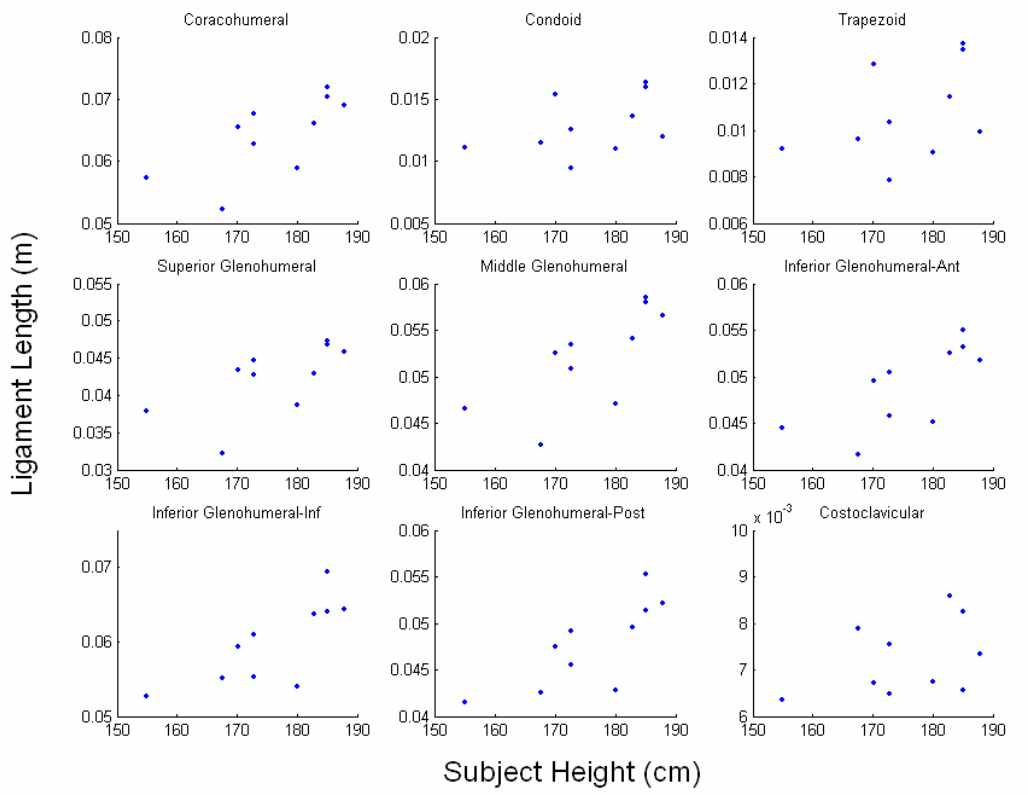

Figure 21: Scatter plots showing relationship of subject height and ligament length. Trends indicate that ligament length may increase as height increases.

5.4 Effect of Glenohumeral Ligaments on Muscle Force Predictions

Several attempts have been made to implement ligaments into musculoskeletal models of the human shoulder. Pronk's (1993) addition of the conoid ligament did not have a great impact on predicted muscle force, while Makhsous'(1999) have not been tested over a large range. Charlton (2006) has also attempted to include ligaments into the Newcastle model, but did not

analyze the effects on muscle forces. Debski's (1999) modeling of the glenohumeral ligaments revealed forces throughout the range of forward flexion, but his model was run without ligaments (Debski, 1999). To the best of our knowledge, this is the first time glenohumeral ligaments have been incorporated into a musculoskeletal model of the shoulder with the purpose of studying their effects on muscle force predictions.

5.4.1 Evaluation Technique

Before discussing the specific effects of our changes on the muscle force predictions of the model, it is important to briefly mention the advantageous and the undesirable characteristics of the evaluation technique. Evaluating the model would be much simpler if muscle or ligament forces could be directly measured in living human subjects. However, this is impractical and invasive. The next best option is using electromyography. Several previous studies have also used EMG to evaluate muscle force predictions (Karlsson, 1992; Van Der Helm, 1994; De Groot, 2004, Dickerson, 2005). However, correlating EMG to MFP is not always precise. EMG amplitude can be influenced by a number of variables, including, but not limited to, muscle length, velocity, fatigue, crosstalk, and inter-subject variability (Basmajian and De Luca, 1989; De Luca, 1997; Dickerson, 2005). While measures were taken to minimize these influences (i.e. by using static postures and providing adequate rest between trials), the use of EMG as a measurement tool remains inherently susceptible to these influences. Furthermore, due to the anatomy of the shoulder, surface EMG could only be

recorded from a subset of the muscles used in the model. Further complicating our evaluation method is the model's tendency to predict zero force in muscles where an EMG signal is present. This is a characteristic common in all optimization models, as they have been shown to poorly predict antagonist activity (Hughes, 1995). However, despite its limitations, EMG remains the most feasible tool available for evaluating the muscle force predictions of our shoulder model.

5.4.2 Effect of Ligament Inclusion on Correlation Coefficients and Slopes

As mentioned earlier, only the effects of adding the GH ligaments on the MFPs of the model were analyzed. Three variables were compared to determine the effects of our modifications;

i) Pearson product correlation coefficients between MFP and EMG.

ii) The slopes of linear regression lines relating MFP to EMG.

iii) The number of zero-force predictions by the model.

While it was expected that ligament additions would make the model more representative of the actual behaviour of the shoulder, the opposite was found. Only significant correlations were found within the lower trapezius and infraspinatus muscles, and both of these correlations decreased when the GH ligaments were added, though not significantly. Three of the r-values showed significant changes (pectoralis sternal, upper trapezius, biceps brachii) however, none of the r-values themselves were significant. Therefore, the modifications

to our model did not have a significant impact on the accuracy of muscle force predictions.

The addition of ligaments was also expected to improve MFP/EMG correlations in extreme postures. However the comparison of extreme postures versus non-extreme postures only showed one significant difference (middle deltoid). Though not statistically significant, there was a noticeable trend across all muscles showing a decrease in correlation when subjects were in extreme postures, despite the inclusions of ligaments. While this result may confirm some of the deficiencies in the ligament modeling, it also emphasizes a very important point: muscle forces are difficult to predict in extreme postures. It highlights the need for representative modeling of shoulder ligaments.

Given the differences between males and females in height, weight, and range of motion it was decided that effects of gender on model predictions should also be explored. Correlations coefficients were divided by gender and the means were compared. Table 23 shows the means and standard deviations of the correlation coefficients derived using the GH model, separated by gender.

Table 23: Averages and standard deviations of correlation coefficients across males and females.

	Lat	Pec Stern	Pec Clav	Upper Trap	Lower Trap	Mid Delt	Ant Delt	Post Delt	Infra	Biceps	Triceps
Male Avg	0.01	0.05	0.08	-0.14	**0.51**	0.21	0.12	0.17	**0.56**	0.20	-0.13
SD	0.12	0.08	0.15	0.15	**0.17**	0.17	0.13	0.20	**0.20**	0.21	0.10
Female Avg	0.08	0.12	0.12	-0.02	**0.27**	0.14	0.09	0.14	**0.37**	0.16	-0.01
SD	0.07	0.20	0.14	0.23	**0.20**	0.07	0.15	0.17	**0.19**	0.07	0.10

Of interest are the differences in correlation between males and females within the lower trapezius and the infraspinatus. Though not supported by statistical differences, the coefficients seen in women for these two muscles are much lower than seen in men. The model itself does not differentiate between males and females, so any differences seen are directly caused by the anthropometry of the subjects. As mentioned, anatomical characteristics differ between males and females. Not only do females tend to be shorter, and lighter, but they also tend to be more flexible. Any of these factors could influence ligament lengths and how force is generated, thus impacting MFPs. Anatomical differences between males and females could also impact EMG recordings. Muscle length, tissue thickness, and muscle size can vary between males and females, and all can influence the recorded EMG signal.

5.4.3 Effect of Ligament Inclusion on Slopes

The change in slopes of the regression lines relating EMG and MFP were also examined. Only the changes in slopes of lower trapezius and infraspinatus muscles are of significance as they were the only muscles to show significant correlations between EMG and MFP. The slope in the infraspinatus was significantly different ($p<0.004$), while the decrease in slope for the lower trapezius was nearly significant ($p<0.066$). These results suggest that the GH model predicted more force from the muscles given the same inputs as the original model. Of the other muscles with significant differences, but without significant correlations, all showed a decrease in slope except for the biceps

brachii. This result disproved the hypothesis, as it was expected that muscle force predictions would actually decrease with the addition of ligaments. It appears as though muscles are working in opposition of ligament forces, causing an increase in MFP. The increase in slope of the biceps brachii is explained by the fact that it shares a similar line of action with the CHL and SGHL. With the addition of these ligaments, some of the force previously assigned to the biceps brachii is now being taken up by some of the ligaments (most likely the CHL and SGHL). Conversely, the addition of the glenohumeral ligaments increased the force predicted from the latissimus dorsi, pectoralis sternal, and posterior deltoid muscles.

5.4.4 Effect of Ligament Inclusion on Zero-Force Prediction

In the evaluation of the original model low correlation levels and a tendency for the model to predict zero force for some muscles led to the conclusion that the optimization approach under-predicts antagonist co-contraction (Dickerson, 2005). While there were no significant changes in the correlation coefficients, there were significant differences in the percent of zero-force predictions. For some muscles the percent of zero-force predictions significantly decreased, although some also increased. For the two muscles with significant correlations (lower trapezius and infraspinatus) we see a significant decrease in the percent of zero occurrences. Since ligament forces are posture-dependent, there will be situations where muscles that are not agonist to the shoulder joint reaction moment will be required to generate force in order to

counteract the ligament forces. This fact, along with our results, may lend support to the theory that including ligaments into the model helps better predict antagonist co-contraction. At the very least it may indicate that for the lower trapezius and infraspinatus muscle, more realistic predictions are made when the GH ligaments are included in the model. While these results show promising signs of a more robust model, further evaluation is required before drawing definitive conclusions.

5.5 Limitations

Several limitations of optimization-driven musculoskeletal models, and unique aspects of the model used in this study are provided in the original presentation of the model (Dickerson, 2005; Dickerson et al., 2007). This section focuses primarily on limitations that are novel to this study.

5.5.1 Modeling Assumptions

Use of Generalized Data on a Range of Subjects:

An unavoidable limitation of modeling is the requirement of making assumptions. In an ideal scenario, all data necessary for modeling would be readily available. However, this is simply not feasible. Much of the data used to add ligaments to the Dickerson shoulder model came from studies performed on cadavers. We assumed that the reference lengths and cross sectional areas of ligaments in our model were the same as those reported in the cadaveric studies. We made this assumption even though the age of the specimens was much older

than the age of our subjects. This assumption was necessary for one simple fact: relatively few people in their mid-20s die, and even fewer of them donate their bodies to science.

It was also assumed that each subject had the same stress-strain characteristics in their ligaments. This assumption was made as there are no non-invasive methods of determining the properties of a specific individual's ligaments. The same rationale was used in assuming the same shoulder rhythm for all subjects. Though making these generalizations likely increased the amount of error in our model's predictions, it was necessary in order to make the model more robust, yet keep it simple.

Finally, it was assumed that the scaling of ligament attachment sites was applicable to all subjects, despite varying anthropometry. The technique used assumes the attachment site to be at a certain proportion of bone size (Hogfors, 1987; Dickerson, 2005). However, this assumption has been shown to vary in clinical studies. A study measuring the insertion of the conoid and trapezoid ligaments on the clavicle showed variation of up to two centimeters (Boehm, 2003). Though this may not seem significant, recall how small changes in ligament length can have a dramatic impact on force production. Furthermore, due to a lack of precise literature, estimates were made for the attachment sites of the glenohumeral ligaments. The attachment site of the MGHL, for example, is said to originate between one and three o'clock on the glenoid (Steinbeck, 1998; Itoi, 2004). This sort of description allows for a large amount of variability when estimating the location of a line of action. Modeling ligaments

as single lines of action is an assumption in and of itself. Some ligaments, such as the IGHLI, act more as a pouch than a typical ligament. A ligament like this may require more than one line of action to be modeled accurately.

Definition of Humeral Coordinate System:

The humeral coordinate system was defined according to (Table 24) and is seen in Figure 22 (adapted from Dickerson, 2005).

Table 24: Definition of humeral coordinate system

Body Segment	Neutral x-axis	Neutral Y-axis	Neutral Z-axis
Humerus	Defined along line between glenohumeral joint and elbow joint center (rotation axis)	Cross product of x and z axes, directed anteriorly (ab/adduction axis)	Perpendicular of the forearm and upper arm x axes, passes through acromion (flexion axis)

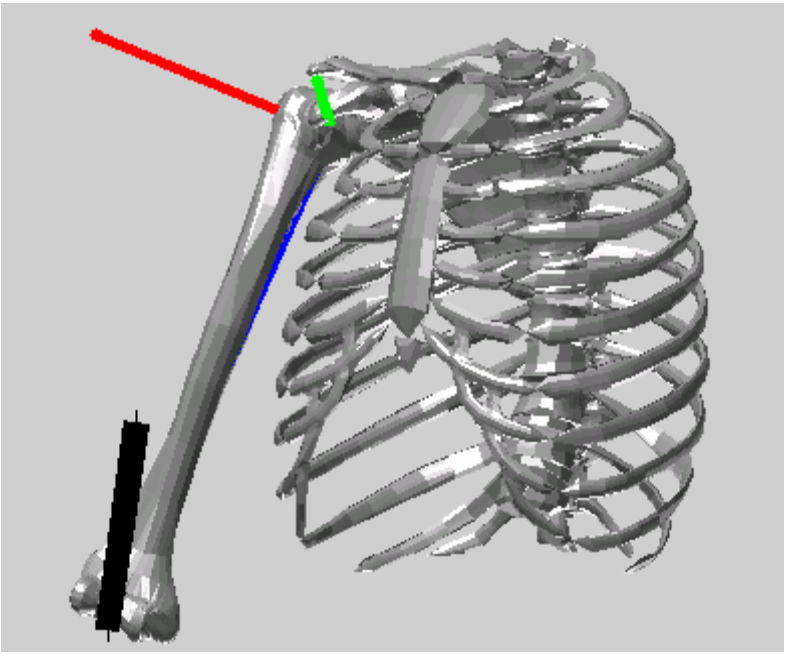

Figure 22: Illustration of humeral coordinate system

The z-axis direction is calculated by taking the cross product of vectors traveling axially through the humerus and forearm. The direction of this axis

defines the amount of rotation (external or internal) present in the humerus. Because our predictions are influenced by humeral rotation, it is tremendously important that the cross product of the humerus and forearm be accurate. The accuracy of the cross product will vary with the magnitude of the angle between the two segments; the greater the angle, the lower the magnitude of the resulting vector and the greater the percentage error therein. This error is not of great concern when the angle between the humerus and forearm is close to 90°. Unfortunately, many of our postures involved a fully extended elbow, which puts the angle between the humerus and forearm at approximately 175°. Furthermore, this method of defining the axis system is sensitive to forearm pronation (Wu et al., 2005). Errors in z-axis definition may have resulted in excessive external humeral rotation, and contributed to some of the inaccuracies seen during model evaluation. It is also suspected that an over-rotated humerus was influential in trials that did not converge. Wu et al. (2005) proposed an alternative method to define a humeral coordinate system, but concluded by recommending that the method used in this model be implemented whenever the forearm is available.

5.5.2 Experimental Data Collection

Level of Force Produced at Hand:

Several methods were proposed when determining how subjects should be instructed to exert against the force transducer. Recall, the primary means of analysis of the model's outputs was comparison with EMG. Thus, a level of

force that would noticeably activate muscles was required. Ideally, the magnitude of force would be normalized to some percentage of a maximum. However, the wide range of postures chosen would require maximum exertions for all 56 postures. Several reference exertions would not be feasible due to the varying ability to generate force in these different postures. Keeping the force constant for all 56 postures was also discussed. However, it was felt that this method would place minimal demands on the shoulder in some postures, and put excessive demands in others. Ultimately, subjects were asked to exert at a "comfortable" level for several reasons. For one, it eliminated the risk of fatiguing any of the muscles, which would hamper our EMG analyses. Secondly, it provided a method of eliciting adequate EMG signals in all postures, which was the primary concern. Though the term "comfortable" is subject to interpretation and perception, and is not quantifiable, it was felt that this method best suited our experimental design and analysis desires.

Variation in Experimental Postures:

Performing a study involving a number of different postures is inherently associated with a degree of error. Errors in measurement with the goniometer were expected. To neutralize its effects, one experimenter was in control of measurements throughout each experimental session. The same experimenter was used to measure arm angles for all subjects except the first subject.

5.5.3 Comparison Method

The relationship between EMG and muscle force has been reported to be non-linear (Dowling, 1997; DeGroot, 2004). Approximation of this non-linear relationship is complicated, especially given the changes in arm posture of our experimental protocol. Thus, for the sake of simplicity EMG was assumed to be linearly related to MFP. It was decided that at this point, the use of higher order relationships was unnecessary.

The comparison method also assumes consistent motor patterns between subjects. That is to say, for a given posture and force, EMG activity will be consistent both between subjects and within subjects. However, EMG will differ both between subjects and within a subject for identical tasks (Deluca, 1997).

Several factors influencing EMG signals were noticed that also had an impact on our analyses. Two muscles, the biceps and triceps, cross both the shoulder joint and the elbow joint. Activities producing moments at the elbow would result in EMG activation, but would not increase MFP for these two muscles.

Changing postures also have a significant impact on both EMG and MFP. Changes in posture can cause changes in EMG pick up area and changes in distance between electrodes and motor units. The former can result in electrodes recording signals from different motor units, while the latter can affect the amplitude of the recorded signal (DeLuca, 1997). Changing postures results in changes to muscle moment arms. Changes in mechanical advantage of a muscle

will inherently make it more or less likely to be activated by the model, but not necessarily by the body.

Some researchers have used EMG-driven muscle force prediction models to evaluate their optimization predictions (Makhsous, 1999). While methods exist to predict muscle force from an EMG signal (Hof, 1981; McGill, 1992; Laursen, 1998; Potvin, 2004), each is accompanied by its own set of assumptions and limitations. To make an evaluation of the presented optimization model by comparing its predictions directly to the predicted values of an EMG driven model would be problematic. As has been shown in the current study, making assumptions when modeling will increase the amount of potential error in the model's outputs. EMG driven models also use a number of assumptions, therefore outputs from these models are also accompanied by a degree of error. If one model is used to evaluate another, the amount of error in the comparison could potentially be large. High error values make comparisons between the two models less reliable, thus rendering the comparison method inadequate.

5.5.4 Error Propagation

In a multi-stage biomechanical model, individual sources of error will contribute to total error in final model outputs. Nine force producing ligament elements were incorporated into the model with the intention of improving its outputs (MFPs). To determine the values of these ligament elements, a number of assumptions and estimations were made. Assumptions and estimations are

accompanied by an amount of error, and this amount of error was often unknown. When the variables connected to the assumptions and estimations (for example ligament maximum stress and ligament cross-sectional area) are used in a function determining a third variable there is a potential increase in total error of the function. Total error may further increase by including more variables in the function, and incorporating variables associated with high errors. When calculating ligament forces, six variables were estimated and in cases assumed to be the same across subjects (Equations 2-5). Each one of these variables is associated with a degree of error. Thus, as the calculation progressed from Equation 2 to Equation 5, the total error associated with ligament forces may have become large. Because ligament force error is potentially large, when ligament force values are included in the determination of MFPs, the error associated with the MFPs will also be correspondingly large. Calculated ligament forces would not be representative of actual (in vivo) ligament forces. Therefore, integration of the nine shoulder ligament elements may have a net negative impact on the physiological realism of model muscle force predictions.

5.6 Future Directions

While the changes made did not overwhelmingly improve the model, they represent an important step towards more robust musculoskeletal models of the shoulder. In the future more steps can be taken to improve both the modeling of ligaments and the techniques used to evaluate them.

One of the difficulties with our method of modeling was attempting to apply averaged ligament reference length data to a number of subjects with different anthropometry. This difficulty was compounded by the fact that much of the ligament data were taken from cadaver studies in which the subjects were much older than the experimental population used in this study. In the future, a method of scaling ligament properties to individuals of different sizes needs to be developed.

A change to our mathematical modeling of the ligaments may also improve the model's force predictions. Generalizations of ligament properties could be made for individual ligaments as opposed to all ligaments. For example, each ligament should be assigned its own maximum strain as opposed to assuming 140% to be maximum strain for all ligaments. More radical changes may also be helpful. An approach involving two separate stress-strain relationships (an exponential relationship in the toe region, followed by a linear relationship) may prove to more accurately simulate ligament activities *in vivo* (Charlton, 2006). In his study, Charlton (2006) noted that this method would help circumvent some of the problems experienced with modeling ligament force-length characteristics using only one equation.

While it was noted that some measures were undertaken to minimize the error incurred from our evaluation technique, further measures could be taken. One such method involves applying the force at the elbow instead of the hand, thus neutralizing the impact of forearm muscles. In future studies it would be wise to use a bent elbow during experimentation in order to minimize error

when defining the local coordinate systems of the humerus. A second alternative would be to define the segment using the epicondyle markers that were tracked during experimental trials.

Future studies should also address the number of muscles being evaluated, for it is important to determine the model's accuracy across all muscles, not just those near the surface. In order to do so, indwelling EMG could be used to access the deeper muscles, in particular the muscles of the rotator cuff. These muscles are of particular interest as they are greatly involved in glenohumeral stability and are responsible for rotation of the arm. Using indwelling EMG may provide the advantage of measuring activity from a different set of muscles, and would also guard against some of the errors encountered when using surface EMG (Stokes, 2003). However, use of indwelling electrodes also introduces many other methodological and interpretation concerns. Despite being less susceptible to crosstalk, electrode movement over a muscle belly, and errors inherent with tissue, indwelling electrodes is also influenced by a number of factors (Turker, 1993). Indwelling EMG is easily hampered by movement artifact, picks up signals from only a very localized part of the muscle, and can short out if the two leads come in contact with each other (Turker, 1993). Regardless of EMG recording methods, sources of error exist and necessary precautions must be taken to minimize their impacts.

VI SUMMARY & CONCLUSIONS

Seven shoulder ligaments were systematically incorporated into a computerized muscle force prediction model. Data from the literature, a pre-existing shoulder model, computerized simulations, and experimental evaluations were used in the process.

The costoclavicular, conoid, and trapezoid ligaments were not included in the muscle force prediction of the model due to a poor convergence rate and our primary interest in the GH ligaments. Thus, muscle force predictions of the original model were only compared with the muscle force predictions of a model with only the glenohumeral ligaments added. All the ligaments were qualitatively analyzed and compared, based on length and force production, with the literature.

Changes in ligament length compared well with the literature. Though they occasionally exceeded their theoretical maximum length, patterns of increase and decrease in length were as expected. In terms of force production, ligament forces occasionally had to be constrained by its maximum value. This led to the conclusion that the model is often overestimating ligament force, because of an overestimation in ligament length and/or an underestimation of ligament reference length.

This study represents an important first attempt to integrate ligaments crossing the glenohumeral joint into a MFP model of the shoulder. Evaluation of the model changes was done by examining correlation coefficients between EMG amplitude and predicted muscle force, and comparing these coefficients

between the two models. The slope of regression lines used to determine correlation coefficients, and the frequency of zero-force predictions were also compared for each muscle between models. EMG from only two muscles (lower trapezius and infraspinatus) correlated significantly with MFP. These results led to the conclusion that the addition of glenohumeral ligaments to the model did not influence the model's ability to predict muscle force. The changes in slope indicated that the addition of glenohumeral ligaments to the model caused an increase in muscle force prediction. The changes in zero-force prediction frequency indicate that ligaments caused muscles to become active in postures where the original model predicts them to be inactive. This finding led to the theory that including GH ligaments may help the model predict antagonist co-contraction, but more evidence would help to support this conclusion.

Overall, this study has shown a method for identifying and integrating ligament properties (particularly the GH ligaments) into musculoskeletal models of the shoulder. The results highlight the sensitivity of ligament forces to small changes in ligament length, and demonstrate the sensitivity of computational musculoskeletal models to ligament forces. The wide range of postures evaluated in this study will be helpful for comparison of EMG data with muscle force predictions by researchers in the future. Our evaluation over these postures has also shown that additional work needs to be done to achieve better muscle forces predictions in the human shoulder. Despite the room for improvement it is believed that this work is vital towards developing a more robust model of the shoulder.

A primary application of the model is for assessing worker risk in ergonomics and occupational biomechanics. It is felt that by adding ligaments to this model, more accurate and more representative muscle force predictions can be garnered, and used in preventing musculoskeletal injury. The added model capability will enhance its effectiveness across a host of applications, and thereby magnify its societal relevance and impact. Although shoulder biomechanical modeling is still in its infancy, this study has highlighted areas that require further study while confirming the sensitivity of large-scale models to many different assumptions.

VII REFERENCES

Bigliani, L.U., Pollock, R.G., Soslowsky, L.J., Flatow, E.L., Pawluk, R.J., Mow, Van C., 1992. Tensile properties of the inferior glenohumeral ligament. Journal of Orthopaedic Research 10, 187-197

Boardman, N.D., Debski, R.E., Warner, J.J.P., Taskiran, E., Maddox, L., Imhoff, A.B., Fu, F.H., Woo, S.L.-Y., 1996. Tensile properties of the superior glenohumeral and coracohumeral ligaments. Journal of Shoulder and Elbow Surgery 5, 249-254.

Boehm, T.D., Kirschner, S., Fischer, A., Gohlke, F., 2003. The relation of the coracoclavicular ligament insertion to the acromioclavicular joint. Acta Orthopaedica Scandinavica 74, 718-721.

Brox, J.I., 2003. Regional musculoskeletal conditions: shoulder pain. Best Practice and Research: Clinical Rheumatology 17, 33-56. Review.

Cave, A.J.E., 1961. The nature and morphology of the costoclavicular ligament. Journal of Anatomy 95, 170-179.

Charlton, I.W., Johnson, G.R., 2001. Application of spherical and cylindrical wrapping algorithms in a musculoskeletal model of the upper limb. Journal of Biomechanics 34, 1209-1216.

Charlton, I.W., Johnson, G.R., 2006. A model for the prediction of the forces at the glenohumeral joint. Proceedings of the Institution of Mechanical Engineers. Part H, Journal of engineering in medicine 220, 801-813.

Cram, J.R., and Kasman G.S., 1998. Introduction to Surface Electromyography, Aspen, Gaithersburg, MD

Culham, E., Peat, M.1993. Functional anatomy of the shoulder complex. Journal of Orthopedic and Sports Physical Therapy 18, 342-350. Review.

Costic, R.S., Vangura, A. Jr., Fenwick, J.A., Rodosky, M.W., Debski, R.E., 2003. Viscoelastic behavior and structural properties of the coracoclavicular ligaments. Scandinavian Journal of Medicine and Science in Sports 13, 305-10.

Debski, R.E., Wong, E.K., Woo, S.L., Fu, F.H., Warner, J.J., 1999. An analytical approach to determine the in situ forces in the glenohumeral ligaments. Journal of Biomechanical Engineering 121, 311-315.

De Luca, C.J., 1997. The use of surface electromyography in biomechanics. Journal of Applied Biomechanics 13, 135-163.

Dickerson, C.R., 2005. A biomechanical analysis of shoulder loading and effort in load-transfer tasks - Dissertation, University of Michigan.

Dickerson, C. R., Martin, B.J., Chaffin, D.B., 2006. The relationship between shoulder torques and the perception of muscular effort in loaded reaches. Ergonomics 49, 1036-1051.

Dickerson, C.R., 2007. A mathematical musculoskeletal shoulder model for proactive ergonomic analysis. Computer Methods in Biomechanics and Biomedical Engineering 10, 389-400.

Dowling, J.J., 1997. The use of electromyography for the non-invasive prediction of muscle forces. Sports Medicine 2, 82-96.

Edelson, J.G., Taitz, C., Girshkan, A., 1991. The coracohumeral ligament. Anatomy of a substantial but neglected structure. Journal of Bone and Joint Surgery of Britain 73, 150-153.

Frievalds, A., 2004. Biomechanics of Upper Limbs: Mechanics, Modelling and Musculoskeletal Injuries. Stockholm, Sweden. Taylor and Francis.

Fukuda, K., Craig, E.V., An, K.N., Cofield, R.H., Chao, E.Y., 1986. Biomechanical study of the ligamentous system of the acromioclavicular joint. Journal of Bone Joint Surgery of America 68, 434–440.

Herberts, P., Kadefors, R., Hogfors, C., Sigholm, G., 1984. Shoulder pain and heavy manual labour. Clinical Orthopaedics 191,161-178.

Hof, A.L., Van den Berg, J.,1981. EMG to force processing I: An electrical analogue of the Hill muscle model. Journal of Biomechanics 14, 747-758.

Hogfors, C., Sigholm, G., Herberts, P., 1987. Biomechanical model of the human shoulder - I. Elements. Journal of Biomechanics 20, 157-166.

Hogfors C., Peterson, B., Sigholm, G., Herberts, P., 1991. Biomechanical model of the human shoulder – II. The shoulder rhythm. Journal of Biomechanics 24, 699-709.

Itoi, E., Morrey, B.F., An, K.N., 2004. Biomechanics of the shoulder. In C.A. Rockwood, F.A Matsen III, M. A. Wirth, & S.B. Lippitt (Eds.), The shoulder (pp. 223-267). Philadelphia, PE: Elsevier.

Janwantanakul, P., Magarey, M.E., Jones, M.A., Brenton, R.D., 2001. Variation in Shoulder Position Sense at Mid and Extreme Range of Motion. Arch Phys Med Rehabil 82, 840-4.

Jerosch, J., Moersler, M., Castro, W.H., 1990. The function of passive stabilizers of the glenohumeral joint-a biomechanical study. Z Orthop Ihre Grenzgeb 128, 206-212.

Johnson, G.R., Spalding, D., Nowitzke, A., Bogduk, N., 1996. Modelling the muscles of the scapula morphometric and coordinate data and functional implications. Journal of Biomechanics 8, 1039-1051

Laursen, B., Jensen, B.R., Nemeth, G., Sjogaard, G.,1998. A model predicting individual shoulder muscle forces based on relationship between electromyographic and 3D external forces in static position. Journal of Biomechanics 31,731-739.

Makhsous, M., 1999. Improvements, Validation and Adaptation of a Shoulder Model. Doctoral Dissertation, Chalmers University of Technology, Gothenburg, Sweden .

McAtamney, L., and Corlett, E.N., 1993. RULA: a survey method for the investigation of work-related upper limb disorders. Applied Ergonomics 24, 91-99.

McGill, S.M., 1992. A myoelectrically based dynamic three-dimensional model to predict loads on lumbar spine tissues during lateral bending. Journal of Biomechanics 25, 395–414.

Neer II, C.S., Satterlee, C.C., Dalsey, R.M., Flatow, E.L., 1992. The anatomy and potential effects of contracture of the coracohumeral ligament. Clinical Orthopaedics and Related Research 280, 182-185.

Nieminen, H., Niemi, J., Takala, EP., Viikari-Juntura, E., 1995. Load-sharing patterns in the shoulder during isometric flexion tasks. Journal of Biomechanics 28, 555-566.

Novotny, J.E., Beynnon, B.D., Nichols, C.E., 2000. Modeling the stability of the human glenohumeral joint during external rotation. Journal of Biomechanics 33, 345-354.

Nussbaum, M.A., Zhang, X, 2000. Heuristics for locating upper extrimeity joint centres from a reduced set of surface markers. Human Movement Science 19, 797-816.

O'Brien, S.J., Neves, M.C., Arnoczky, S.P., Rozbruck, S.R., Dicarlo, E.F., Warren, R.F., Schwartz, R., Wickiewicz, T.L., 1990. The Anatomy and histology of the inferior glenohumeral ligament complex of the shoulder. American Journal of Sports and Medicine 18, 449-456.

O'Connell, P.W., Nuber, G.W., Mieski, R.A., Lautenschlager, E. The contribution of the glenohumeral ligaments to anterior stability of the shoulder joint. American Journal of Sports Medicine 18, 579-584.

Potvin, J.R., Brown, S.H.M., 2004. Less is more: High pass filtering out up to 99% of the surface EMG signal power improves EMG-based biceps brachii muscle force estimates. Journal of Electromyography and Kinesiology 14, 389–399.

Pronk, G.M., van der Helm, F.C.T., Rozendaal, L.A., 1993. Interaction between the joints in the shoulder mechanism: the function of the costoclavicular, conoid and trapezoid ligaments. Proceedings of the Institution of Mechanical Engineers 207, 219-229.

Reynolds, L., 1999. Zeroing in on ergonomics costs and solutions. HR Today 7.

Seeley, R.R., Stephens, T.D., Tate, P., 2000. Anatomy and Physiology: 5th Ed. Boston, MA. McGraw-Hill.

Spencer, E.E., Kuhn, J.E., Huston, L.J., Carpenter, J.E., Hughes, R.E., 2002. Ligamentous restraints to anterior and posterior translation of the sternoclavicular joint. Journal of Shoulder and Elbow Surgery 11, 43-47.

Steinbeck, J., Liljenqvist, U., Jerosch, J., 1998. The anatomy of the glenohumeral ligamentous complex and its contribution to anterior shoulder stability. Journal of Shoulder and Elbow Surgery 7, 122-126

Stokes, I.A.F., Henry, S.M., Single, R.M., 2003. Surface EMG electrodes do not accurately record from lumbar multifidus muscles. Clinical Biomechanics 19, 9-13.

Svendsen, S.W., Bonde, J.P., Mathiassen, S.E., Stengaard-Pedersen, K., Frich, L.H., 2004. Work related shoulder disorders: quantitative exposure-response relations with reference to arm posture. Occupational Environmental Medicine 61, 844-853.

Turkel, S.J., Panio, M.W., Marshall, J.L., Girgis, F.G., 1991. Stabilizing mechanisms preventing anterior dislocation of the glenohumeral joint. Journal of Bone Joint Surgery of America 63, 1208-17.

Turker, K.S., 1993. Electromyography: Some Methodological Problems and Issues. Physical Therapy 73, 698-710.

Urayama, M., Itoi, E., Hatakeyama, Y., Pradhan, R.L., Sato, K., 2001. Function of the 3 portions of the inferior glenohumeral ligament: A cadaveric study. Journal of Shoulder and Elbow Surgery 10, 589-94.

Van der Helm, F.C.T., Veeger, H.E.J., Pronk, G.M., Van Der Woude, L.H.V., Rozendal, R.H., 1992. Geometry parameters for musculoskeletal modelling of the shoulder mechanism. Journal of Biomechanics 25, 129-144.

Van der Helm, F.C.T., 1994a. Analysis of the kinematic and dynamic behavior of the shoulder mechanism. Journal of Biomechanics 27, 527}550.

Van der Helm, F.C.T., 1994b. A finite element musculoskeletal model of the shoulder mechanism. Journal of Biomechanics 27, 551}569.

Veeger, H.E.J., Van Der Helm, F.C.T., Van Der Woude, L.H.V., Pronk, G.M., Rozendal, R.H., 1991. Inertia and muscle contraction parameters for musculoskeletal modelling of the shoulder mechanism. Journal of Biomechanics 24, 615-629.

Werner, S.L., Guido, J.A., Steward, G.W., McNeice, R.P., VanDyke, T., Jones, D.G., 2007. Relationships between throwing mechanics and shoulder distraction in collegiate baseball pitchers. Journal of Shoulder and Elbow Surgery 16, 37-42.

Winter, D.A., 2005. Biomechanics and motor control of human movement 3rd Edition, Toronto: Wiley and Sons.

Winters, J.M., Stark L., 1985. Analysis of fundamental human movement patterns through the use of in-depth antagonistic muscle models. IEEE Transactions on Biomedical Engineering 32, 826-839.

Wood, J.E., Meek, S.G., Jacobsen, S.C., 1989. Quantitation of human shoulder anatomy for prosthetic arm control-I. Surface modeling. Journal of Biomechanics 22, 273-292.

Wood, J.E., Meek, S.G., Jacobsen, S.C., 1989. Quantitation of human shoulder anatomy for prosthetic arm control-II. Anatomy Matrices. Journal of Biomechanics 22, 309-325.

Wu G., van der Helm F.C., Veeger H.E., Makhsous M., Van Roy P., Anglin C., Nagels J., Karduna A.R., McQuade K., Wang X., Werner F.W., Buchholz B.; International Society of Biomechanics, 2005. ISB recommendation on definitions of joint coordinate systems of various joints for the reporting of human joint motion--Part II: shoulder, elbow, wrist and hand. Journal of Biomechanics 38, 981-992.

VIII APPENDICES

APPENDIX A

IDENTIFICATION OF 56 EXPERIMENTAL TRIALS

Posture	Abduction(°)	Flexion(°)	Ext Rot(°)	Hor	Elbow(°)	Force
1	0	0	0	0	0	AB
2	30	0	0	0	0	AB
3	60	0	0	0	0	AB
4	90	0	0	0	0	AB
5	120	0	0	0	0	AB
6	150	0	0	0	0	AB
7	180	0	0	0	0	AB
8	0	-60	0	0	0	FLEX
9	0	-30	0	0	0	FLEX
10	0	0	0	0	0	FLEX
11	0	30	0	0	0	FLEX
12	0	60	0	0	0	FLEX
13	0	90	0	0	0	FLEX
14	0	120	0	0	0	FLEX
15	0	150	0	0	0	FLEX
16	0	180	0	0	0	FLEX
17	90	0	-60	0	90	EXT ROT
18	90	0	-35	0	90	EXT ROT
19	90	0	-10	0	90	EXT ROT
20	90	0	15	0	90	EXT ROT
21	90	0	40	0	90	EXT ROT
22	90	0	65	0	90	EXT ROT
23	90	0	90	0	90	EXT ROT
24	0	90	0	-60	90	HOR AB
25	0	90	0	-15	90	HOR AB
26	0	90	0	30	90	HOR AB
27	0	90	0	75	90	HOR AB
28	0	90	0	120	90	HOR AB
29	0	0	0	0	0	ADD
30	30	0	0	0	0	ADD
31	60	0	0	0	0	ADD
32	90	0	0	0	0	ADD
33	120	0	0	0	0	ADD
34	150	0	0	0	0	ADD
35	180	0	0	0	0	ADD
36	0	-60	0	0	0	EXT
37	0	-30	0	0	0	EXT
38	0	0	0	0	0	EXT
39	0	30	0	0	0	EXT
40	0	60	0	0	0	EXT
41	0	90	0	0	0	EXT
42	0	120	0	0	0	EXT
43	0	150	0	0	0	EXT
44	0	180	0	0	0	EXT
45	90	0	-60	0	90	INT ROT
46	90	0	-35	0	90	INT ROT
47	90	0	-10	0	90	INT ROT
48	90	0	15	0	90	INT ROT
49	90	0	40	0	90	INT ROT
50	90	0	65	0	90	INT ROT
51	90	0	90	0	90	INT ROT
52	0	90	0	-60	90	HOR ADD
53	0	90	0	-15	90	HOR ADD
54	0	90	0	30	90	HOR ADD
55	0	90	0	75	90	HOR ADD
56	0	90	0	120	90	HOR ADD

APPENDIX B

ATTACHMENT SITES FOR MODELING GLENOHUMERAL LIGAMENTS

Ligament	Site	x-coordinate	y-coordinate	z-coordinate
Superior Glenohumeral	Origin	-0.021*h*	0.08*h*	0.05*h*
	Insertion	0.13*s*	-0.028*s*	0.09*s*
Middle Glenohumeral	Origin	-0.022*h*	0.09*h*	0.022*h*
	Insertion	0.22*s*	-0.085*s*	0.105*s*
Inferior Glenohumeral (Anterior)	Origin	0.026*h*	0.065*h*	-0.026*h*
	Insertion	0.251*s*	-0.108*s*	0.086*s*
Inferior Glenohumeral (Inferior)	Origin	0.1*h*	-0.01*h*	-0.015*h*
	Insertion	0.272*s*	-0.125*s*	0.01*s*
Inferior Glenohumeral (Posterior)	Origin	0.026*h*	-0.087*h*	0.012*h*
	Insertion	0.23*s*	-0.065*s*	-0.05*s*

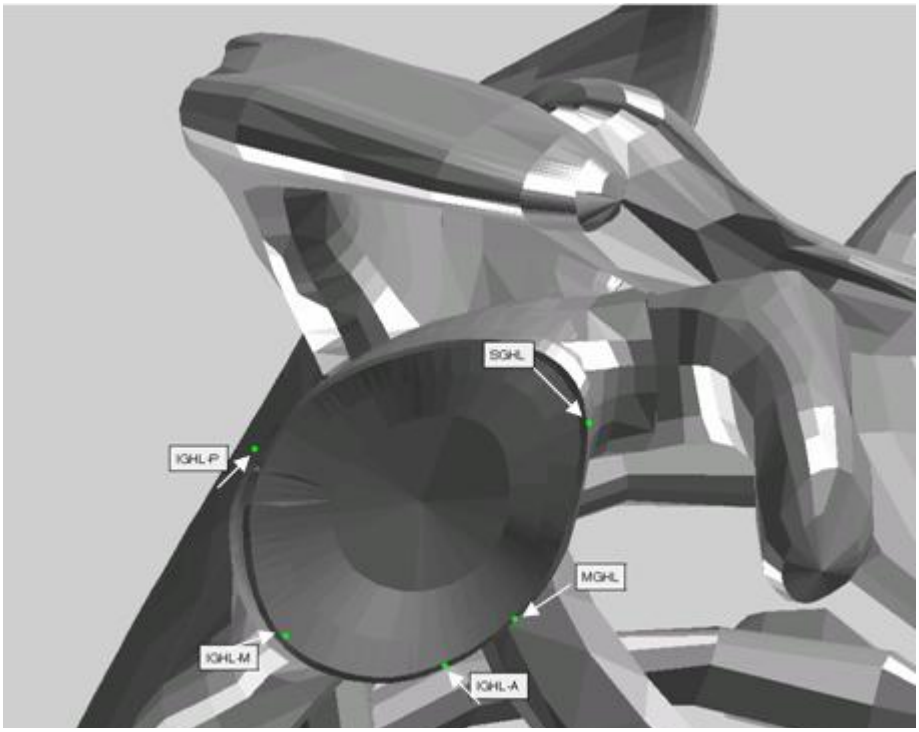

APPENDIX C

NON-CONVERGING TRIALS FOR EACH SUBJECT AND MODEL

TRIAL	S1	S2	S3	S4	S5	S6	S7	S8	S9	S10
1								AL	AL	
2					AL			AL	AL	AL
3		NL/GH/AL					NL/GH/AL	AL		
4										
5										
6	GH/AL	GH/AL	GH/AL			AL		GH/AL		
7	GH/AL	GH	AL				AL	AL	AL	AL
8		NL/GH/AL	NL/GH/AL	NL/ GH/AL	NL/GH/AL					
9		NL/GH/AL			NL/GH/AL		NL/GH/AL	GH/AL	GH/AL	
10		NL/GH/AL								
11	AL		AL	AL				AL		AL
12			AL					AL		
13			AL					AL		
14										
15		AL					GH/AL	AL		
16						AL	AL	AL		
17										
18										
19										
20										
21										
22										
23		AL	AL		AL					
24		AL						AL		
25										
26										
27										
28										
29										
30					AL			AL	AL	
31								AL		
32		AL								
33										
34			AL	AL		AL		AL		
35	GH/AL	GH/AL	GH/AL		AL		AL	AL	GH/AL	AL
36										
37		AL								
38				GH/AL	AL			NL/ GH/AL		
39	AL	NL/GH/AL						AL	AL	AL
40		AL	AL					AL		
41										
42		AL						AL		
43					NL/GH/AL			AL		
44	GH/AL		AL		NL/GH/AL		AL	AL		
45										
46										
47										
48										
49		NL/AL								
50		AL						AL		
51										
52		AL								
53										
54										
55								AL		
56										

APPENDIX D

LIGAMENT LENGTH OF NINE LIGAMENT PLOTTED AGAINST VARYING POSTURES

A graph of ligament length as predicted by the model for all 56 postures is shown for each subject.
Postures 1-7: Abduction; Postures 8-16: Extension-Flexion; Postures 17-23: Internal/External rotation; Postures 24-28: Horizontal Ad/Abduction. Postures 29-56 are a repetition of postures 1-28.

Subject #1

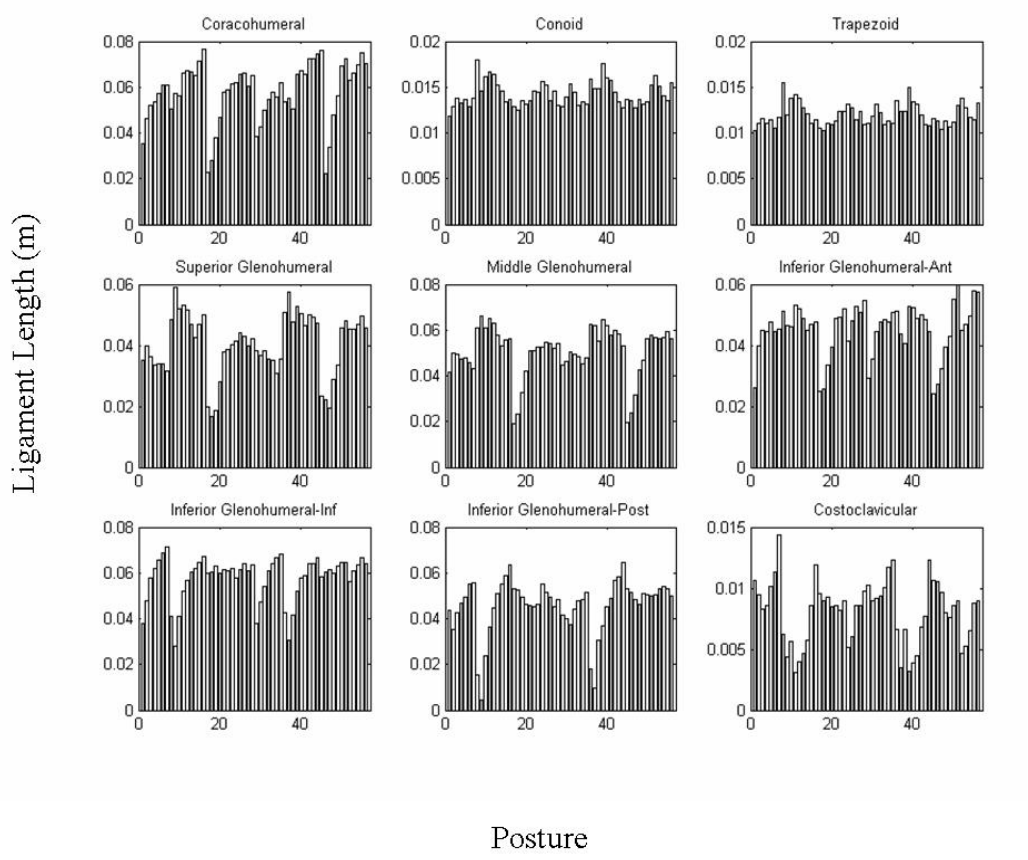

Subject #2

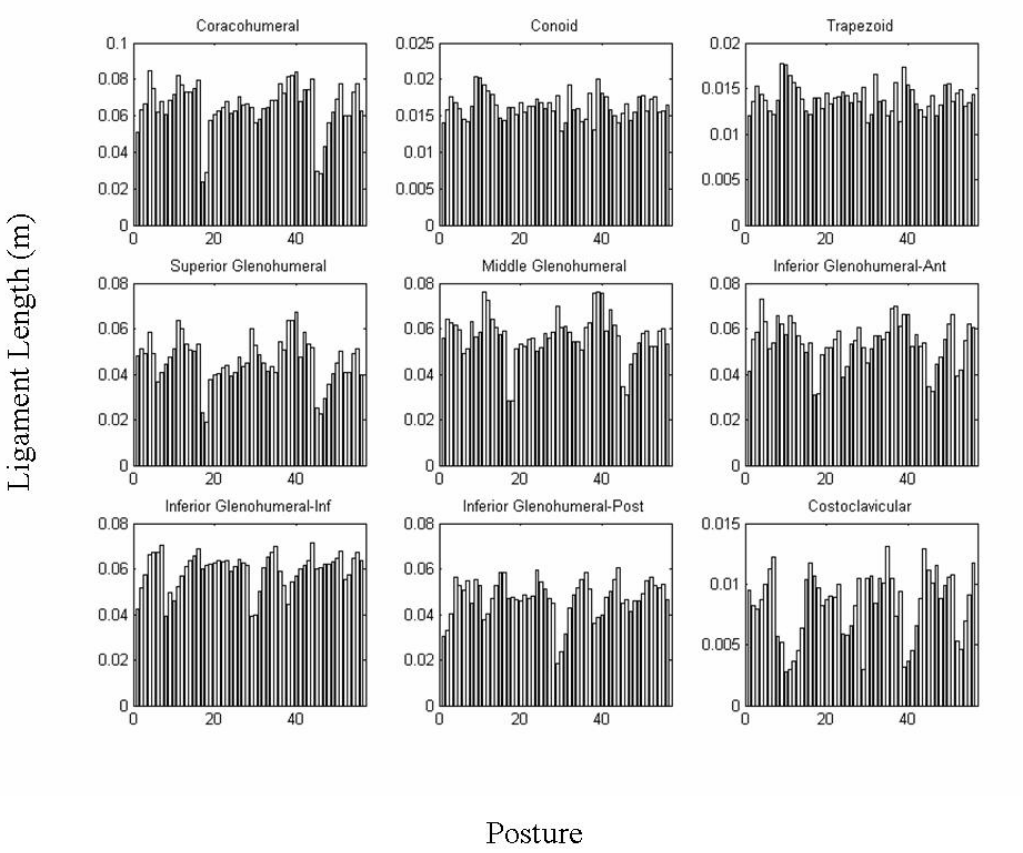
Coracohumeral
Conoid
Trapezoid
Superior Glenohumeral
Middle Glenohumeral
Inferior Glenohumeral-Ant
Inferior Glenohumeral-Inf
Inferior Glenohumeral-Post
Costoclavicular
Ligament Length (m)
Posture

Subject #3

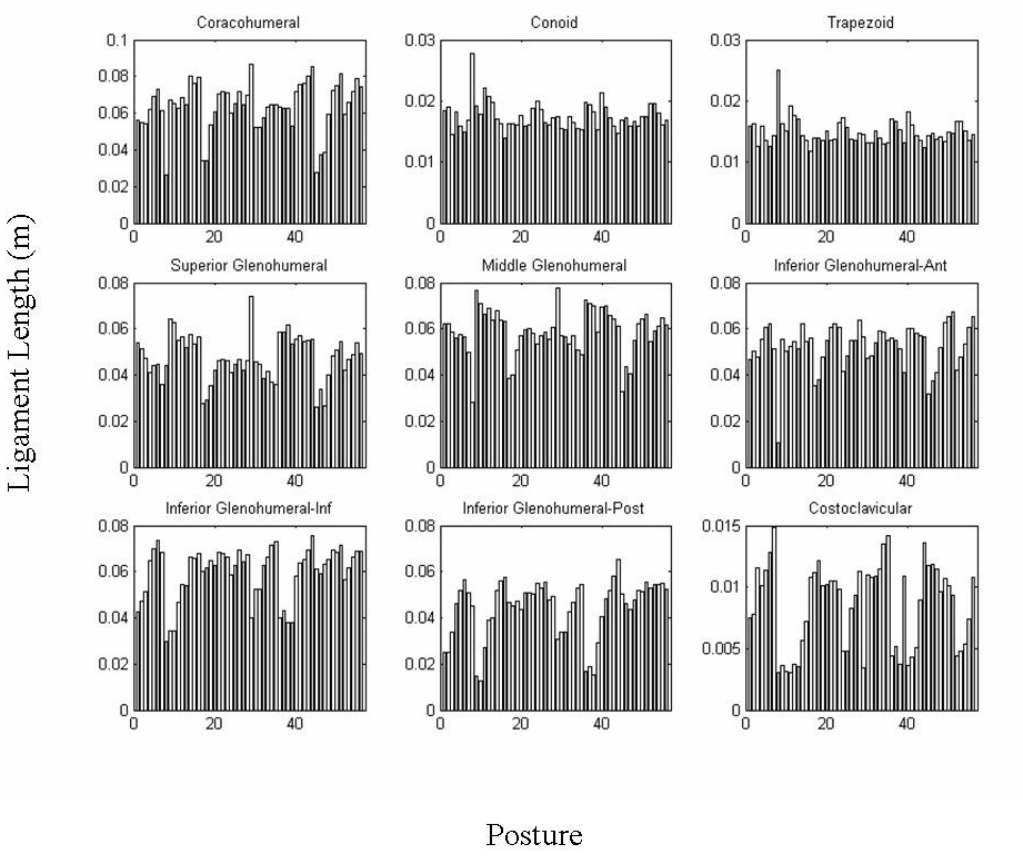
Coracohumeral
Conoid
Trapezoid
Superior Glenohumeral
Middle Glenohumeral
Inferior Glenohumeral-Ant
Inferior Glenohumeral-Inf
Inferior Glenohumeral-Post
Costoclavicular
Ligament Length (m)
Posture

Subject #4

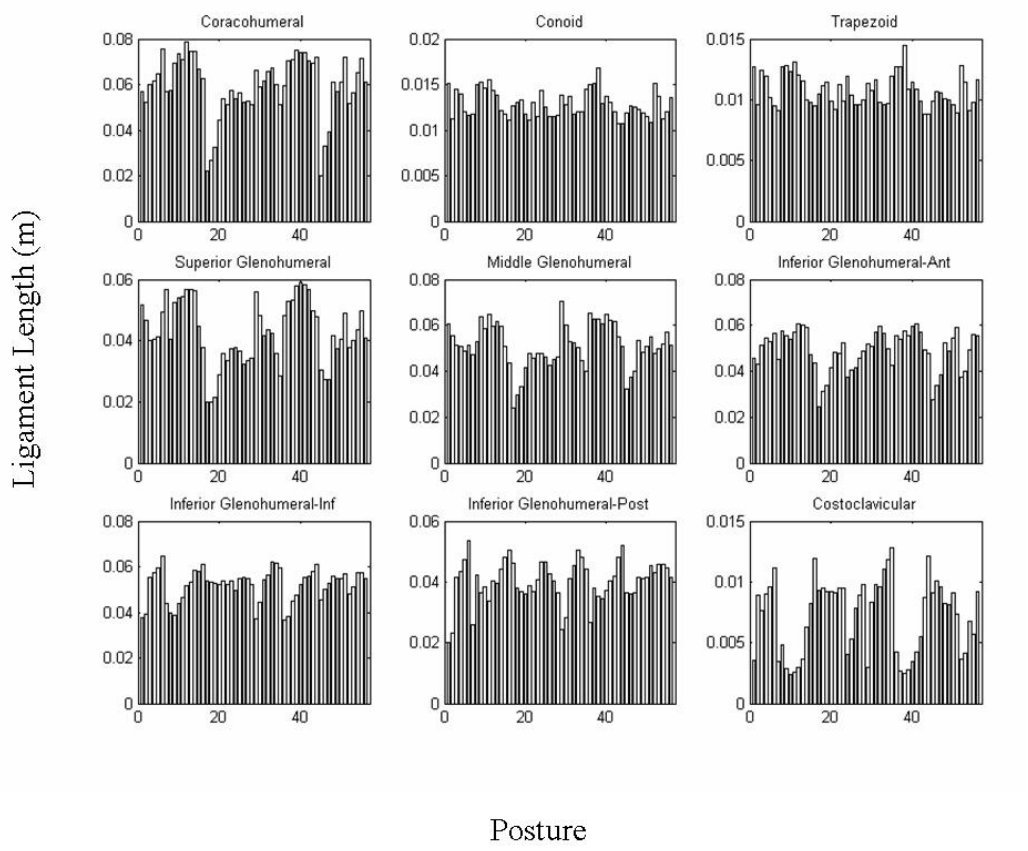
Coracohumeral
Conoid
Trapezoid
Superior Glenohumeral
Middle Glenohumeral
Inferior Glenohumeral-Ant
Inferior Glenohumeral-Inf
Inferior Glenohumeral-Post
Costoclavicular
Ligament Length (m)
Posture

Subject #5

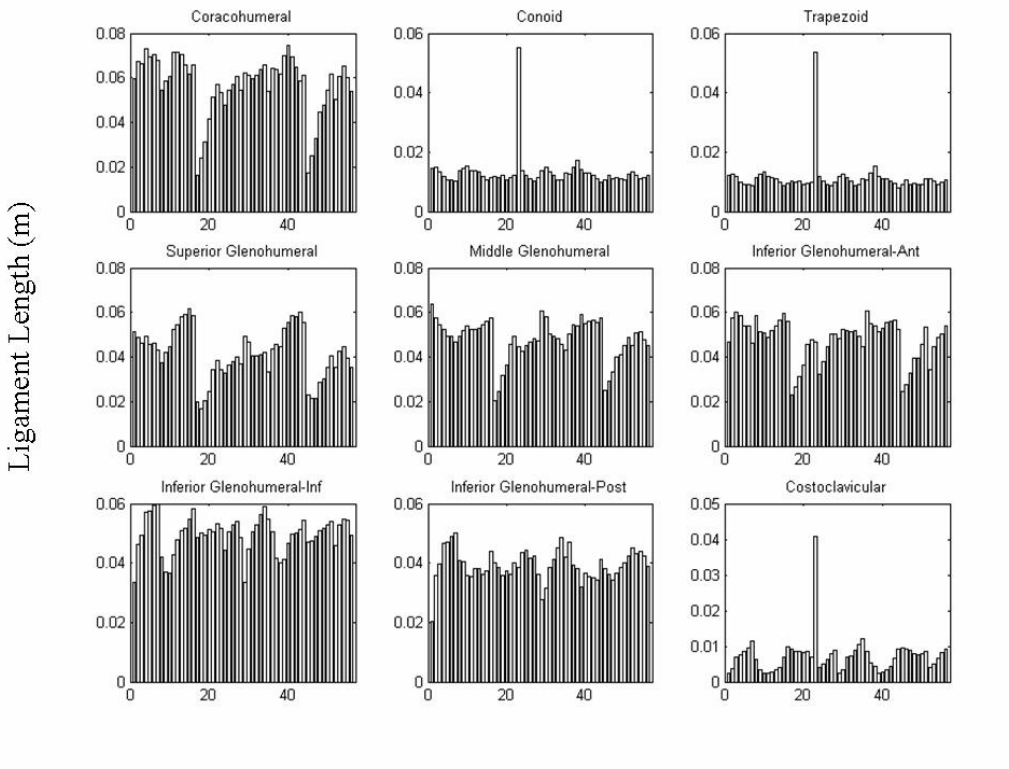
Coracohumeral
Conoid
Trapezoid
Superior Glenohumeral
Middle Glenohumeral
Inferior Glenohumeral-Ant
Inferior Glenohumeral-Inf
Inferior Glenohumeral-Post
Costoclavicular
Ligament Length (m)
Posture

Subject #6

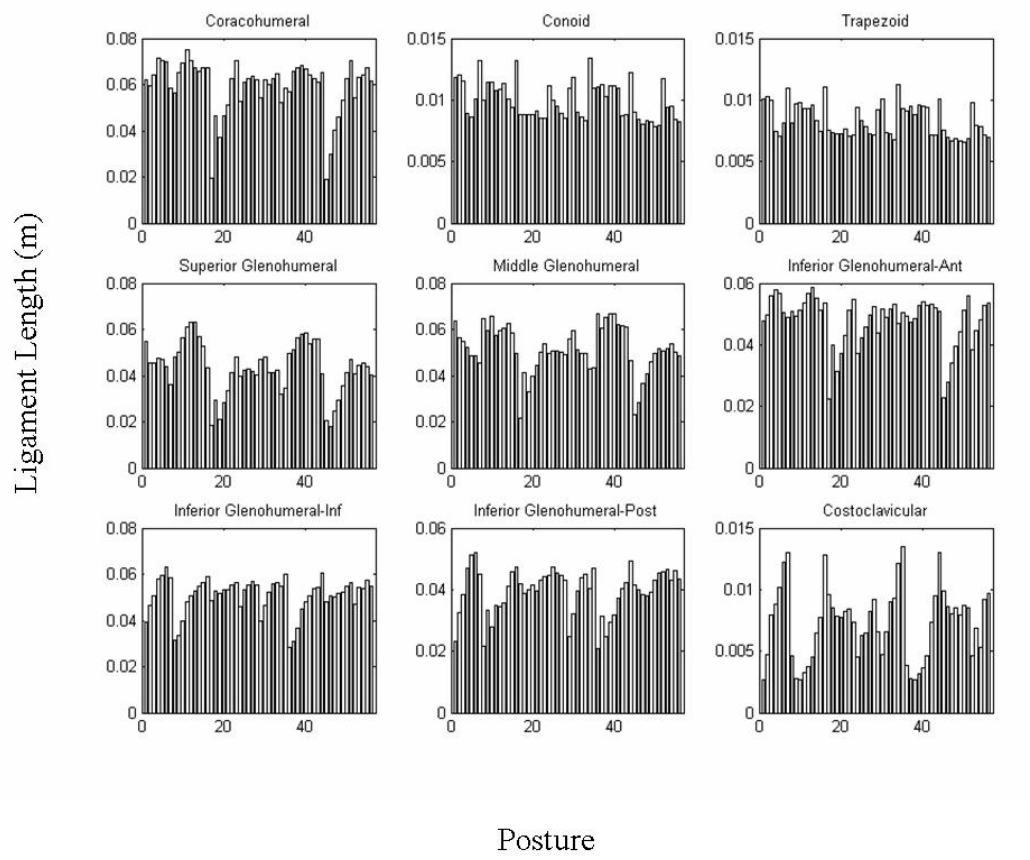
Coracohumeral
Conoid
Trapezoid
Superior Glenohumeral
Middle Glenohumeral
Inferior Glenohumeral-Ant
Inferior Glenohumeral-Inf
Inferior Glenohumeral-Post
Costoclavicular
Ligament Length (m)
Posture

Subject #7

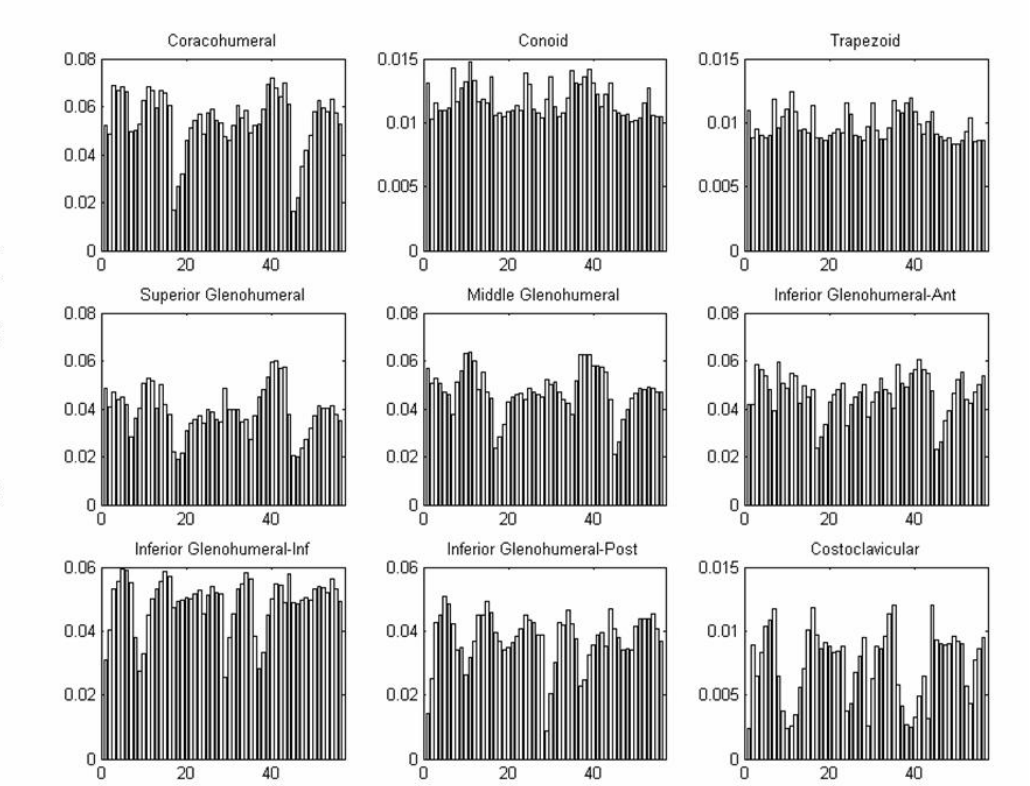
Coracohumeral
Conoid
Trapezoid
Superior Glenohumeral
Middle Glenohumeral
Inferior Glenohumeral-Ant
Inferior Glenohumeral-Inf
Inferior Glenohumeral-Post
Costoclavicular
Posture

Subject #8

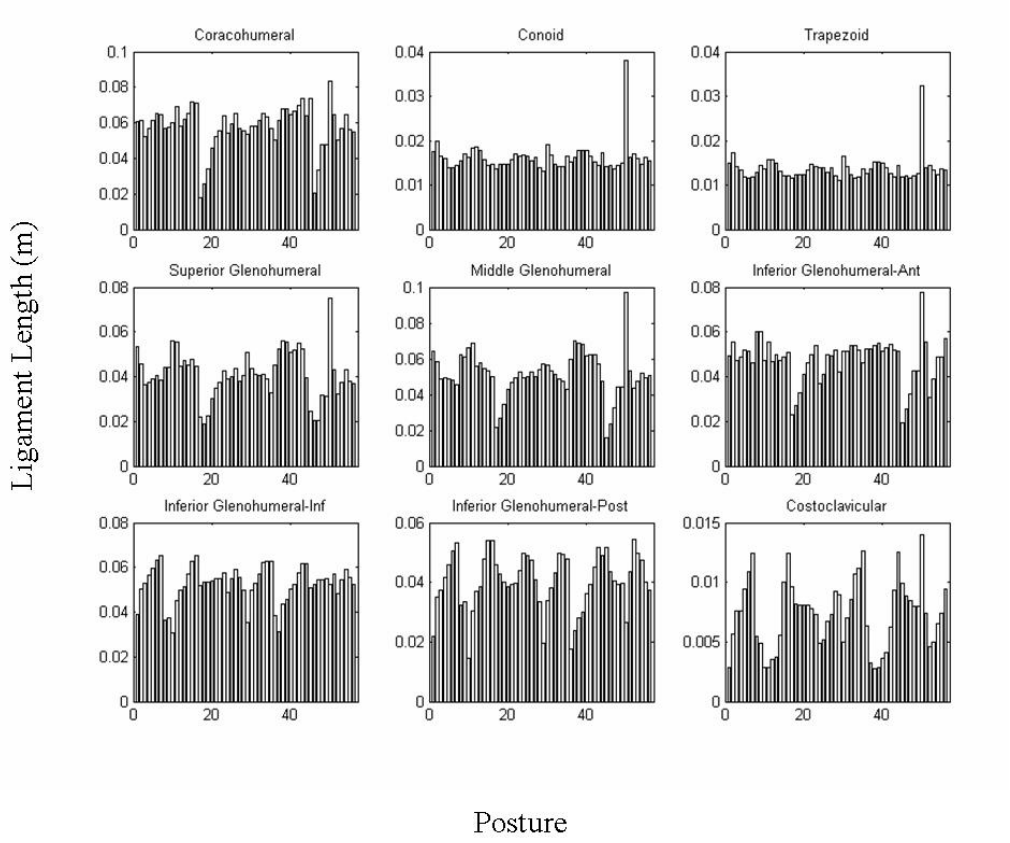
Coracohumeral
Conoid
Trapezoid
Superior Glenohumeral
Middle Glenohumeral
Inferior Glenohumeral-Ant
Inferior Glenohumeral-Inf
Inferior Glenohumeral-Post
Costoclavicular
Ligament Length (m)
Posture

Subject #9

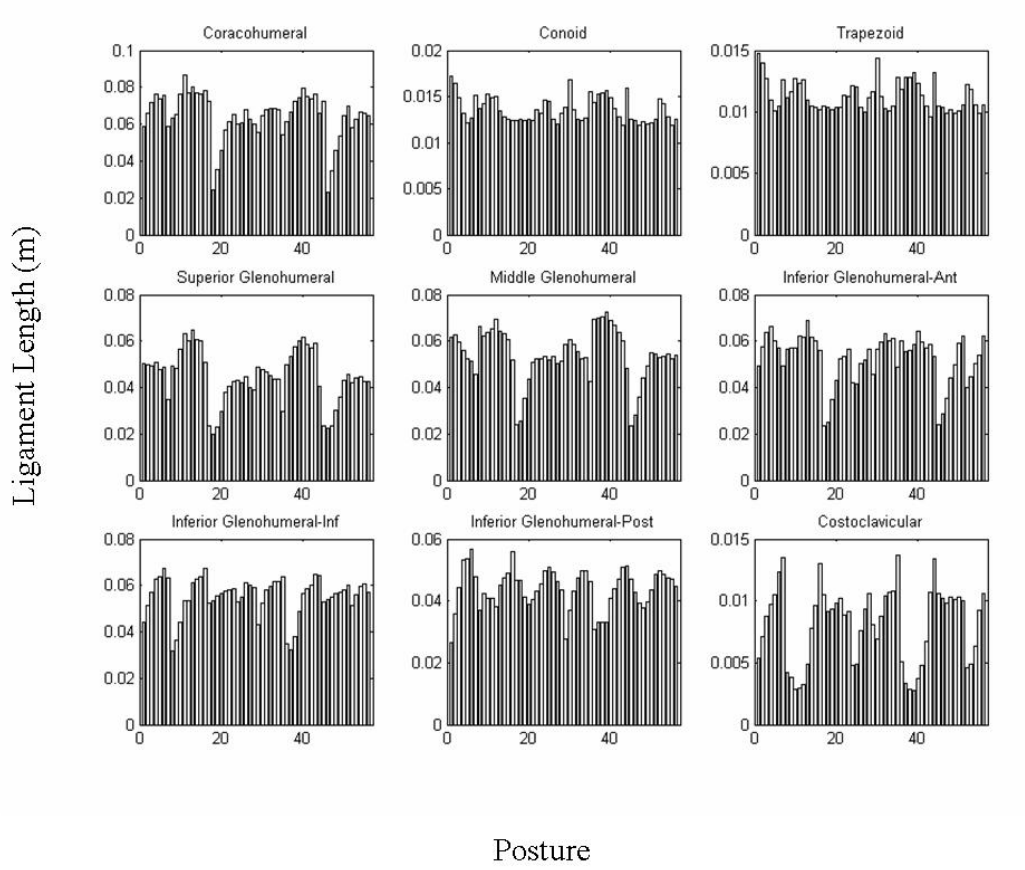
Coracohumeral
Conoid
Trapezoid
Superior Glenohumeral
Middle Glenohumeral
Inferior Glenohumeral-Ant
Inferior Glenohumeral-Inf
Inferior Glenohumeral-Post
Costoclavicular
Ligament Length (m)
Posture

Subject #10

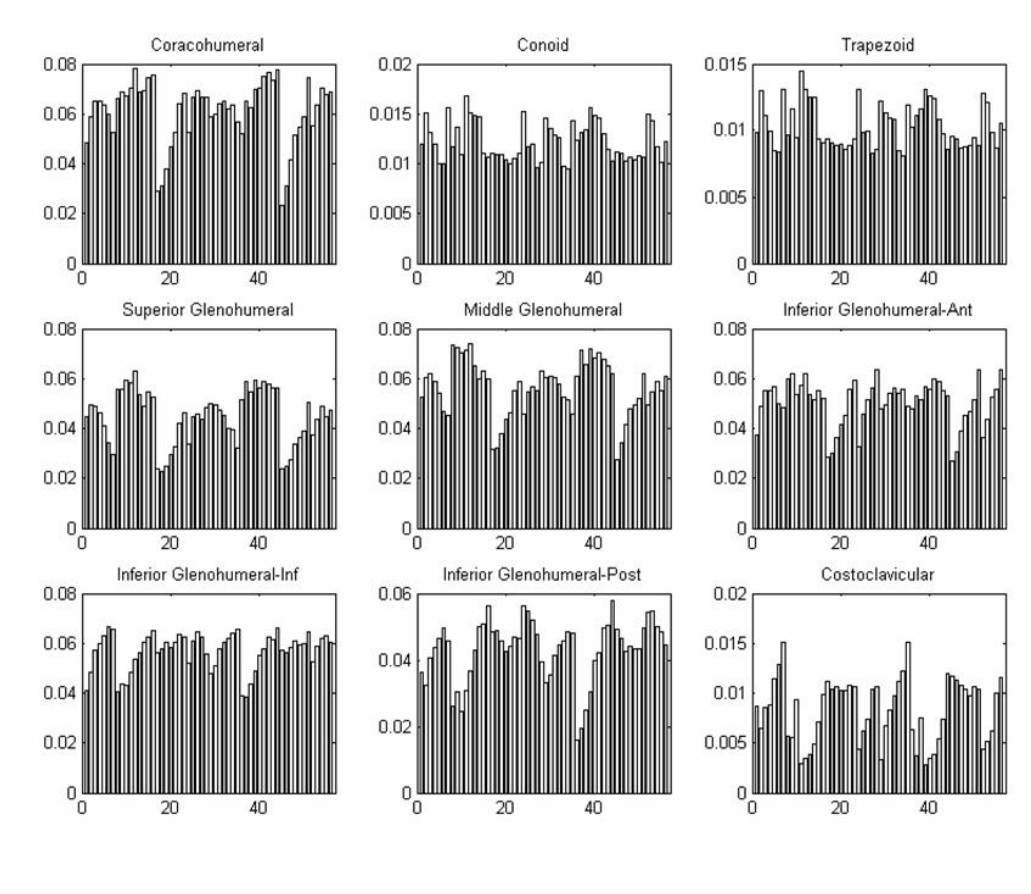

Posture

APPENDIX E

LIGAMENT FORCE OF NINE LIGAMENTS PLOTTED AGAINST VARYING POSTURES

A graph of the force in each ligament as predicted by the model for all 56 postures is shown for each subject.
Postures 1-7: Abduction; Postures 8-16: Extension-Flexion; Postures 17-23: Internal/External rotation; Postures 24-28: Horizontal Ad/Abduction. Postures 29-56 are a repetition of postures 1-28.

Subject #1

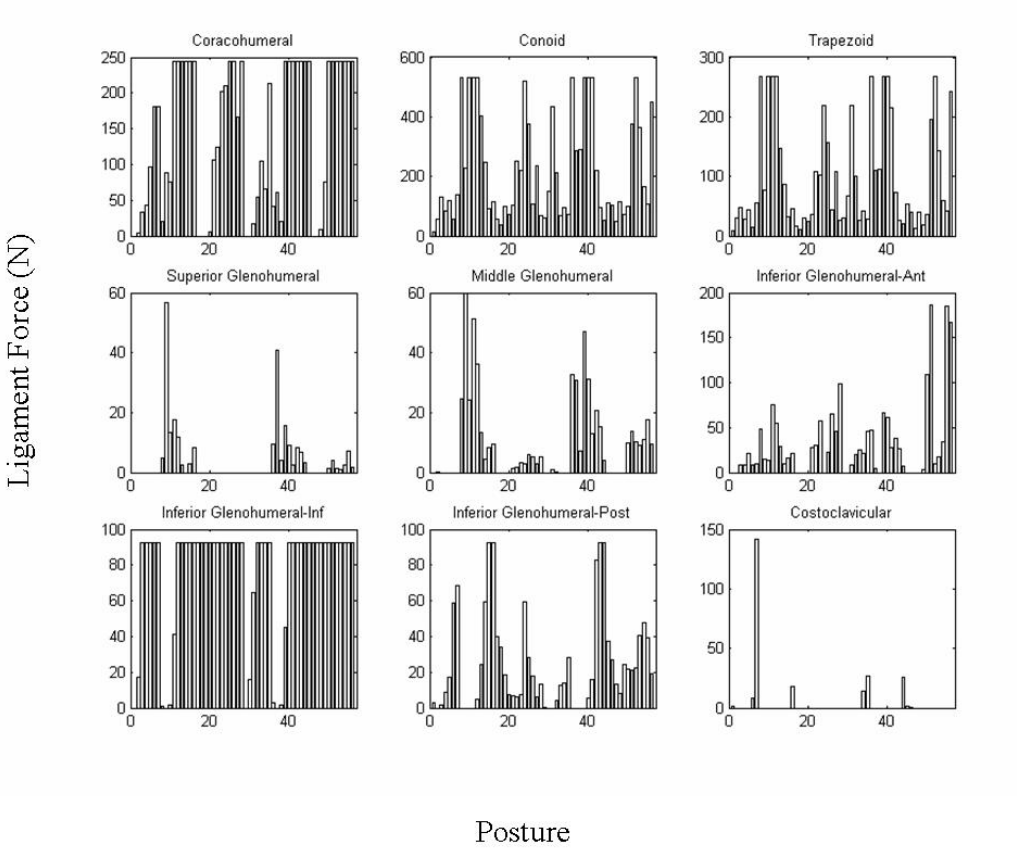

Subject #2

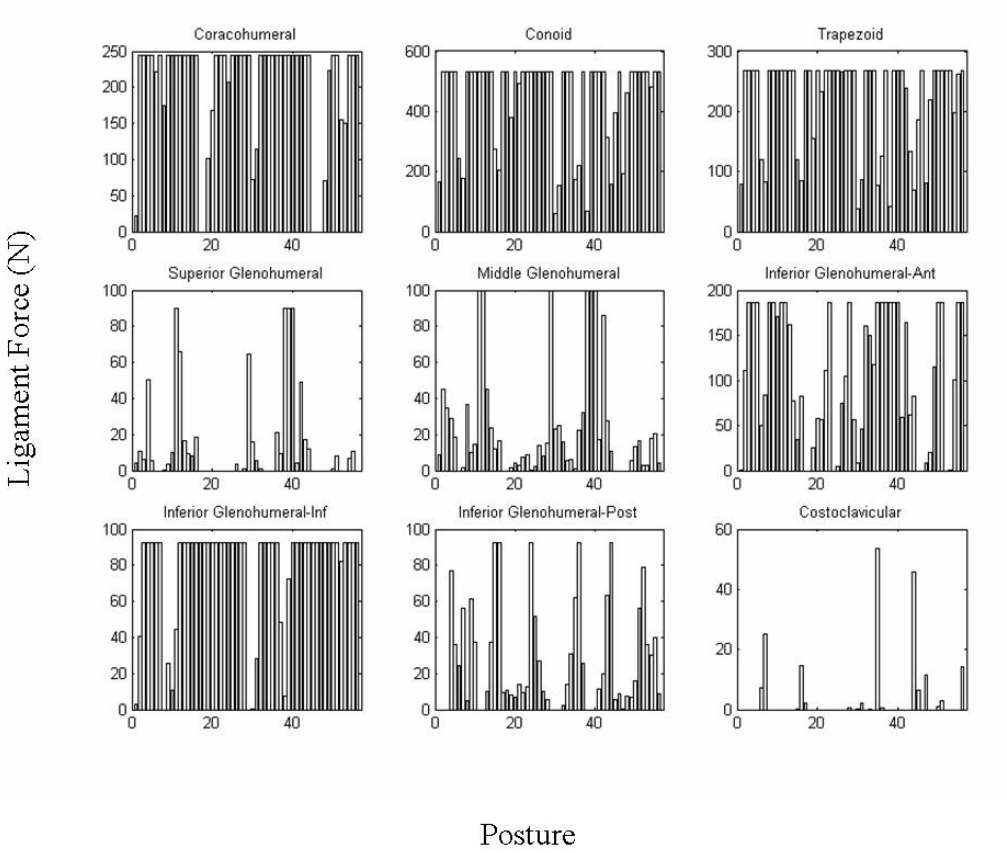
Coracohumeral
Conoid
Trapezoid
Superior Glenohumeral
Middle Glenohumeral
Inferior Glenohumeral-Ant
Inferior Glenohumeral-Inf
Inferior Glenohumeral-Post
Costoclavicular
Ligament Force (N)
Posture

Subject #3

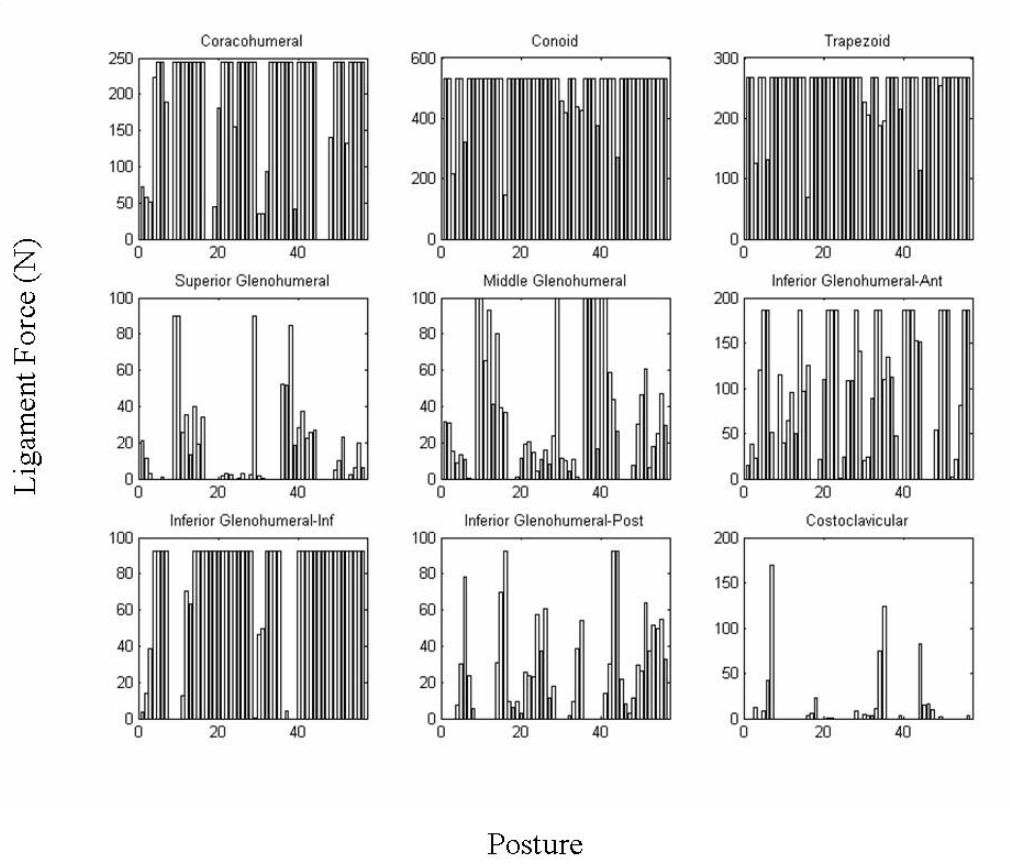
Coracohumeral
Conoid
Trapezoid
Superior Glenohumeral
Middle Glenohumeral
Inferior Glenohumeral-Ant
Inferior Glenohumeral-Inf
Inferior Glenohumeral-Post
Costoclavicular
Ligament Force (N)
Posture

Subject #4

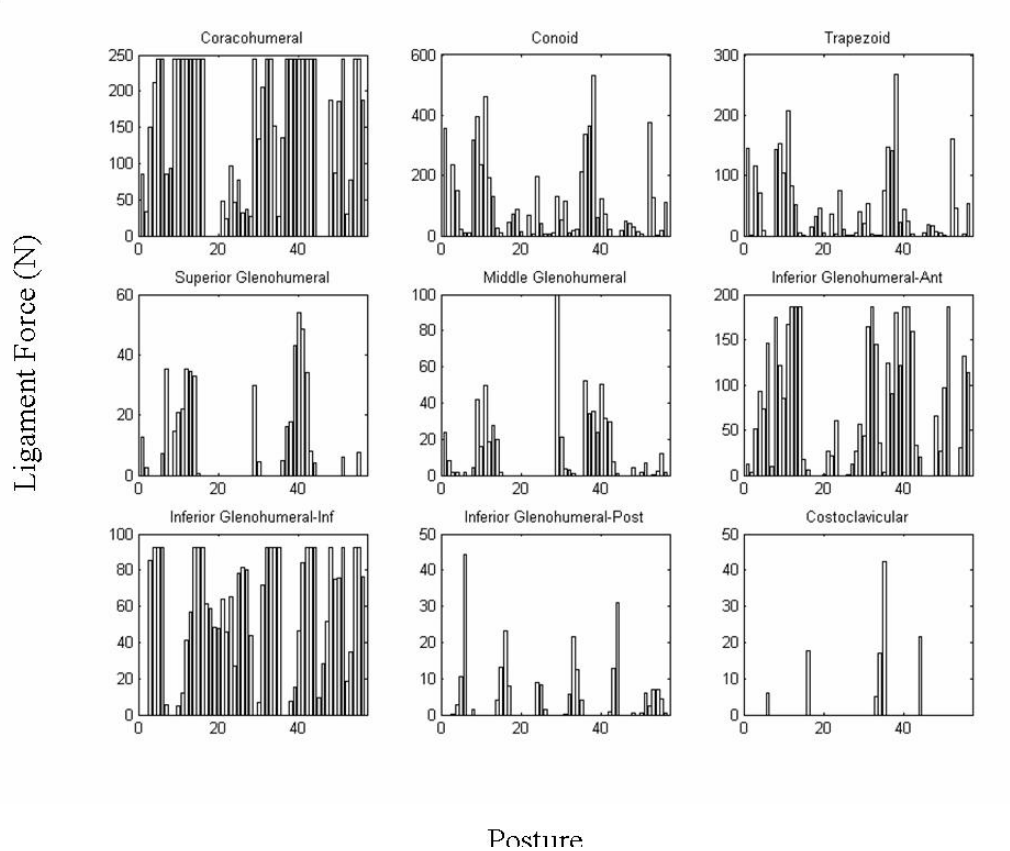
Coracohumeral
Conoid
Trapezoid
Superior Glenohumeral
Middle Glenohumeral
Inferior Glenohumeral-Ant
Inferior Glenohumeral-Inf
Inferior Glenohumeral-Post
Costoclavicular
Ligament Force (N)
Posture

Subject #5

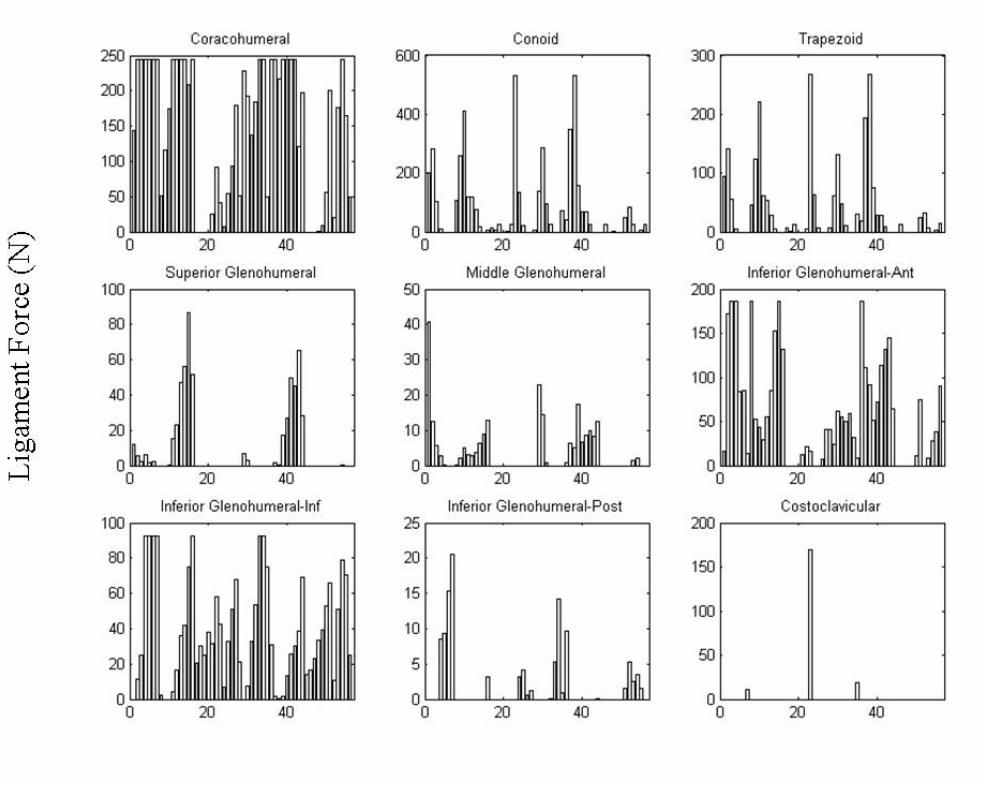
Coracohumeral
Conoid
Trapezoid
Superior Glenohumeral
Middle Glenohumeral
Inferior Glenohumeral-Ant
Inferior Glenohumeral-Inf
Inferior Glenohumeral-Post
Costoclavicular
Ligament Force (N)
Posture

Subject #6

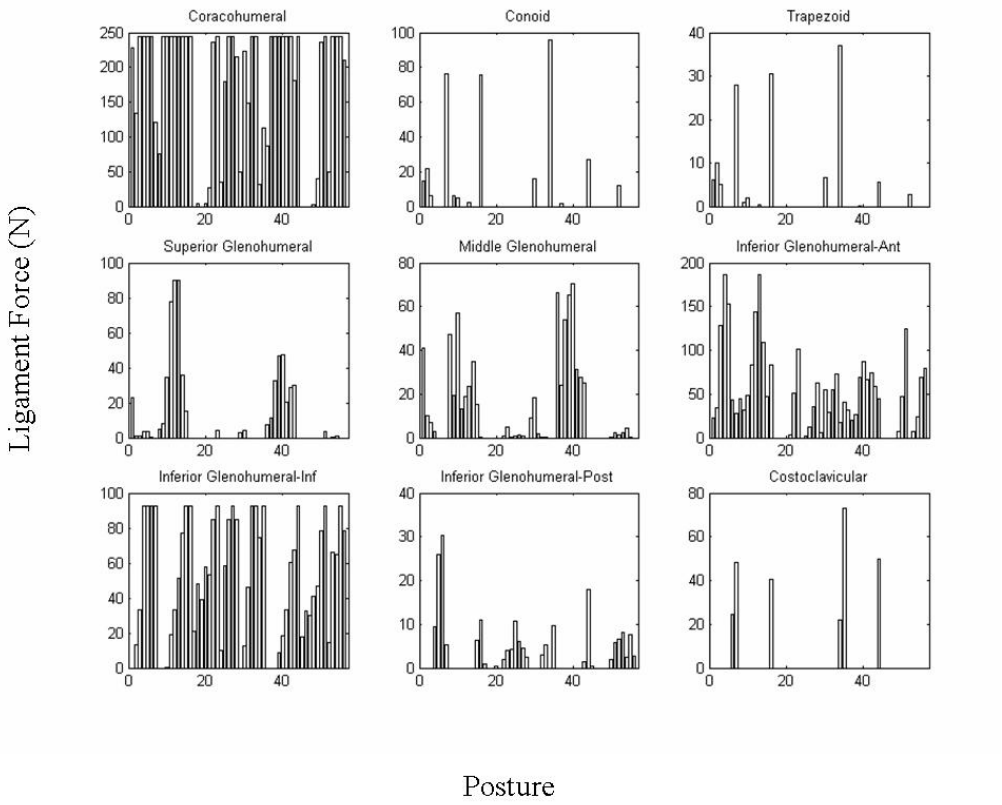
Coracohumeral
Conoid
Trapezoid
Superior Glenohumeral
Middle Glenohumeral
Inferior Glenohumeral-Ant
Inferior Glenohumeral-Inf
Inferior Glenohumeral-Post
Costoclavicular
Ligament Force (N)
Posture

Subject #7

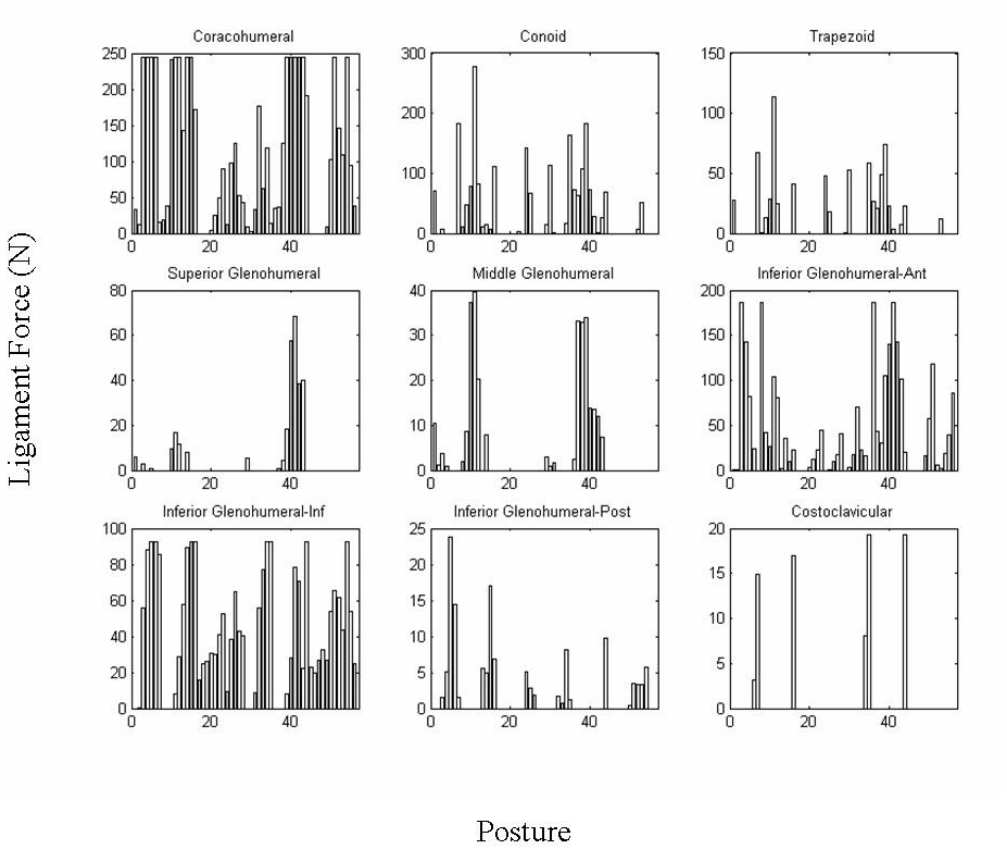
Coracohumeral
Conoid
Trapezoid
Superior Glenohumeral
Middle Glenohumeral
Inferior Glenohumeral-Ant
Inferior Glenohumeral-Inf
Inferior Glenohumeral-Post
Costoclavicular
Ligament Force (N)
Posture

Subject #8

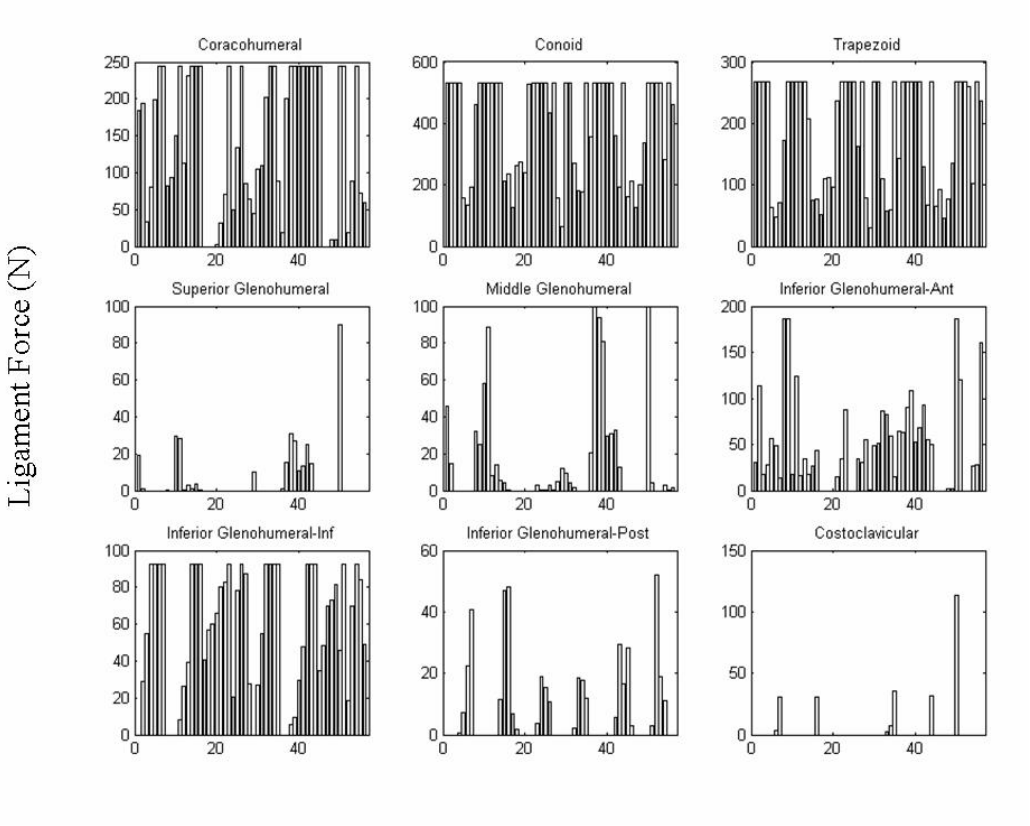
Coracohumeral
Conoid
Trapezoid
Superior Glenohumeral
Middle Glenohumeral
Inferior Glenohumeral-Ant
Inferior Glenohumeral-Inf
Inferior Glenohumeral-Post
Costoclavicular
Ligament Force (N)
Posture

Subject #9

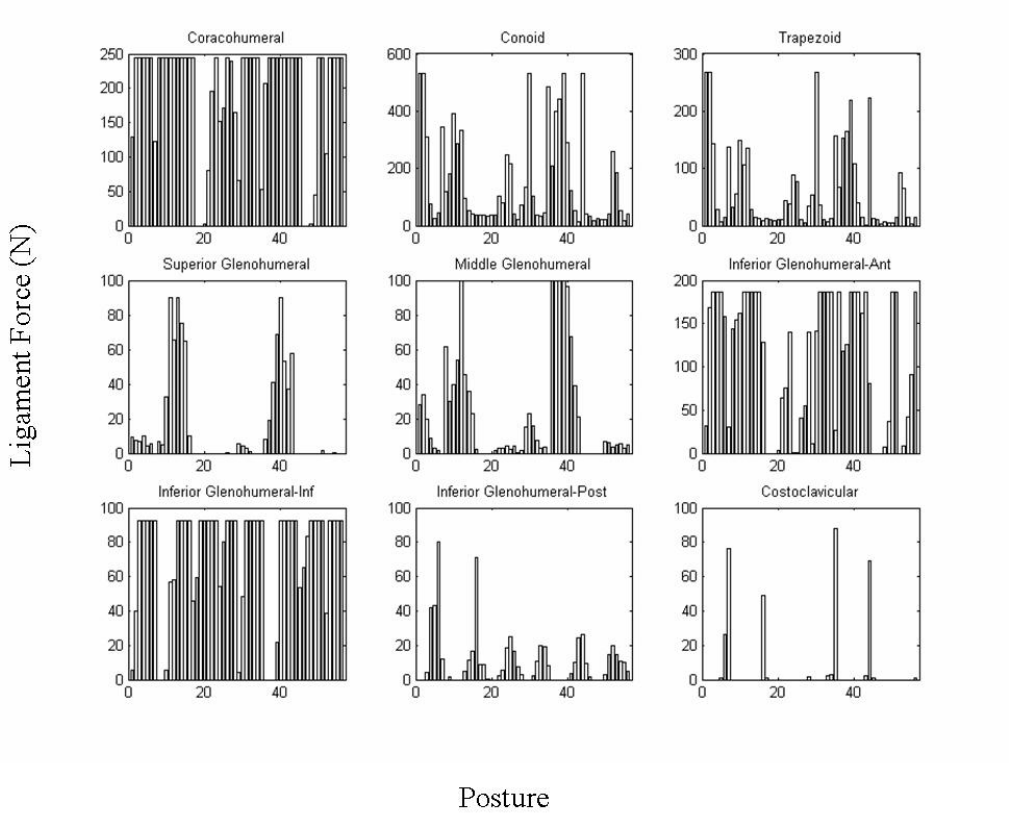
Coracohumeral
Conoid
Trapezoid
Superior Glenohumeral
Middle Glenohumeral
Inferior Glenohumeral-Ant
Inferior Glenohumeral-Inf
Inferior Glenohumeral-Post
Costoclavicular
Ligament Force (N)
Posture

Subject #10

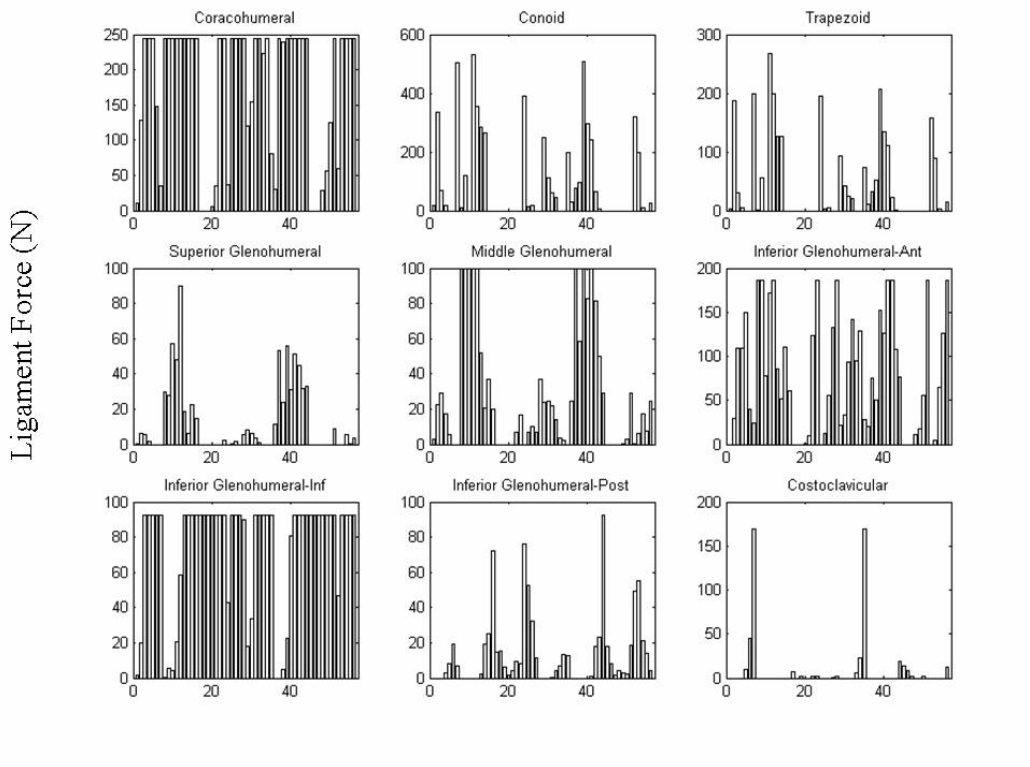
Coracohumeral
Conoid
Trapezoid
Superior Glenohumeral
Middle Glenohumeral
Inferior Glenohumeral-Ant
Inferior Glenohumeral-Inf
Inferior Glenohumeral-Post
Costoclavicular
Ligament Force (N)
Posture

APPENDIX F

EMG AMPLITUDE COMPARED WITH PREDICTED MUSCLE FORCE FOR EACH SUBJECT AND MUSCLE - NL MODEL

A scatter plot of predicted muscle force from the No-Ligament model versus EMG amplitude is shown for 11 muscles for each subject.

Subject #1

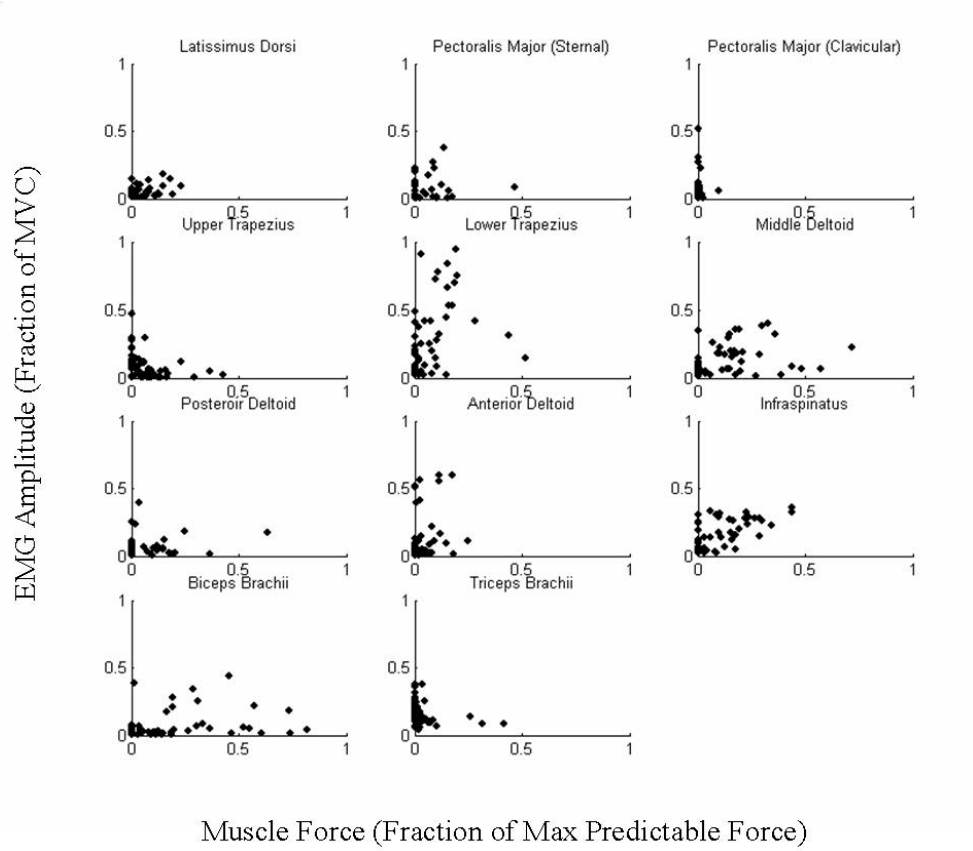

Subject #2

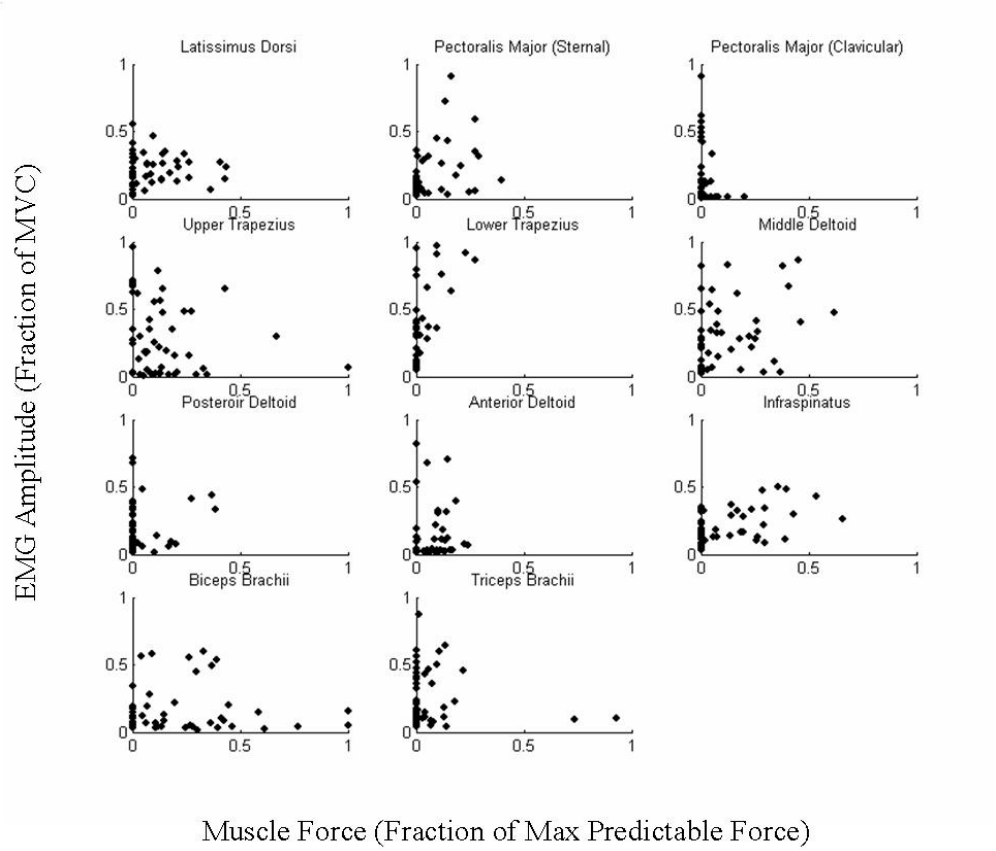
Latissimus Dorsi
Pectoralis Major (Sternal)
Pectoralis Major (Clavicular)
Upper Trapezius
Lower Trapezius
Middle Deltoid
Posteroir Deltoid
Anterior Deltoid
Infraspinatus
Biceps Brachii
Triceps Brachii
EMG Amplitude (Fraction of MVC)
Muscle Force (Fraction of Max Predictable Force)

Subject #3

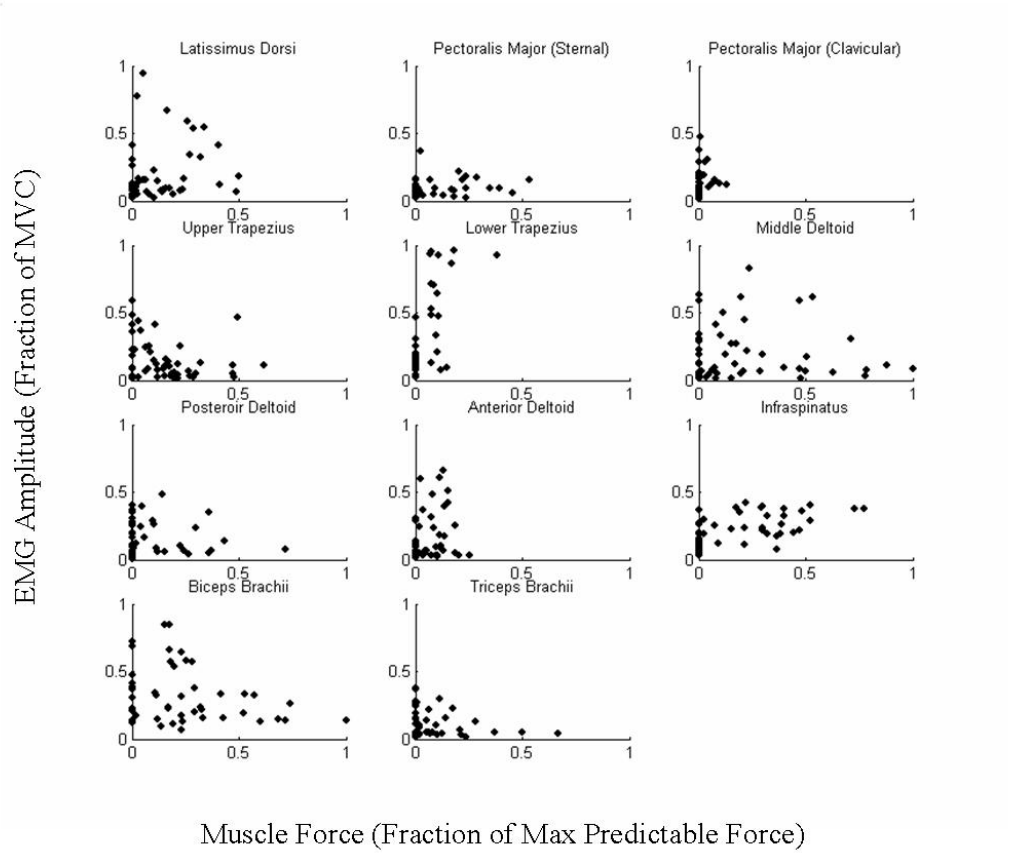
Latissimus Dorsi
Pectoralis Major (Sternal)
Pectoralis Major (Clavicular)
Upper Trapezius
Lower Trapezius
Middle Deltoid
Posteroir Deltoid
Anterior Deltoid
Infraspinatus
Biceps Brachii
Triceps Brachii
EMG Amplitude (Fraction of MVC)
Muscle Force (Fraction of Max Predictable Force)

Subject #4

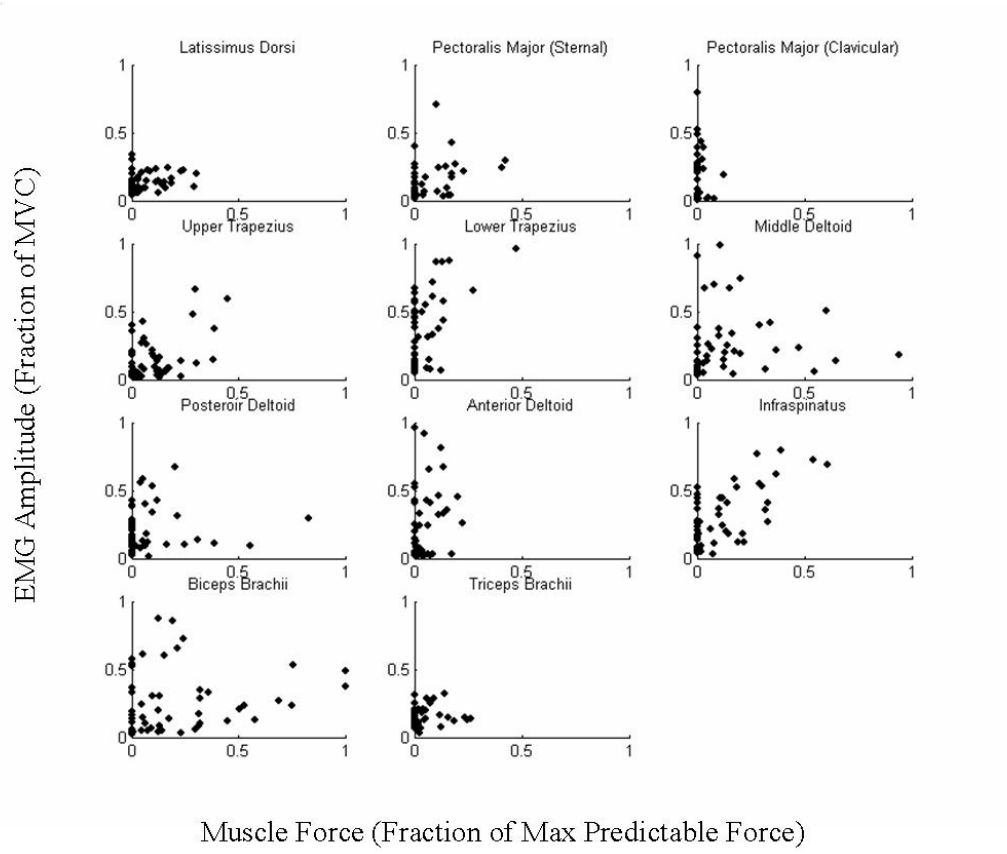
Latissimus Dorsi
Pectoralis Major (Sternal)
Pectoralis Major (Clavicular)
Upper Trapezius
Lower Trapezius
Middle Deltoid
Posteroir Deltoid
Anterior Deltoid
Infraspinatus
Biceps Brachii
Triceps Brachii
EMG Amplitude (Fraction of MVC)
Muscle Force (Fraction of Max Predictable Force)

Subject #5

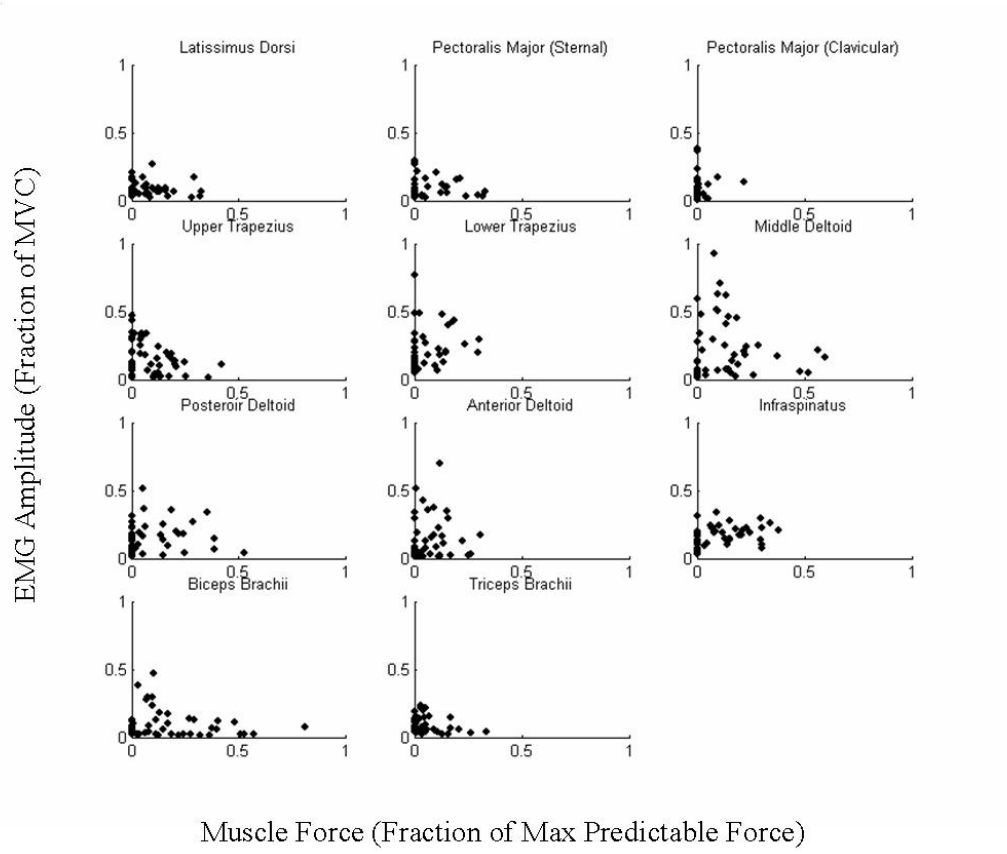
Latissimus Dorsi
Pectoralis Major (Sternal)
Pectoralis Major (Clavicular)
Upper Trapezius
Lower Trapezius
Middle Deltoid
Posteroir Deltoid
Anterior Deltoid
Infraspinatus
Biceps Brachii
Triceps Brachii
EMG Amplitude (Fraction of MVC)
Muscle Force (Fraction of Max Predictable Force)

Subject #6

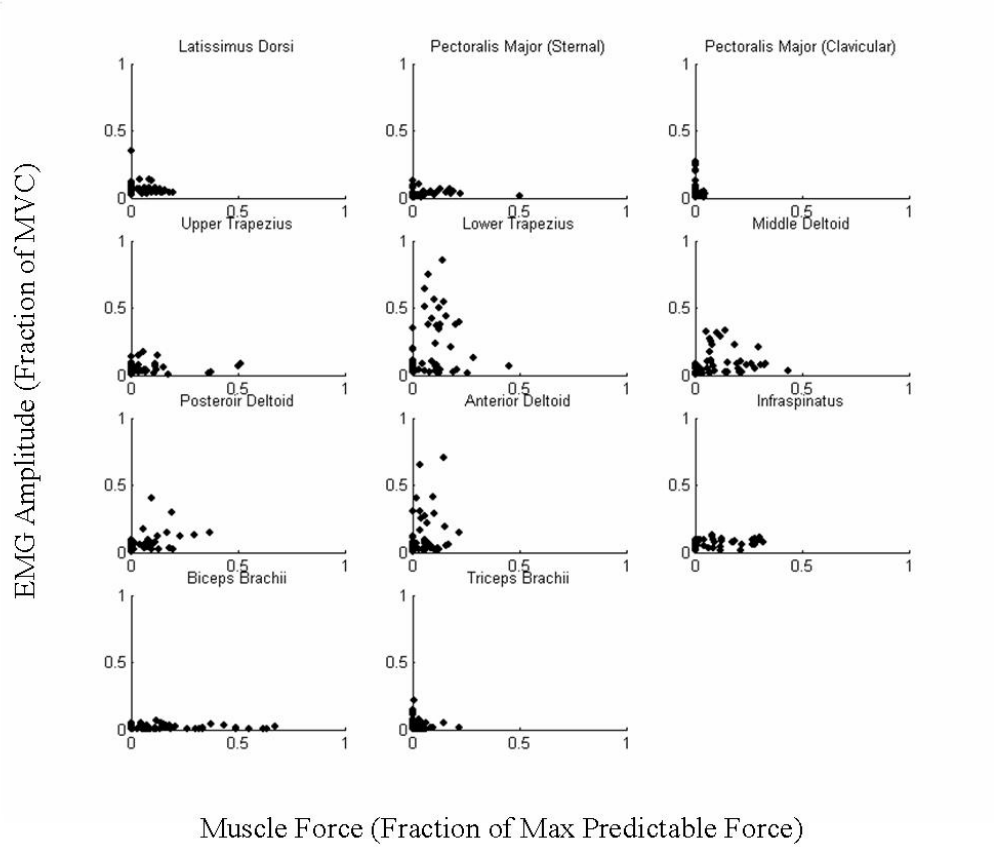
Latissimus Dorsi
Pectoralis Major (Sternal)
Pectoralis Major (Clavicular)
Upper Trapezius
Lower Trapezius
Middle Deltoid
Posteroir Deltoid
Anterior Deltoid
Infraspinatus
Biceps Brachii
Triceps Brachii
EMG Amplitude (Fraction of MVC)
Muscle Force (Fraction of Max Predictable Force)

Subject #7

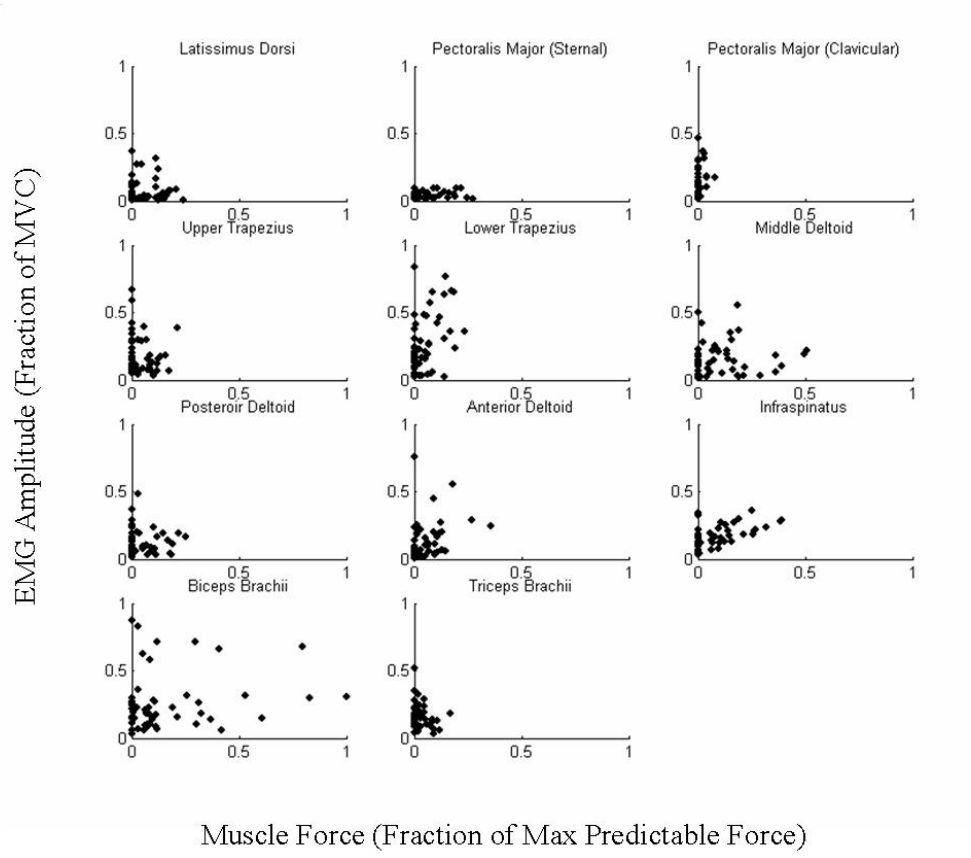
Latissimus Dorsi
Pectoralis Major (Sternal)
Pectoralis Major (Clavicular)
Upper Trapezius
Lower Trapezius
Middle Deltoid
Posteroir Deltoid
Anterior Deltoid
Infraspinatus
Biceps Brachii
Triceps Brachii
EMG Amplitude (Fraction of MVC)
Muscle Force (Fraction of Max Predictable Force)

Subject #8

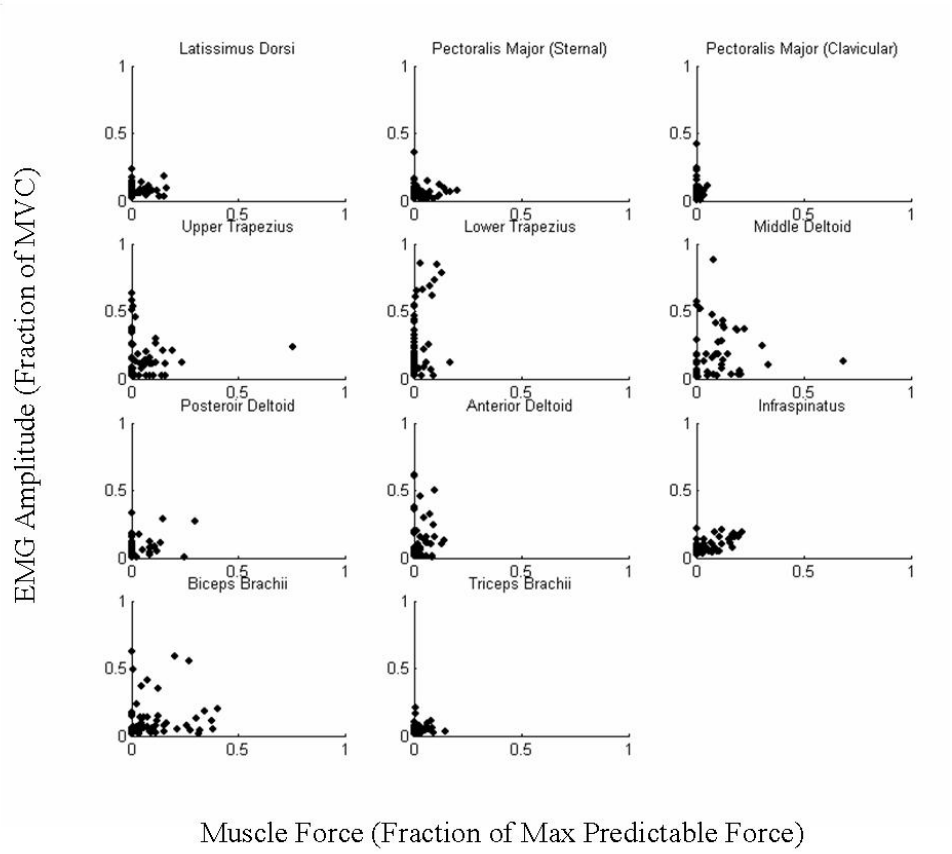
Latissimus Dorsi
Pectoralis Major (Sternal)
Pectoralis Major (Clavicular)
Upper Trapezius
Lower Trapezius
Middle Deltoid
Posteroir Deltoid
Anterior Deltoid
Infraspinatus
Biceps Brachii
Triceps Brachii
EMG Amplitude (Fraction of MVC)
Muscle Force (Fraction of Max Predictable Force)

Subject #9

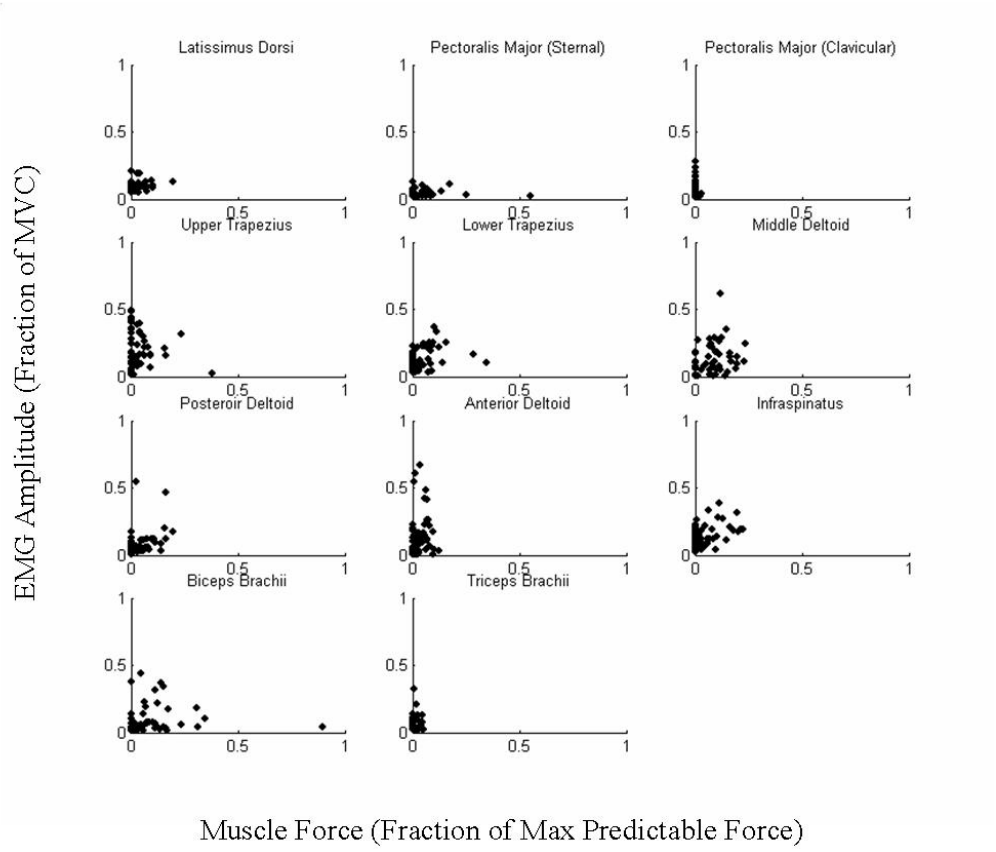
Latissimus Dorsi
Pectoralis Major (Sternal)
Pectoralis Major (Clavicular)
Upper Trapezius
Lower Trapezius
Middle Deltoid
Posteroir Deltoid
Anterior Deltoid
Infraspinatus
Biceps Brachii
Triceps Brachii
EMG Amplitude (Fraction of MVC)
Muscle Force (Fraction of Max Predictable Force)

Subject #10

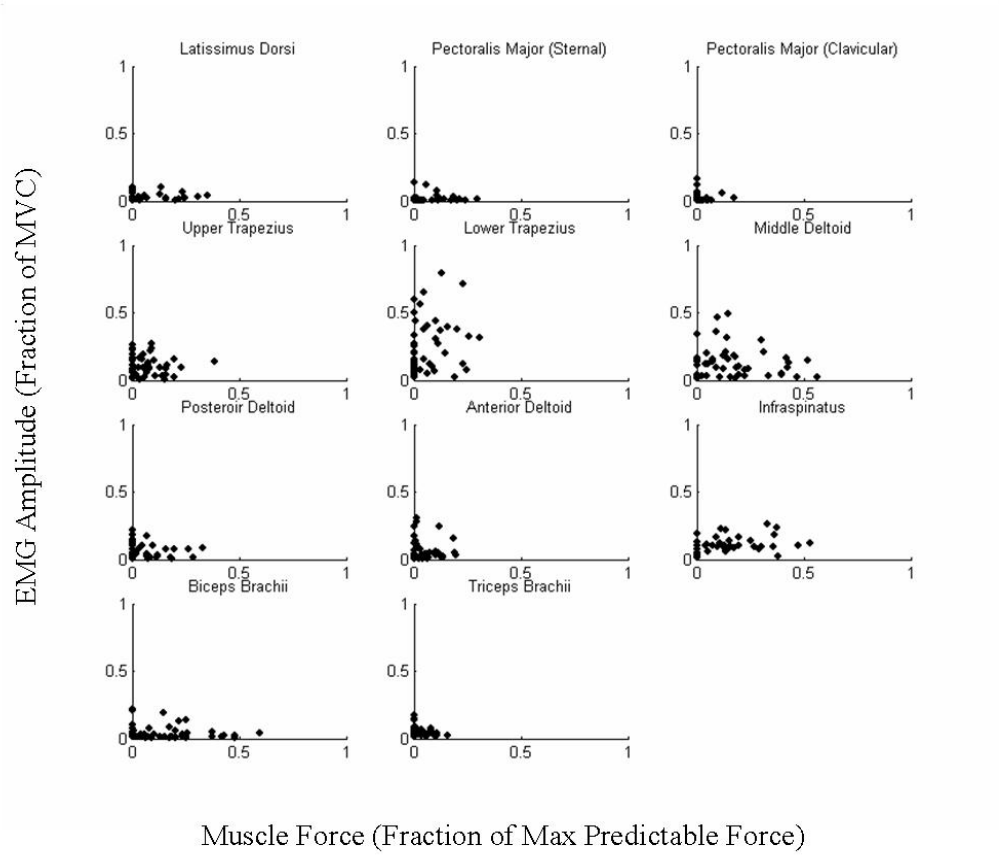
Latissimus Dorsi
Pectoralis Major (Sternal)
Pectoralis Major (Clavicular)
Upper Trapezius
Lower Trapezius
Middle Deltoid
Posteroir Deltoid
Anterior Deltoid
Infraspinatus
Biceps Brachii
Triceps Brachii
EMG Amplitude (Fraction of MVC)
Muscle Force (Fraction of Max Predictable Force)

APPENDIX G

EMG AMPLITUDE COMPARED WITH PREDICTED MUSCLE FORCE FOR EACH SUBJECT AND MUSCLE - GH MODEL

A scatter plot of predicted muscle force from the Glenohumeral-Ligament model versus EMG amplitude is shown for 11 muscles for each subject.

Subject #1

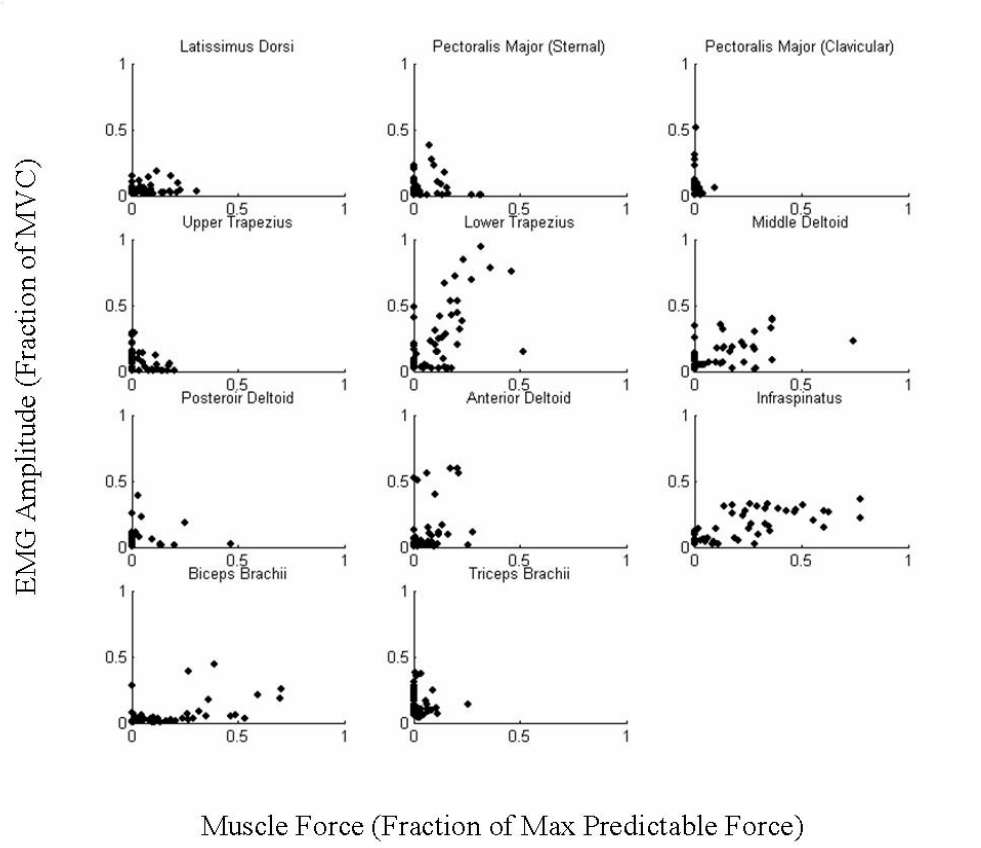

Subject #2

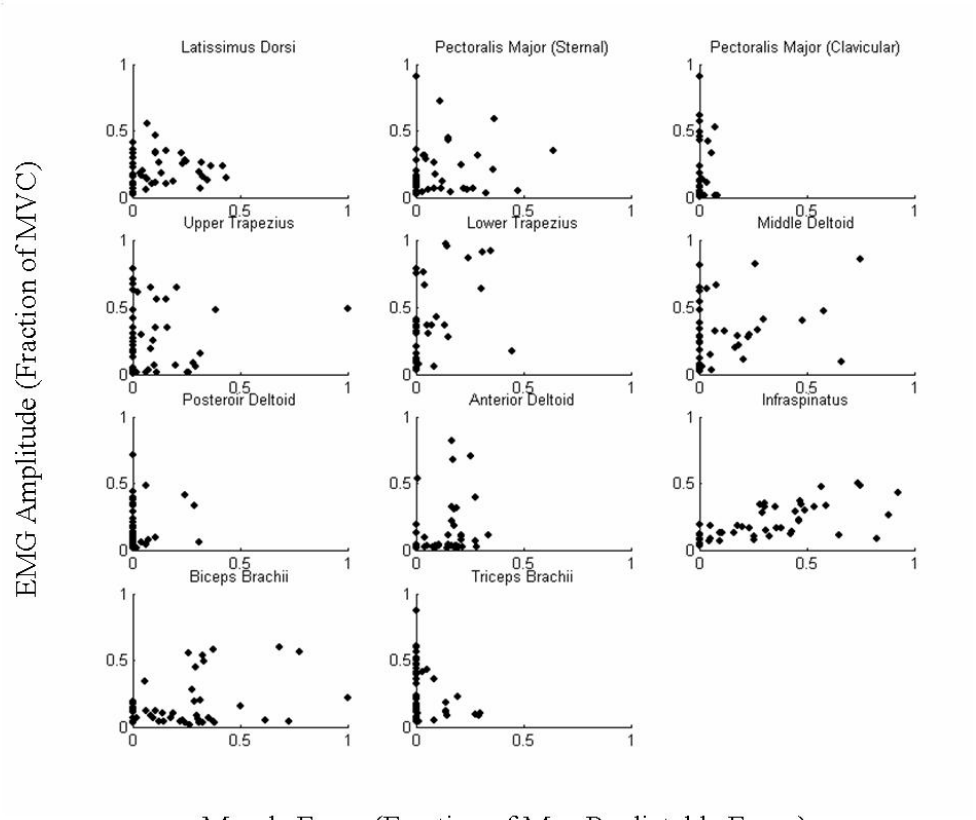
Latissimus Dorsi
Pectoralis Major (Sternal)
Pectoralis Major (Clavicular)
Upper Trapezius
Lower Trapezius
Middle Deltoid
Posteroir Deltoid
Anterior Deltoid
Infraspinatus
Biceps Brachii
Triceps Brachii
EMG Amplitude (Fraction of MVC)
Muscle Force (Fraction of Max Predictable Force)

Subject #3

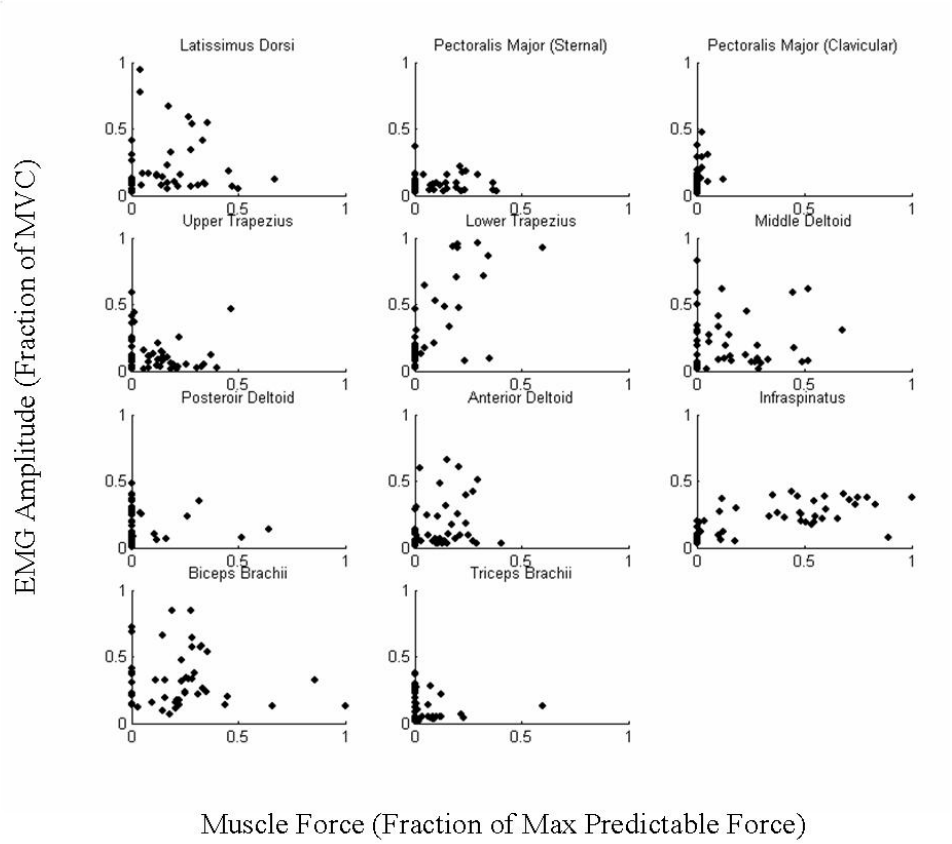
Latissimus Dorsi
Pectoralis Major (Sternal)
Pectoralis Major (Clavicular)
Upper Trapezius
Lower Trapezius
Middle Deltoid
Posteroir Deltoid
Anterior Deltoid
Infraspinatus
Biceps Brachii
Triceps Brachii
EMG Amplitude (Fraction of MVC)
Muscle Force (Fraction of Max Predictable Force)

Subject #4

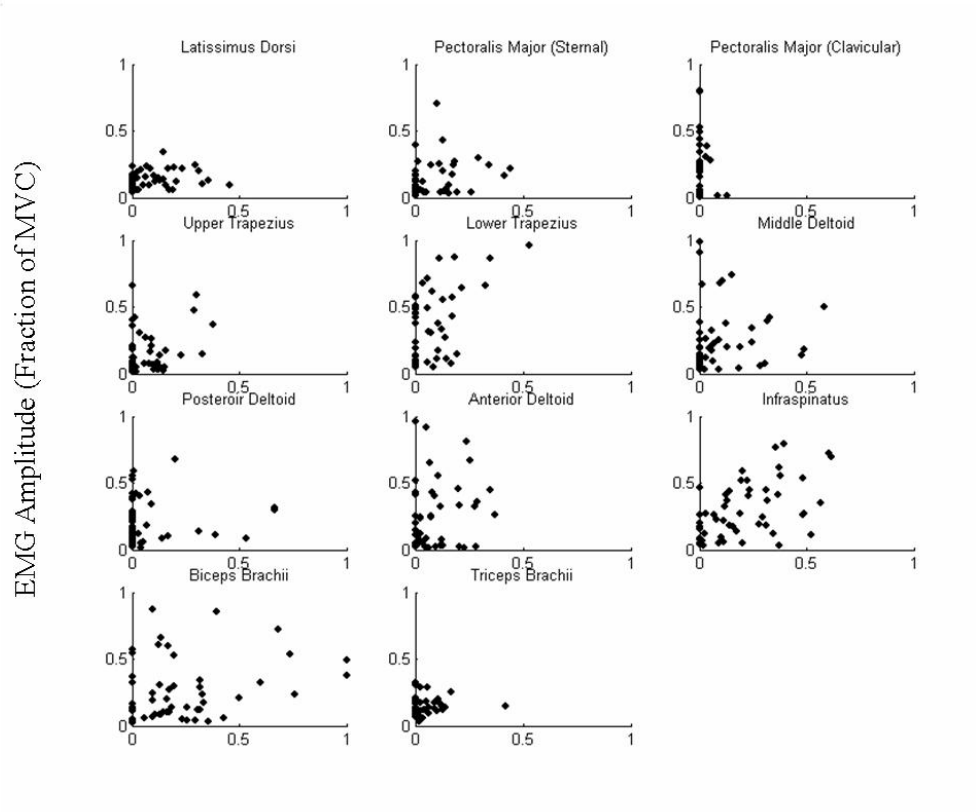
Latissimus Dorsi
Pectoralis Major (Sternal)
Pectoralis Major (Clavicular)
Upper Trapezius
Lower Trapezius
Middle Deltoid
Posteroir Deltoid
Anterior Deltoid
Infraspinatus
Biceps Brachii
Triceps Brachii
EMG Amplitude (Fraction of MVC)
Muscle Force (Fraction of Max Predictable Force)

Subject #5

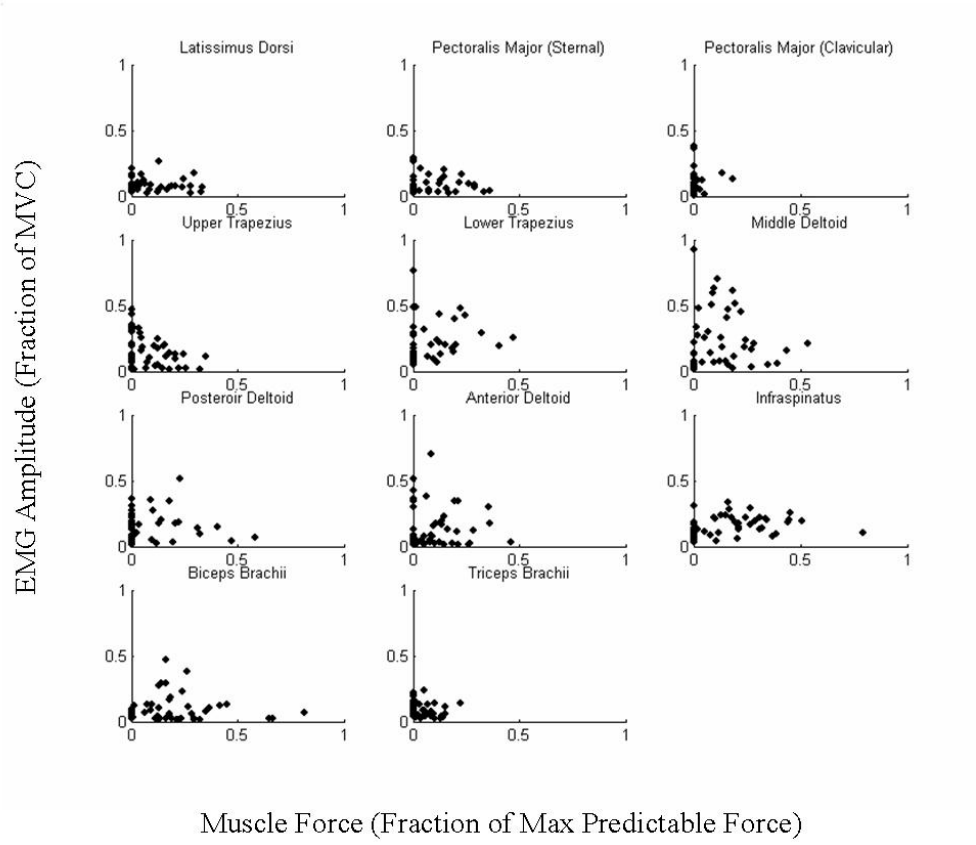
Latissimus Dorsi
Pectoralis Major (Sternal)
Pectoralis Major (Clavicular)
Upper Trapezius
Lower Trapezius
Middle Deltoid
Posteroir Deltoid
Anterior Deltoid
Infraspinatus
Biceps Brachii
Triceps Brachii
EMG Amplitude (Fraction of MVC)
Muscle Force (Fraction of Max Predictable Force)

Subject #6

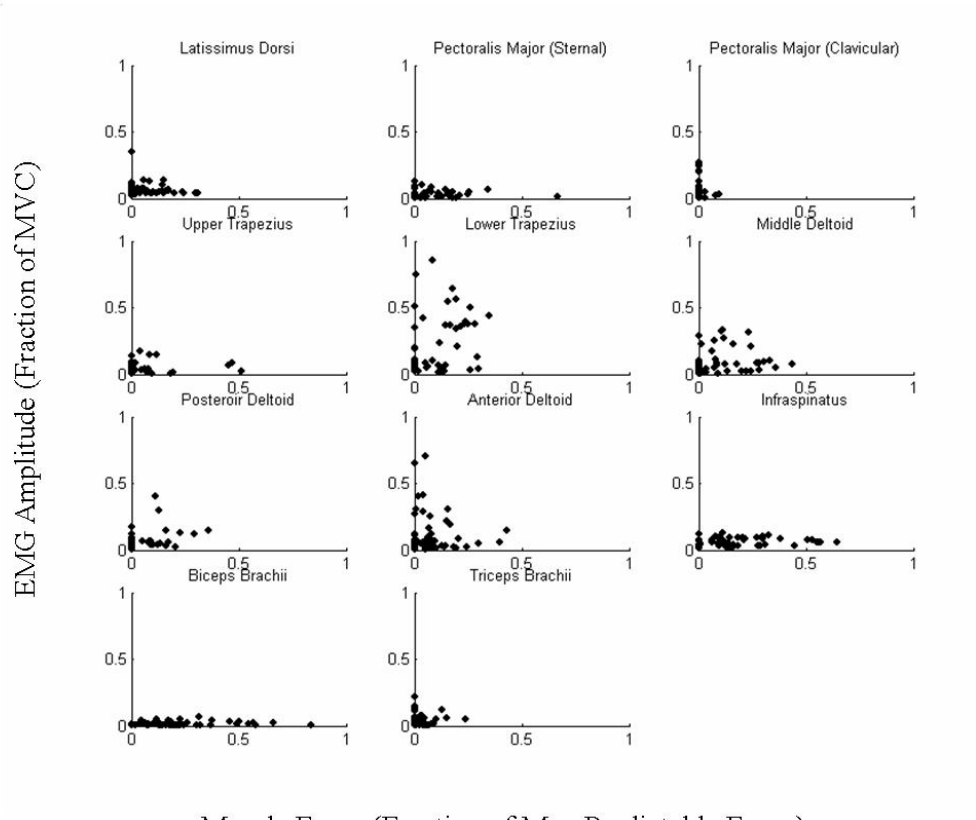
Latissimus Dorsi
Pectoralis Major (Sternal)
Pectoralis Major (Clavicular)
Upper Trapezius
Lower Trapezius
Middle Deltoid
Posteroir Deltoid
Anterior Deltoid
Infraspinatus
Biceps Brachii
Triceps Brachii
EMG Amplitude (Fraction of MVC)
Muscle Force (Fraction of Max Predictable Force)

Subject #7

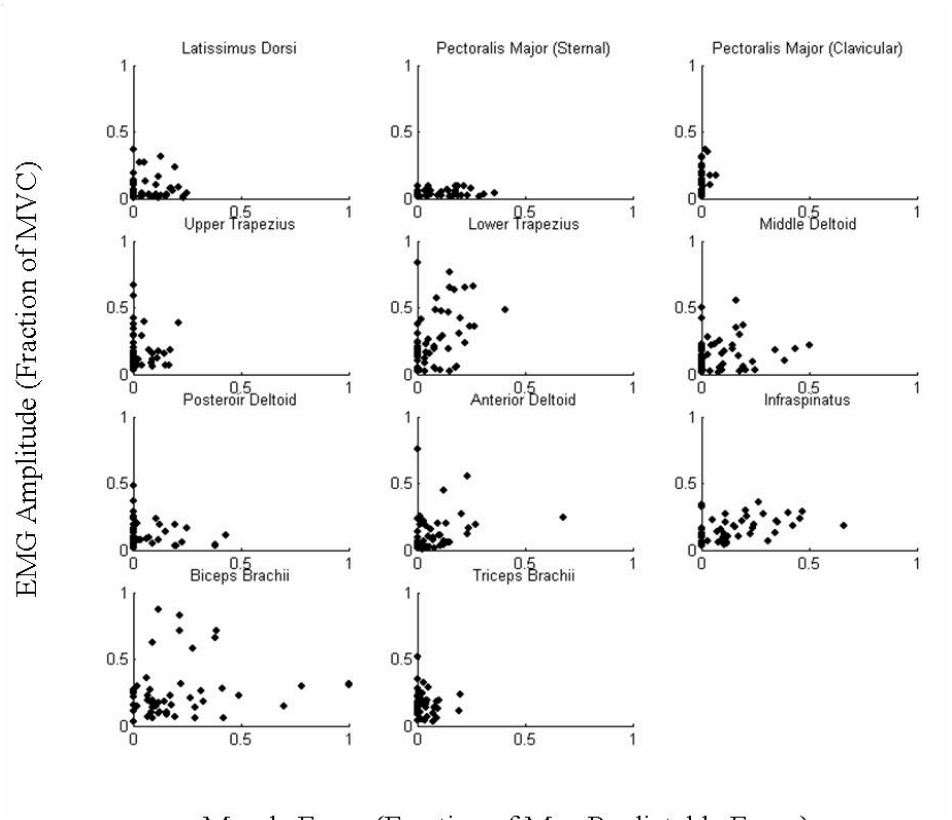
Latissimus Dorsi
Pectoralis Major (Sternal)
Pectoralis Major (Clavicular)
Upper Trapezius
Lower Trapezius
Middle Deltoid
Posteroir Deltoid
Anterior Deltoid
Infraspinatus
Biceps Brachii
Triceps Brachii
EMG Amplitude (Fraction of MVC)
Muscle Force (Fraction of Max Predictable Force)

Subject #8

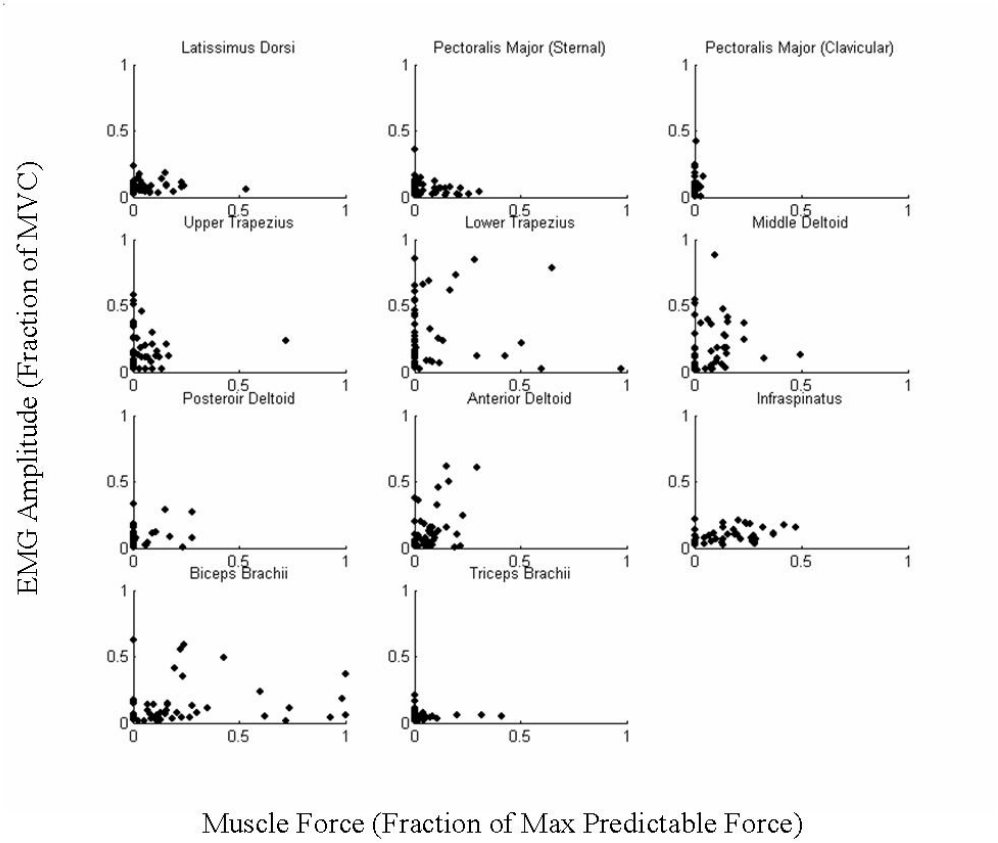
Latissimus Dorsi
Pectoralis Major (Sternal)
Pectoralis Major (Clavicular)
Upper Trapezius
Lower Trapezius
Middle Deltoid
Posteroir Deltoid
Anterior Deltoid
Infraspinatus
Biceps Brachii
Triceps Brachii
EMG Amplitude (Fraction of MVC)
Muscle Force (Fraction of Max Predictable Force)

Subject #9

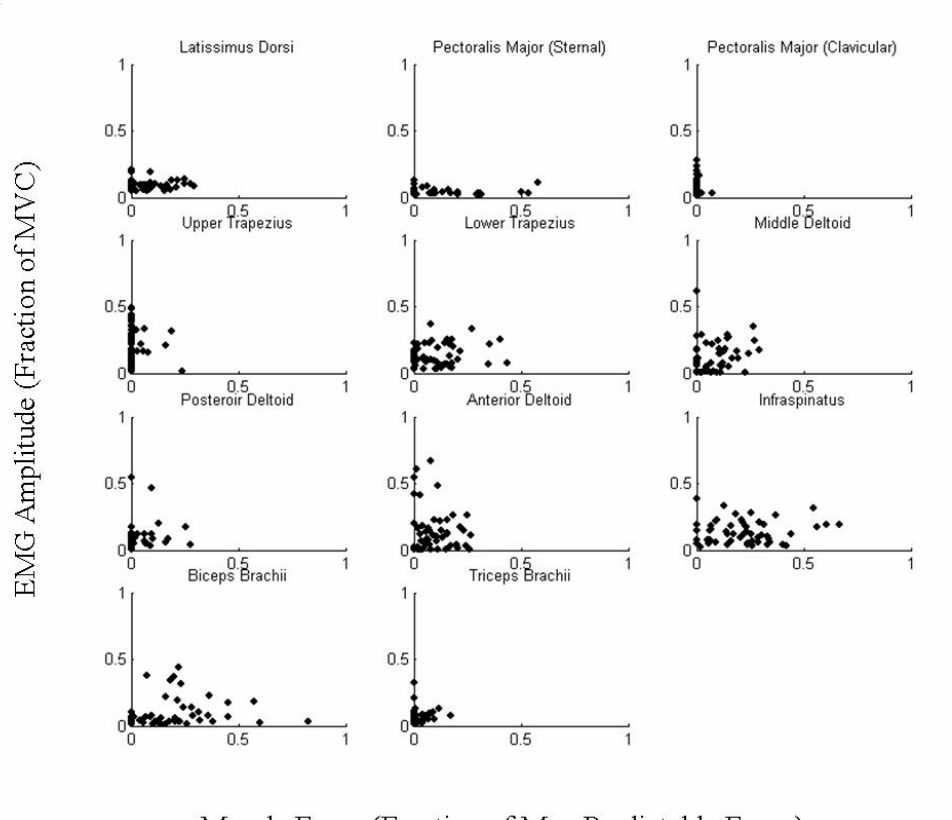
Latissimus Dorsi
Pectoralis Major (Sternal)
Pectoralis Major (Clavicular)
Upper Trapezius
Lower Trapezius
Middle Deltoid
Posteroir Deltoid
Anterior Deltoid
Infraspinatus
Biceps Brachii
Triceps Brachii
EMG Amplitude (Fraction of MVC)
Muscle Force (Fraction of Max Predictable Force)

Subject #10

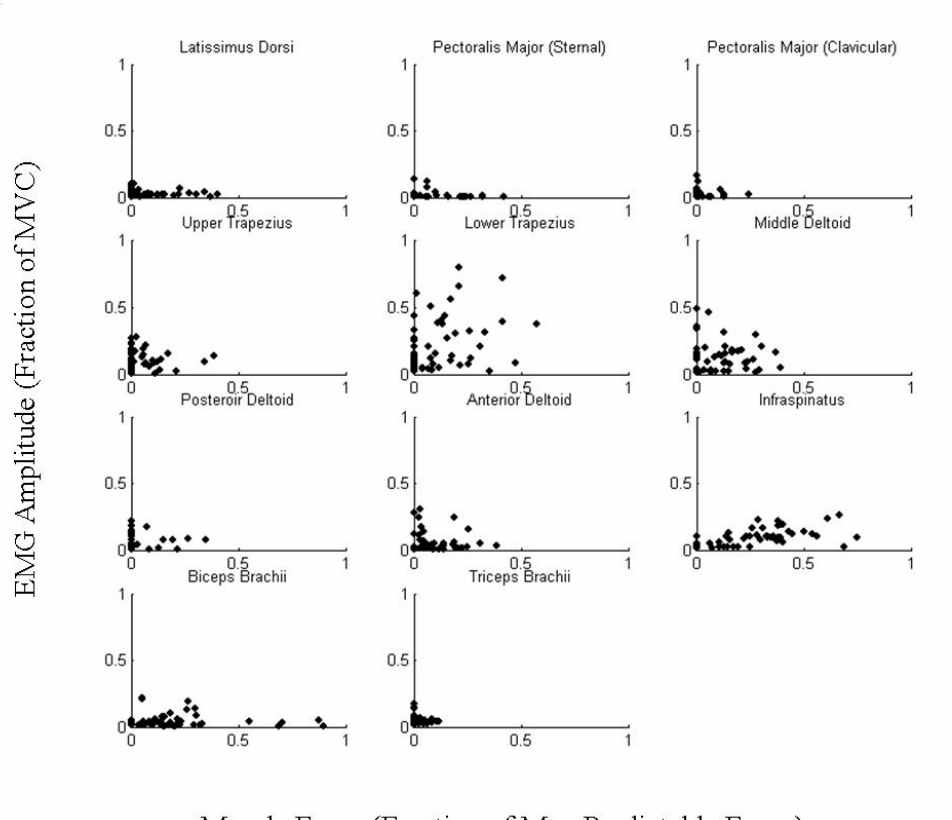
Latissimus Dorsi
Pectoralis Major (Sternal)
Pectoralis Major (Clavicular)
Upper Trapezius
Lower Trapezius
Middle Deltoid
Posteroir Deltoid
Anterior Deltoid
Infraspinatus
Biceps Brachii
Triceps Brachii
EMG Amplitude (Fraction of MVC)
Muscle Force (Fraction of Max Predictable Force)